

NANOPORE BIOSENSORS FOR MOLECULAR DETECTION AND ANALYSIS

By

Muhammad Usman Raza

Presented to the Faculty of the Graduate School of

The University of Texas at Arlington

in Partial Fulfillment of the Requirements for the Degree of

DOCTOR OF PHILOSOPHY

THE UNIVERSITY OF TEXAS AT ARLINGTON

May 2018

Copyrights © Muhammad Usman Raza

May 2018

All Rights Reserved

ACKNOWLEDGEMENTS

All praise to Allah Almighty, creator of this world and the hereafter.

Praise to Prophet Muhammad, Sallallahu Alaihi Wasallam.

I would like to thank my Mom who bore me and brought me into this world. She instilled empathy, love and care in me. She juggled her teaching job and household duties for over two decades to fulfil her desire to get us the best education. My father who was the reason I did well in studies because he was a constant support. He worked day and night to bring food on the table. My parents never took vacations or afforded luxuries of life for themselves so that they could send me and my siblings to the best schools. My father nudged me in the right direction for pursuing higher studies.

I thank my wife for supporting me each and every day of my PhD. For the tremendous buck up talks that lifted my spirits when things were not working out. For working 9 hours a day just so that we can afford a living, while I complete my doctoral studies. For supporting me in times of distress.

I thank my PhD advisor Dr. Samir M. Iqbal for giving me a chance to work in Nanobio lab. For guiding me and supporting me during my research. I would also express my gratitude to Dr George Alexandrakis for his guidance and encouragement. I thank Dr. Zeynep Celik-Butler, Dr. Yuze Sun and Dr Ali Davoudi for being in my PhD dissertation committee. I especially thank Dr. Zeynep Celik-Butler for choosing me as her lab teaching assistant.

Also, I would like to thank my coworkers in NanoBio Lab especially Sai Santosh Sasank Peri for helping me and patiently being the support system in my PhD. I would also thank Dr. Nader Hozhabri and the Nanotechnology Research center staff for their technical help.

May, 4, 2018

DEDICATION

This work is dedicated to the memory of my late grandfather, who passed away due to lung cancer. His cancer was detected when it had reached stage 4 metastasis and doctors could not save him. It was due to this that I became interested in Nanobio Lab at UTA which was working on biosensors for early detection of cancer and I decided that I wanted to do my doctoral research here. If he was here today with us, he would have been so proud.

ABSTRACT

Nanopore Biosensors for Molecular Detection and Analysis

By

Muhammad Usman Raza, PhD

University of Texas at Arlington, 2018

Supervising professor: Dr Samir M. Iqbal

Nanoscale fabrication techniques have led the march towards a new class of biosensors that were not possible to build in the past due to technological limitations. These molecular nanosensors can have biochemical, electromagnetic, acoustic, optical or electrophoretic detection modalities. One of these nanosensors, is solid state nanopores which use resistive pulse sensing in nanometer apertures in thin dielectric membranes. Solid state nanopores have been fabricated using cutting edge fabrication techniques to detect and analyze nanoscale biomolecules such as DNA, proteins, miRNA, viruses etc. These biosensors can be used as electronic sensors for biomarkers of certain diseases such as cancer and can form effective tools for early detection which can eventually save lives. Solid state nanopores have also been used as a novel way for cheap DNA sequencing. In the case for early detection of cancer, molecular biology plays a critical role and solid state nanopores can be used to study that and provide effective ways for the effect.

In this dissertation we work on solid state nanopores and try to improve them using the cutting-edge fabrication techniques and optical modalities to make them ultrasensitive biomarker detection and multiplexed sensing biosensors. In the first project, we use solid state nanopores in silicon nitride membranes to detect epidermal growth factor receptor (EGFR) protein which is overexpressed in many cancers and is a cancer biomarker. We use an RNA Aptamer to selectively bind to the EGFR which increases the selectivity for this cancer biomarker through solid state nanopores. In the second project, we

simulate two adjacent nanopores on a single membrane in the quest to find the adjacent nanopore distance for reduced electronic crosstalk. The optical parameters derived from the simulations can be used as a blueprint for fabrication of nanopore arrays on single membranes to increase the throughput and self-referencing capability for noise cancellation. The final project reinvents the solid state nanopore with the inclusion of an optical plasmonic trap cavity at the mouth of the nanopore. We are the first ones to report this type of nanopore device. This novel sensor provides dual mode optical and electrical sensing capability. In addition, the localized plasmon field can trap the nanoparticles for up to 7 seconds at the mouth of the nanopore, which was previously not possible due to the electrophoretic translocation. It is shown that nanoparticles oscillate in the trap, which results in high frequency electrical noise that is synchronous to the mass loading of the plasmonic cavity.

TABLE OF CONTENTS

ACKNOWLEDGEMENTS	I
DEDICATION	II
ABSTRACT	III
TABLE OF CONTENTS	V
1. INTRODUCTION	1
2. DIFFERENTIATION OF SPECIFIC CANCER BIOMARKERS WITH SOLID STATE NANOPORES	18
3. CROSSTALK BETWEEN ADJACENT NANOPORES IN A SOLID-STATE MEMBRANE ARRAY FOR MULTI-ANALYTE HIGH-THROUGHPUT BIOMOLECULE DETECTION	41
4. SIBA ACTUATED NANOPORE ELECTROPHORESIS (SANE)	63
5. CONCLUSION	86
6. APPENDICES	88

1. INTRODUCTION

1.1. BACKGROUND

Over the past millennia, healers have been diagnosing diseases in humans using physical and psychological markers that become apparent when the disease had progressed throughout the human body. The diagnosis would be based on anecdotal knowledge about certain apparent symptoms and the cure would be administered based on trial and error over numerous patients suffering similar symptoms in the past [1]. The general attributes of herbs and other complex medicines were part of the base knowledge for healers of that time. With the advent of modern medicine, it became necessary to understand the prognosis of diseases so that solutions to diagnosis, prevention and cure are based on biological evidence [2-4]. The need for knowledge on biological basis of disease progression is where the field of molecular biology became vital in the biology of drug action [5-8]. Hence, as human knowledge about molecular biology increased, the cures of previously deadly diseases were discovered [9-12]. As biomolecular analytical technologies evolved as tools to study disease the interest in development of ever more sensitive and specific biosensors increased. This also resulted in the development of new biosensors which used the biomolecular changes in the human body, that result from certain diseases, to be used as markers for disease detection and prognosis [13-15]. Miniaturization of sensors down to the nanoscale promises to fulfill the sensitivity-specificity goals, which in turn can enable early detection of deadly diseases such as cancer.

Cancer is one of the deadliest diseases, with abnormal cell growth resulting in the formation of tumors in the body. Cancer cells develop out of healthy cells due to DNA mutations that result in altered signaling pathways that may help the cell evade cell cycle checkpoints and programmed death. [16]. When cancer starts, it has no apparent symptoms that only become apparent once the mass of the tumor grows. For example, in the case of colorectal cancer, this may lead to bowel blockage [17]. In the case of lung cancer this may lead to cough, flu or pneumonia symptoms[18]. Many apparent symptoms caused by cancer are non-specific in nature as cancer imitates symptoms of other diseases [19, 20]. So, if proper diagnosis is not

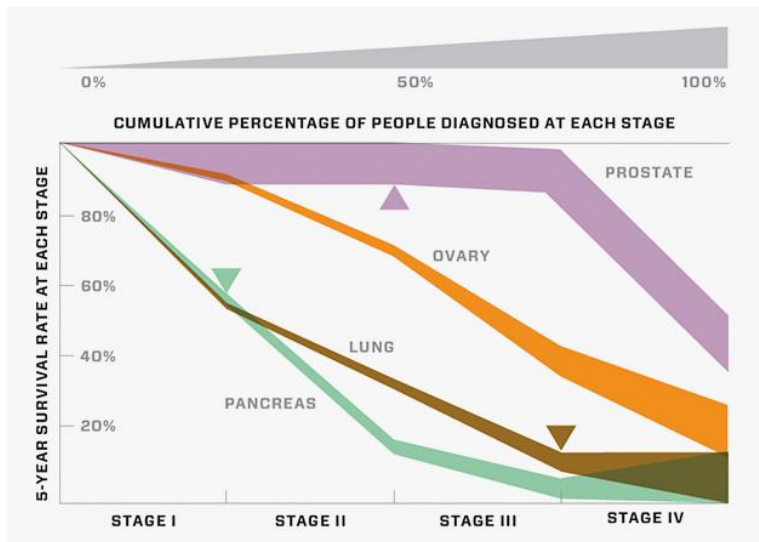


Fig 1.1: Early cancer diagnosis results in higher 5-year survival rates. If the cancer is detected in stage IV the chances of survival are less [25].

performed and testing does not take into consideration the biomarkers of cancer, the cancer could progress into a more aggressive metastatic stage, in which the abnormal cells proliferate throughout the body by being transported through blood vessels at which point a cure is often not feasible [21-24].

In cancer, early stage detection and diagnosis, when the tumor is at its primary site can result in the difference between life and death [25]. However, the most common stage of detection is different between cancer types and heavily skewed towards late detection [Fig 1.1]. Cancer is the second most prevalent

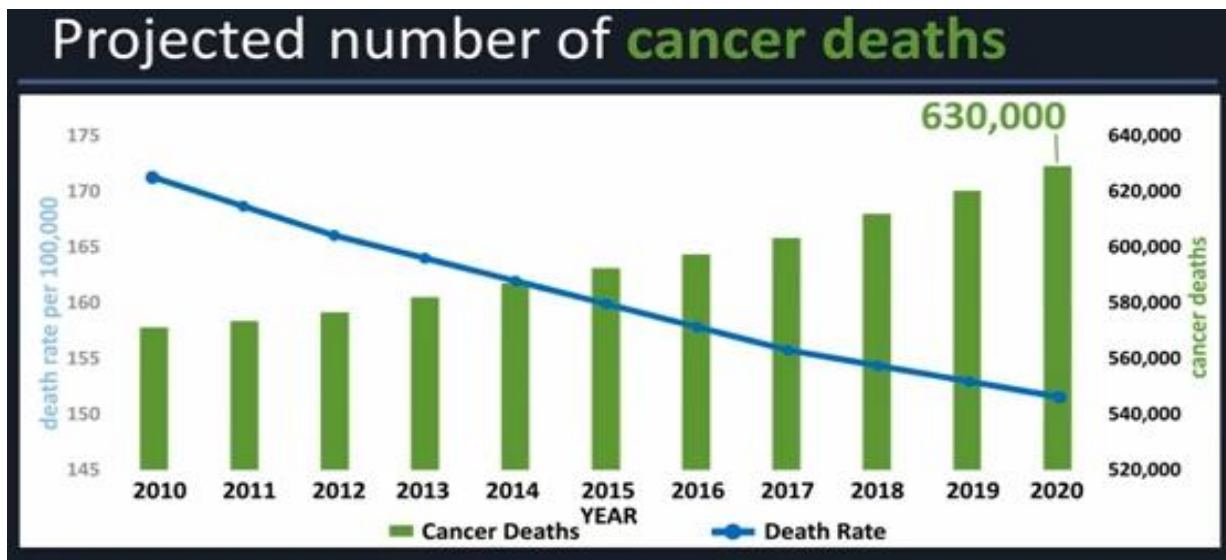


Fig 1.2: Cancer deaths are going to increase as overall death rates due to other diseases decrease [26]

disease in the world only next to heart disease. However, as the number of deaths for heart disease patients have halved for those under 85 years of age, those of cancer patients are almost stagnant. This shows the importance of research on cancer biology to further understand the prognosis of cancer from start. As the number of deaths per 100,000 people decrease due to medical advances the deaths due to cancer is projected to increase in the next few years in US [26] [Fig 1.2].

Progression of cancer in the human body is referred to as carcinogenesis [27]. Normal cells mutate in to abnormal cells with changes in the characteristics at the genetic, epigenetic and cellular level leading to abnormal cell division [28]. Additionally, DNA mutations disrupt the process of programmed cell death, or apoptosis. Whereas normal cells are eliminated with apoptosis, cancer cells skip apoptosis and multiply uncontrollably. These cells form local tumor sites in organs called primary sites [29, 30]. Cancer cells in tumor sites over time mutate into malignant cells, which are invasive, and they enter nearby vascular tracts and start their journey in the blood stream. In the blood stream, malignant cells can migrate into distant organs and start remote tumor sites as they proliferate [31, 32]. When metastasis has established itself in the host body, many apparent signs of the disease are established, which leads to a diagnosis that is too late in most cases to be cured fully. Hence, the most effective way to cure cancer is to detect it in its early stages[33-36].

The study of DNA mutations and subsequent proteomics has led to the belief that early detection of cancer progression can be achieved through detection of minute changes in DNA sequences or the up-regulated expression of cancer specific biomarkers [37, 38]. The biomarkers are molecular signatures made by tumor or by the body in response to the tumor. These biomarkers can be detected either in biopsied tissue from the tumor sites or in blood, urine and other fluids in the body[14]. Cutting-edge research in cancer detection focuses on biosensors, which can target circulating molecular biomarkers in the bodily fluids such as blood, urine because they are easily accessible. These biosensors can utilize electrical, optical, chemical, physical, magnetic properties of a specific biomarker or coterie of biomarkers to detect the advent of a tumor at nascent Stage 1 when it is bound to its primary tumor site, which maybe small enough to evade detection using current Point of Care (POC) testing facilities. The hope is that these nanoscale molecular biosensors may become efficient, robust and cheap tools to detect cancers in early stages so that lives are

saved. It is projected that in 2020, 158 billion USD [39] will be spent on cancer care and this can be significantly reduced if tumors are detected at early stages where they can be cured effectively at a lesser cost.

1.2. NANOPORE BIOSENSORS

A human cell is replete with various kinds of biological nanopores which regulate the transport of ions, nutrients and biomolecules in and out of its nuclear, mitochondrial and outer cell membranes. This becomes the basic mechanism by which a human cell interacts and lives in its environment. However, if we take this idea from nature and regulate the transport of disease biomarkers through manmade nanopores under certain conditions and monitor the results we may be able to study, identify and quantify those biomarkers. Biological nanopores, occur in nature, regulating the transport of ions and molecules across the cell membrane. Electrophysiology experiments of single ion channel nanopores in cells membranes was done decades ago [40]. It was in the 1990's that first work on DNA sequencing using biological nanopores based on α -hemolysin [41, 42] was accomplished. In subsequent works, it was shown that translocating ssDNA across the α -hemolysin nanopore would produce a characteristic current and have different translocation times based on its composition. Nanopores based on α -hemolysin which is a protein toxin created by a bacterium called *Staphylococcus Aureus*, makes 1.4 nm diameter nanopores that spontaneously insert themselves into a lipid membrane. This resulted in the hypothesis that cheap and fast DNA sequencing

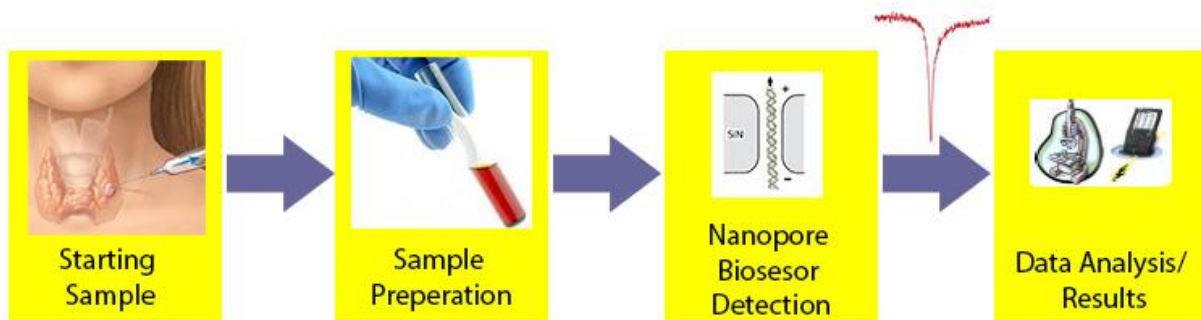


Fig 1.3: Process flow of Point of Care solid state nanopore biomarker detection

could be accomplished using these nanometer-size natural pores. However, the limitations of these biological nanopores consisting of fixed size, inability to detect single base pairs due to fast translocation

and structural instability caused by external factors like salt concentration, pH and mechanical stress, lead to the fabrication of nanopores through solid state materials which are more robust to external factors.

Solid state nanopores are fabricated using silicon nanoscale fabrication techniques. The elementary idea behind solid state nanopores is that they can become robust analytical devices for any kind of bio molecule as their structure and size can be tuned to match the size of the target analyte [43]. The target analyte can be a disease biomarker in a patient sample. The sample after going through required pre-processing can be analyzed using a solid state nanopore biosensor at the point of care [Fig 1.3]. This idealized use case scenario is what makes the field of nanopore biosensing important for the future [44]. With scale, solid state nanopore biosensors can be fabricated inexpensively, leading to greater financial reach for average POC facility.

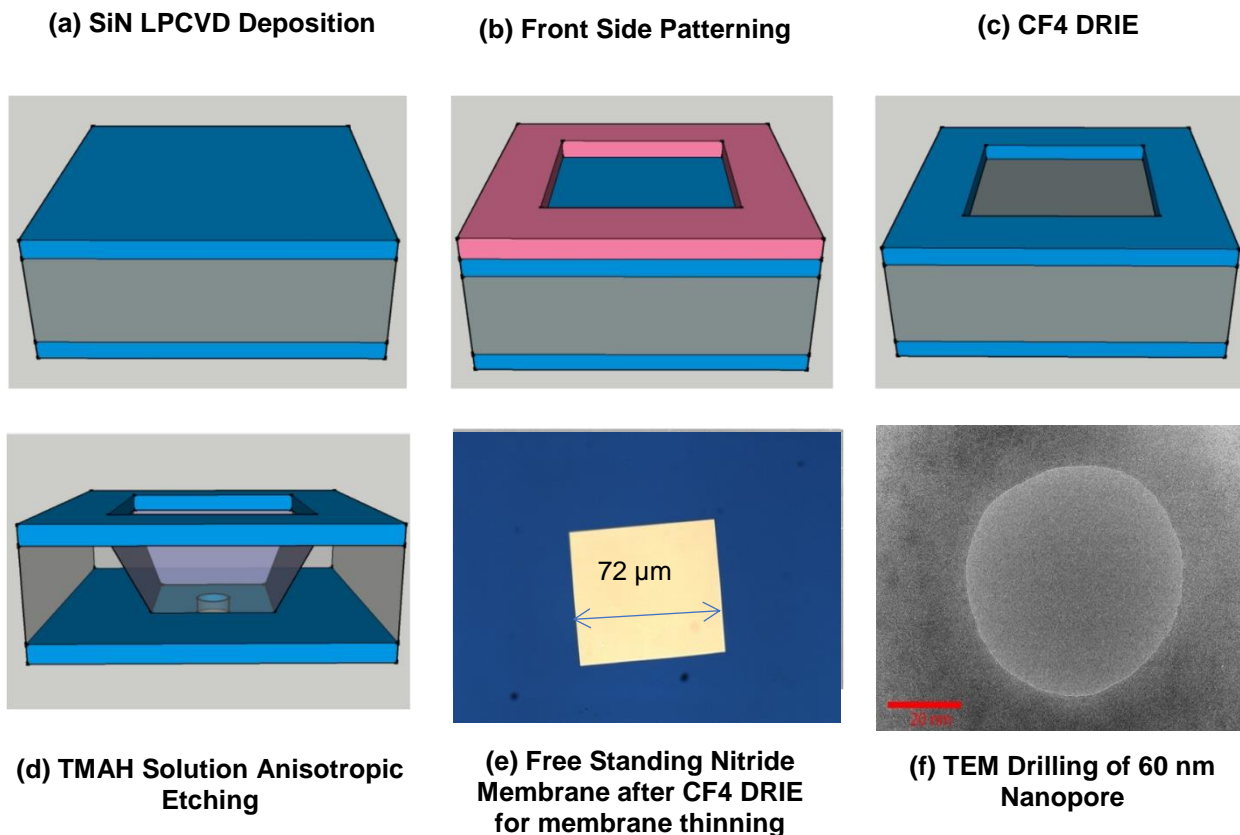


Fig 1.4: Steps to fabricate a simple solid state nanopore on a silicon wafer.

Solid state nanopores are nanometer holes drilled into thin dielectric membranes suspended on silicon chips [45, 46]. These nanopore dielectrics can use silicon nitride, silicon oxide, graphene or other materials based on the requirements of the application[47, 48]. The fabrication can incorporate complex techniques

for certain applications such as DNA sequencing [49]. Fig 1.4 shows the steps required to fabricate solid state nanopores in dielectric membranes using silicon nanofabrication techniques. Fabrication is started by depositing a thin silicon nitride layer on top of a 525 μm thick (100) silicon wafer [Fig 1.4 (a)]. The wafer is patterned using optical lithography and a 780 μm square window is opened in the photoresist [Fig 1.4 (b)]. CF_4 chemistry is used in the Deep Reactive Ion Etcher (DRIE) to etch away the silicon nitride exposed inside the patterned square windows [Fig 1.4 (c)]. Tetra Methyl Ammonium Hydroxide (TMAH) anisotropic wet etching is used to etch the silicon all the way to the other side of the wafer till the silicon nitride on the other side remains suspended [Fig 1.4 (d)]. The suspended membrane in this design is 75 ± 10 μm squares in size [Fig 1.4 (e)]. After this, the chips are placed in a high energy beam which can be a Transmission Electron Microscope or Focused Ion Beam to drill the nanometer sized nanopore in the thin silicon nitride membrane [Fig 1.4 (f)]. This chip is sandwiched between two containers of ionic solution with bio-analyte suspended in the cis container. Voltage bias is applied to the cis and trans containers via Ag/AgCl electrodes leading to electrophoresis of ionic solution through the nanopore and translocation of analyte through the nanopore. As the analyte translocates through the ion channel it gives a characteristic resistive pulse which is detected by the measuring equipment [50]. This procedure has been used for the past two decades for many biological applications. Solid state nanopores with three-dimensional dielectric materials silicon nitride (Si_3N_4) and two-dimensional materials such as graphene and molybdenum disulphide (MoS_2) have been used for DNA sequencing [51-54]. The two-dimensional materials provide the extraordinary characteristic of less than 1 nm thin nanopores leading to precise base pair detection in nanopores. Solid state nanopores can also be functionalized with certain biomolecules to improve the detection capability of a target analyte [55-57]. Nanopores have also been used to detect and analyze bio molecules such as miRNA, proteins, enzymes and others which may be disease biomarkers [58-64]. Larger size nanopores have also been used to investigate large entities such as viruses, bacteria and big biomolecules [65-67]. The breadth of reported sensing applications illustrates the extraordinary capability of solid state nanopores of different structures and sizes to be used for individualized bio-applications where the nanopore design parameters are built to suit the constraints of the analyte.

The work in this dissertation focuses on the use of simple solid state nanopores for early detection of cancer using the proteomic indicators that are overexpressed in cancers of different types. We also use selective

binding agents called aptamers, for targeted binding on the protein biomarker which causes the spread of cancer through abnormal cell growth. We show that solid state nanopores can be used to selectively detect cancer molecular biomarkers which can be found at the tumor site or in bodily fluids, albeit at a smaller scale. Furthermore, we try to improve the throughput and self-referencing capability of solid state nanopores by conducting simulations for array of nanopores on a single chip and find out the distance requirement between adjacent nanopores for actual fabrication. Finally, we build an original optical and electrical dual modality, plasmonic solid state nanopore which can be thought as the solid state nanopore for the future. This dual modality nanopore uses plasmonic force to trap the individual molecules and particles at the mouth of the nanopore.

1.3. CANCER BIOMARKER DETECTION USING SOLID STATE NANOPORES

In the first project, we use solid state nanopores to detect extracellular domain of Epidermal Growth Factor Receptor (EGFR) and use a bare nanopore that is not functionalized to detect characteristic translocation of this protein that is highly overexpressed in many tumors. We can selectively detect presence of this protein with the help of its RNA Aptamer binding. This can be used as a biosensor for certain cancers in which EGFR concentrations can be found to detect cancer or it can be used for cancer prognosis studies.

1.4. NANOPORE ARRAYS CROSSTALK SIMULATIONS

In the second project, we simulate electrical crosstalk between adjacent nanopores that can be used to fix the distance between adjacent nanopores. This distance is necessary to avoid electronic crosstalk between adjacent nanopores. This simulation provides a mechanism to determine the adjacent nanopore distance based on the requirements of a certain application. We simulate for different applied voltages, adjacent nanopore distances and nanopore sizes for a characteristic thickness of the membrane. Finally, a particle is simulated translocating inside a nanopore and it is shown that there is no measurable effect in electrical field in the adjacent nanopore as both are more than one debye length away from each other.

1.5. DUAL MODALITY PLASMONIC SOLID STATE NANOPORES

In the last project, we fabricate a new kind of dual modality nanopore trying to resolve the technological difficulties in molecular detection and analysis in simple solid state nanopores. We fabricate Au dual nanohole (DNH) nanoapertures at the mouth of a solid state nanopore. A near-infrared (NIR) laser is focused on the DNH cavity. Due to the previously reported Self Induced Back Action (SIBA) effect, the DNH traps translocating nanoparticles at the mouth of the nanopore for a duration of seconds. This trapping effect provides valuable time to study individual biomolecules and biomarkers. The four orders of magnitude improvement in the time a particle stays in the vicinity of a nanopore, compared to electrical sensing alone, enables detecting high frequency charge oscillations from the detected electrical signal. We interpret these high frequency oscillations to originate from nanoparticle bobbing and the resulting frequency spectrum peaks at lower frequencies when more than one nanoparticle is trapped inside the DNH optical trap. This novel biosensing platform that we have fabricated, offers significant promise to improve the detection of protein biomarkers and DNA, which we propose to explore in future work.

REFERENCES

- [1] J. M. Riddle, "Theory and practice in medieval medicine," *Viator*, vol. 5, pp. 157-184, 1974.
- [2] R. H. Shryock, "The Development of Modern Medicine," ed: LWW, 1948.
- [3] R. H. Bannerman, J. Burton, and W.-C. Chen, "Traditional medicine and health care coverage: a reader for health administrators and practitioners," 1983.
- [4] B. G. Katzung, S. B. Masters, and A. J. Trevor, "Basic & clinical pharmacology," 2004.
- [5] J. D. Watson, "Molecular biology of the gene," *Molecular biology of the gene.*, 1965.
- [6] M. A. Savageau, "Biochemical systems analysis. A study of function and design in molecular biology," in *ADDISON WESLEY PUBL.*, 1976.
- [7] B. Valeur and M. N. Berberan-Santos, *Molecular fluorescence: principles and applications*. John Wiley & Sons, 2012.
- [8] P. D. Josephy and B. Mannervik, *Molecular toxicology*. Oxford University Press on Demand, 2006.

- [9] J. Sato, T. Kawamoto, A. Le, J. Mendelsohn, J. Polikoff, and G. Sato, "Biological effects in vitro of monoclonal antibodies to human epidermal growth factor receptors," *Molecular biology & medicine*, vol. 1, no. 5, pp. 511-529, 1983.
- [10] I. Xenarios, L. Salwinski, X. J. Duan, P. Higney, S.-M. Kim, and D. Eisenberg, "DIP, the Database of Interacting Proteins: a research tool for studying cellular networks of protein interactions," *Nucleic acids research*, vol. 30, no. 1, pp. 303-305, 2002.
- [11] C.-Z. Chen, "MicroRNAs as oncogenes and tumor suppressors," *New England Journal of Medicine*, vol. 353, no. 17, p. 1768, 2005.
- [12] J.-T. Zhang and Y. Liu, "Use of comparative proteomics to identify potential resistance mechanisms in cancer treatment," *Cancer treatment reviews*, vol. 33, no. 8, pp. 741-756, 2007.
- [13] S. R. Horner, C. R. Mace, L. J. Rothberg, and B. L. Miller, "A proteomic biosensor for enteropathogenic E. coli," *Biosensors and Bioelectronics*, vol. 21, no. 8, pp. 1659-1663, 2006.
- [14] A. Rasooly and J. Jacobson, "Development of biosensors for cancer clinical testing," *Biosensors and Bioelectronics*, vol. 21, no. 10, pp. 1851-1858, 2006.
- [15] K. Jain, "Current status of molecular biosensors," *Medical device technology*, vol. 14, no. 4, pp. 10-15, 2003.
- [16] G. Klein, "Cancer, apoptosis, and nonimmune surveillance," *Cell death and differentiation*, vol. 11, no. 1, pp. 13-17, 2004.
- [17] S. J. Winawer *et al.*, "Colorectal cancer screening: clinical guidelines and rationale," *Gastroenterology*, vol. 112, no. 2, pp. 594-642, 1997.
- [18] A. A. Abd-El-Fattah, N. A. H. Sadik, O. G. Shaker, and M. L. Aboulftouh, "Differential microRNAs expression in serum of patients with lung cancer, pulmonary tuberculosis, and pneumonia," *Cell biochemistry and biophysics*, vol. 67, no. 3, pp. 875-884, 2013.
- [19] L. M. DeAngelis, "Primary central nervous system lymphoma imitates multiple sclerosis," *Journal of neuro-oncology*, vol. 9, no. 2, pp. 177-181, 1990.
- [20] D. C. Utz, K. A. Hanash, and G. M. Farrow, "The plight of the patient with carcinoma in situ of the bladder," *The Journal of urology*, vol. 103, no. 2, pp. 160-164, 1970.
- [21] P. M. Lantz *et al.*, "The influence of race, ethnicity, and individual socioeconomic factors on breast cancer stage at diagnosis," *American journal of public health*, vol. 96, no. 12, pp. 2173-2178, 2006.
- [22] M. A. O'Rourke, J. R. Feussner, P. Feigl, and J. Laszlo, "Age trends of lung cancer stage at diagnosis: implications for lung cancer screening in the elderly," *Jama*, vol. 258, no. 7, pp. 921-926, 1987.
- [23] A. Parikh-Patel, J. H. Bates, and S. Campleman, "Colorectal cancer stage at diagnosis by socioeconomic and urban/rural status in California, 1988–2000," *Cancer*, vol. 107, no. S5, pp. 1189-1195, 2006.
- [24] I. E. L. C. A. P. Investigators, "Survival of patients with stage I lung cancer detected on CT screening," *New England Journal of Medicine*, vol. 355, no. 17, pp. 1763-1771, 2006.

- [25] T. Goetz, "Why early detection is the best way to beat cancer," *Wired com*, 2008.
- [26] C. f. D. Control and Prevention, "Expected New Cancer Cases and Deaths in 2020," ed, 2017.
- [27] G. S. Palapattu *et al.*, "Prostate carcinogenesis and inflammation: emerging insights," *Carcinogenesis*, vol. 26, no. 7, pp. 1170-1181, 2004.
- [28] B. E. Henderson and H. S. Feigelson, "Hormonal carcinogenesis," *Carcinogenesis*, vol. 21, no. 3, pp. 427-433, 2000.
- [29] J. S. Nystrom, J. M. Weiner, J. Heffelfinger-Juttner, L. E. Irwin, J. R. Bateman, and R. M. Wolf, "Metastatic and histologic presentations in unknown primary cancer," in *Seminars in oncology*, 1977, vol. 4, no. 1, pp. 53-58.
- [30] M. J. Hayat, N. Howlader, M. E. Reichman, and B. K. Edwards, "Cancer statistics, trends, and multiple primary cancer analyses from the Surveillance, Epidemiology, and End Results (SEER) Program," *The oncologist*, vol. 12, no. 1, pp. 20-37, 2007.
- [31] A. F. Chambers, A. C. Groom, and I. C. MacDonald, "Metastasis: dissemination and growth of cancer cells in metastatic sites," *Nature Reviews Cancer*, vol. 2, no. 8, p. 563, 2002.
- [32] I. J. Fidler, "The pathogenesis of cancer metastasis: the 'seed and soil' hypothesis revisited," *Nature Reviews Cancer*, vol. 3, no. 6, p. 453, 2003.
- [33] J. D. Wulfkuhle, L. A. Liotta, and E. F. Petricoin, "Early detection: proteomic applications for the early detection of cancer," *Nature reviews cancer*, vol. 3, no. 4, p. 267, 2003.
- [34] C. Bettegowda *et al.*, "Detection of circulating tumor DNA in early- and late-stage human malignancies," *Science translational medicine*, vol. 6, no. 224, pp. 224ra24-224ra24, 2014.
- [35] P. T. Scardino, R. Weaver, and A. H. M'Liss, "Early detection of prostate cancer," *Human pathology*, vol. 23, no. 3, pp. 211-222, 1992.
- [36] R. Etzioni *et al.*, "Early detection: The case for early detection," *Nature Reviews Cancer*, vol. 3, no. 4, p. 243, 2003.
- [37] S. Ramaswamy, K. N. Ross, E. S. Lander, and T. R. Golub, "A molecular signature of metastasis in primary solid tumors," *Nature genetics*, vol. 33, no. 1, p. 49, 2003.
- [38] A. J. Minn *et al.*, "Genes that mediate breast cancer metastasis to lung," *Nature*, vol. 436, no. 7050, p. 518, 2005.
- [39] D. Kelly *et al.*, "Cancer Care Costs and Clinical Trials," *Irish medical journal*, vol. 110, no. 4, pp. 557-557, 2017.
- [40] B. Sakmann, *Single-channel recording*. Springer Science & Business Media, 2013.
- [41] D. W. Deamer and M. Akeson, "Nanopores and nucleic acids: prospects for ultrarapid sequencing," *Trends in biotechnology*, vol. 18, no. 4, pp. 147-151, 2000.

- [42] J. J. Kasianowicz, E. Brandin, D. Branton, and D. W. Deamer, "Characterization of individual polynucleotide molecules using a membrane channel," *Proceedings of the National Academy of Sciences*, vol. 93, no. 24, pp. 13770-13773, 1996.
- [43] C. Dekker, "Solid-state nanopores," *Nature nanotechnology*, vol. 2, no. 4, p. 209, 2007.
- [44] S. Choi, M. Goryll, L. Y. M. Sin, P. K. Wong, and J. Chae, "Microfluidic-based biosensors toward point-of-care detection of nucleic acids and proteins," *Microfluidics and Nanofluidics*, vol. 10, no. 2, pp. 231-247, 2011.
- [45] A. Storm, J. Chen, X. Ling, H. Zandbergen, and C. Dekker, "Fabrication of solid-state nanopores with single-nanometre precision," *Nature materials*, vol. 2, no. 8, p. 537, 2003.
- [46] B. N. Miles, A. P. Ivanov, K. A. Wilson, F. Doğan, D. Japrun, and J. B. Edel, "Single molecule sensing with solid-state nanopores: novel materials, methods, and applications," *Chemical Society Reviews*, vol. 42, no. 1, pp. 15-28, 2013.
- [47] M. Firmkes, D. Pedone, J. Knezevic, M. Doblinger, and U. Rant, "Electrically facilitated translocations of proteins through silicon nitride nanopores: conjoint and competitive action of diffusion, electrophoresis, and electroosmosis," *Nano letters*, vol. 10, no. 6, pp. 2162-2167, 2010.
- [48] G. F. Schneider *et al.*, "DNA translocation through graphene nanopores," *Nano letters*, vol. 10, no. 8, pp. 3163-3167, 2010.
- [49] T. Nelson, B. Zhang, and O. V. Prezhdo, "Detection of nucleic acids with graphene nanopores: ab initio characterization of a novel sequencing device," *Nano letters*, vol. 10, no. 9, pp. 3237-3242, 2010.
- [50] Z. Yuan, C. Wang, X. Yi, Z. Ni, Y. Chen, and T. Li, "Solid-State Nanopore," *Nanoscale research letters*, vol. 13, no. 1, p. 56, 2018.
- [51] Y. Qiu, C. Arcadia, M. A. Alibakhshi, J. Rosenstein, and M. Wanunu, "Nanopore Fabrication in Ultrathin HFO2 Membranes for Nanopore-Based DNA Sequencing," *Biophysical Journal*, vol. 114, no. 3, p. 179a, 2018.
- [52] H. Hoi *et al.*, "Biofunctionalized silicon nitride platform for sensing applications," *Biosensors and Bioelectronics*, vol. 102, pp. 497-503, 2018.
- [53] G. F. Schneider and C. Dekker, "DNA sequencing with nanopores," *Nature biotechnology*, vol. 30, no. 4, p. 326, 2012.
- [54] S. K. Min, W. Y. Kim, Y. Cho, and K. S. Kim, "Fast DNA sequencing with a graphene-based nanochannel device," *Nature nanotechnology*, vol. 6, no. 3, p. 162, 2011.
- [55] E. C. Yusko *et al.*, "Controlling protein translocation through nanopores with bio-inspired fluid walls," *Nature nanotechnology*, vol. 6, no. 4, p. 253, 2011.
- [56] V. Mussi *et al.*, "Electrical characterization of DNA-functionalized solid state nanopores for bio-sensing," *Journal of Physics: Condensed Matter*, vol. 22, no. 45, p. 454104, 2010.
- [57] S. W. Kowalczyk, T. R. Blosser, and C. Dekker, "Biomimetic nanopores: learning from and about nature," *Trends in biotechnology*, vol. 29, no. 12, pp. 607-614, 2011.

- [58] M. Wanunu, T. Dadosh, V. Ray, J. Jin, L. McReynolds, and M. Drndić, "Rapid electronic detection of probe-specific microRNAs using thin nanopore sensors," *Nature nanotechnology*, vol. 5, no. 11, p. 807, 2010.
- [59] X. Zhang, Y. Wang, B. L. Fricke, and L.-Q. Gu, "Programming nanopore ion flow for encoded multiplex microRNA detection," *ACS nano*, vol. 8, no. 4, pp. 3444-3450, 2014.
- [60] R. Wei, V. Gatterdam, R. Wieneke, R. Tampé, and U. Rant, "Stochastic sensing of proteins with receptor-modified solid-state nanopores," *Nature nanotechnology*, vol. 7, no. 4, p. 257, 2012.
- [61] D. S. Talaga and J. Li, "Single-molecule protein unfolding in solid state nanopores," *Journal of the American Chemical Society*, vol. 131, no. 26, pp. 9287-9297, 2009.
- [62] Q. Wei *et al.*, "Nanoporous gold film based immunosensor for label-free detection of cancer biomarker," *Biosensors and Bioelectronics*, vol. 26, no. 8, pp. 3714-3718, 2011.
- [63] B. M. Venkatesan and R. Bashir, "Nanopore sensors for nucleic acid analysis," *Nature nanotechnology*, vol. 6, no. 10, p. 615, 2011.
- [64] W. Ali *et al.*, "Differentiation of Specific Cancer Biomarkers with Solid-state Nanopores."
- [65] H. Wu *et al.*, "Translocation of rigid rod-shaped virus through various solid-state nanopores," *Analytical chemistry*, vol. 88, no. 4, pp. 2502-2510, 2016.
- [66] J. D. Uram, K. Ke, A. J. Hunt, and M. Mayer, "Submicrometer Pore-Based Characterization and Quantification of Antibody–Virus Interactions," *Small*, vol. 2, no. 8-9, pp. 967-972, 2006.
- [67] P. Guo, E. W. Hall, R. Schirhagl, H. Mukaibo, C. R. Martin, and R. N. Zare, "Microfluidic capture and release of bacteria in a conical nanopore array," *Lab on a Chip*, vol. 12, no. 3, pp. 558-561, 2012.
- [68] S. L. Murphy, J. Xu, and K. D. Kochanek, "Deaths: Final Data for 2010," *National Vital Statistics Reports*, vol. 61, no. 4, pp. 1-118, 2013.
- [69] S. M. Iqbal, D. Akin, and R. Bashir, "Solid-State Nanopore Channels with DNA Selectivity," *Nature Nanotechnology*, vol. 2, no. 4, pp. 243-248, 2007.
- [70] H. He *et al.*, "Functionalized Nanopore-Embedded Electrodes for Rapid DNA Sequencing," *The Journal of Physical Chemistry (C)*, vol. 112, no. 10, pp. 3456-3459, 2008.
- [71] T. Osaki, H. Suzuki, B. Le Pioufle, and S. Takeuchi, "Multichannel Simultaneous Measurements of Single-Molecule Translocation in α -Hemolysin Nanopore Array," *Analytical Chemistry*, vol. 81, no. 24, pp. 9866-9870, 2009.
- [72] L. Song, M. R. Hobaugh, C. Shustak, S. Cheley, H. Bayley, and J. E. Gouaux, "Structure of Staphylococcal Alpha-Hemolysin, A Heptameric Transmembrane Pore," (in eng), *Science*, vol. 274, no. 5294, pp. 1859-66, Dec 13 1996.
- [73] G. Maglia, M. R. Restrepo, E. Mikhailova, and H. Bayley, "Enhanced translocation of single DNA molecules through α -hemolysin nanopores by manipulation of internal charge," *Proceedings of the National Academy of Sciences*, vol. 105, no. 50, pp. 19720-19725, 2008.

- [74] J. Li, D. Stein, C. McMullan, D. Branton, M. J. Aziz, and J. A. Golovchenko, "Ion-beam sculpting at nanometre length scales," *Nature*, vol. 412, no. 6843, pp. 166-169, 2001.
- [75] S. Garaj, W. Hubbard, A. Reina, J. Kong, D. Branton, and J. Golovchenko, "Graphene as a subnanometre trans-electrode membrane," *Nature*, vol. 467, no. 7312, p. 190, 2010.
- [76] Z. S. Siwy and M. Davenport, "Nanopores: Graphene opens up to DNA," *Nature Nanotechnology*, vol. 5, no. 10, pp. 697-698, 2010.
- [77] F. Haque, J. Li, H.-C. Wu, X.-J. Liang, and P. Guo, "Solid-state and biological nanopore for real-time sensing of single chemical and sequencing of DNA," *Nano Today*, vol. 8, no. 1, pp. 56-74, 2013.
- [78] G. Maglia, A. J. Heron, D. Stoddart, D. Japrun, and H. Bayley, "Analysis of single nucleic acid molecules with protein nanopores," *Methods in Enzymology*, vol. 475, pp. 591-623, 2010.
- [79] S. Howorka and Z. Siwy, "Nanopore analytics: sensing of single molecules," *Chemical Society Reviews*, vol. 38, no. 8, pp. 2360-2384, 2009.
- [80] R. Wei, T. G. Martin, U. Rant, and H. Dietz, "DNA Origami Gatekeepers for Solid-State Nanopores," *Angewandte Chemie*, vol. 124, no. 20, pp. 4948-4951, 2012.
- [81] Y. Li, H.-H. Yang, Q.-H. You, Z.-X. Zhuang, and X.-R. Wang, "Protein recognition via surface molecularly imprinted polymer nanowires," *Analytical Chemistry*, vol. 78, no. 1, pp. 317-320, 2006.
- [82] J.-R. Ku and P. Stroeve, "Protein diffusion in charged nanotubes: "On-Off" behavior of molecular transport," *Langmuir*, vol. 20, no. 5, pp. 2030-2032, 2004.
- [83] A. Meller, L. Nivon, and D. Branton, "Voltage-driven DNA translocations through a nanopore," *Physical Review Letters*, vol. 86, no. 15, p. 3435, 2001.
- [84] E. C. Yusko *et al.*, "Controlling protein translocation through nanopores with bio-inspired fluid walls," *Nature Nanotechnology*, 10.1038/nnano.2011.12 vol. 6, no. 4, pp. 253-260, 04//print 2011.
- [85] M. A. I. Mahmood, W. Ali, A. Adnan, and S. M. Iqbal, "3D Structural Integrity and Interactions of Single-stranded Protein-binding DNA in a Functionalized Nanopore," *The Journal of Physical Chemistry B*, vol. 118, no. 22, pp. 5799-5806, 2014.
- [86] D. Wang *et al.*, "Fabrication of sub-20 nm Nanopore Arrays in Membranes with Embedded Metal Electrodes at Wafer Scales," *Nanoscale*, 10.1039/C3NR06723H 2014.
- [87] D. Branton *et al.*, "The potential and challenges of nanopore sequencing," *Nature Biotechnology*, vol. 26, no. 10, pp. 1146-1153, 2008.
- [88] L. Movileanu, "Interrogating single proteins through nanopores: challenges and opportunities," *Trends in Biotechnology*, vol. 27, no. 6, pp. 333-341, 2009.
- [89] (2015, Oct 30). *Potassium Chloride* SID=24881796. Available: <https://pubchem.ncbi.nlm.nih.gov/substance/24881796>

- [90] W. Asghar, A. Ilyas, R. R. Deshmukh, S. Sumitsawan, R. B. Timmons, and S. M. Iqbal, "Pulsed plasma polymerization for controlling shrinkage and surface composition of nanopores," *Nanotechnology*, vol. 22, no. 28, p. 285304, 2011.
- [91] W. Shi, A. K. Friedman, and L. A. Baker, "Nanopore sensing," *Analytical chemistry*, vol. 89, no. 1, pp. 157-188, 2016.
- [92] T. Z. Butler, M. Pavlenok, I. M. Derrington, M. Niederweis, and J. H. Gundlach, "Single-molecule DNA detection with an engineered MspA protein nanopore," *Proceedings of the National Academy of Sciences*, vol. 105, no. 52, pp. 20647-20652, 2008.
- [93] C. C. Harrell, Y. Choi, L. P. Horne, L. A. Baker, Z. S. Siwy, and C. R. Martin, "Resistive-pulse DNA detection with a conical nanopore sensor," *Langmuir*, vol. 22, no. 25, pp. 10837-10843, 2006.
- [94] D. Fologea, M. Gershow, B. Ledden, D. S. McNabb, J. A. Golovchenko, and J. Li, "Detecting single stranded DNA with a solid state nanopore," *Nano letters*, vol. 5, no. 10, pp. 1905-1909, 2005.
- [95] S. M. Iqbal, D. Akin, and R. Bashir, "Solid-state nanopore channels with DNA selectivity," *Nature nanotechnology*, vol. 2, no. 4, p. 243, 2007.
- [96] M. R. Hasan, M. A. I. Mahmood, R. R. Khanzada, N. Mansur, A. Adnan, and S. M. Iqbale, "Molecular Dynamics Study of Protein Deformation through Solid-State Nanopore."
- [97] M. S. Khan, N. S. Dosoky, G. Mustafa, D. Patel, B. Berdiev, and J. D. Williams, "Electrophysiology of Epithelial Sodium Channel (ENaC) Embedded in Supported Lipid Bilayer Using a Single Nanopore Chip," *Langmuir*, vol. 33, no. 47, pp. 13680-13688, 2017/11/28 2017.
- [98] I. Nir, D. Huttner, and A. Meller, "Direct sensing and discrimination among Ubiquitin and Ubiquitin chains using solid-state nanopores," *Biophysical journal*, vol. 108, no. 9, pp. 2340-2349, 2015.
- [99] N. Varongchayakul, D. Huttner, M. W. Grinstaff, and A. Meller, "Sensing Native Protein Solution Structures Using a Solid-state Nanopore: Unraveling the States of VEGF," *Scientific reports*, vol. 8, no. 1, p. 1017, 2018.
- [100] K. J. Freedman, S. R. Haq, J. B. Edel, P. Jemth, and M. J. Kim, "Single molecule unfolding and stretching of protein domains inside a solid-state nanopore by electric field," *Scientific reports*, vol. 3, p. 1638, 2013.
- [101] D. Japrun *et al.*, "Single-molecule studies of intrinsically disordered proteins using solid-state nanopores," *Analytical chemistry*, vol. 85, no. 4, pp. 2449-2456, 2013.
- [102] L.-Q. Gu, M. Wanunu, M. X. Wang, L. McReynolds, and Y. Wang, "Detection of miRNAs with a nanopore single-molecule counter," *Expert review of molecular diagnostics*, vol. 12, no. 6, pp. 573-584, 2012.
- [103] O. K. Zahid, F. Wang, J. A. Ruzicka, E. W. Taylor, and A. R. Hall, "Sequence-specific recognition of microRNAs and other short nucleic acids with solid-state nanopores," *Nano letters*, vol. 16, no. 3, pp. 2033-2039, 2016.
- [104] D. Deamer, M. Akeson, and D. Branton, "Three decades of nanopore sequencing," *Nature biotechnology*, vol. 34, no. 5, p. 518, 2016.

- [105] L. Steinbock and A. Radenovic, "The emergence of nanopores in next-generation sequencing," *Nanotechnology*, vol. 26, no. 7, p. 074003, 2015.
- [106] M. S. Khan, N. S. Dosoky, B. K. Berdiev, and J. D. Williams, "Electrochemical impedance spectroscopy for black lipid membranes fused with channel protein supported on solid-state nanopore," *European Biophysics Journal*, journal article vol. 45, no. 8, pp. 843-852, December 01 2016.
- [107] E. A. Manrao *et al.*, "Reading DNA at single-nucleotide resolution with a mutant MspA nanopore and phi29 DNA polymerase," *Nature biotechnology*, vol. 30, no. 4, p. 349, 2012.
- [108] J. Li, D. Stein, C. McMullan, D. Branton, M. J. Aziz, and J. A. Golovchenko, "Ion-beam sculpting at nanometre length scales," *Nature*, vol. 412, no. 6843, p. 166, 2001.
- [109] C. J. Lo, T. Aref, and A. Bezryadin, "Fabrication of symmetric sub-5 nm nanopores using focused ion and electron beams," *Nanotechnology*, vol. 17, no. 13, p. 3264, 2006.
- [110] J. Gierak *et al.*, "Exploration of the ultimate patterning potential achievable with high resolution focused ion beams," *Applied Physics A*, vol. 80, no. 1, pp. 187-194, 2005.
- [111] D. Emmrich *et al.*, "Nanopore fabrication and characterization by helium ion microscopy," *Applied Physics Letters*, vol. 108, no. 16, p. 163103, 2016.
- [112] M. U. Raza, S. Saleem, W. Ali, and S. M. Iqbal, "Crosstalk between adjacent nanopores in a solid-state membrane array for multi-analyte high-throughput biomolecule detection," *Journal of Applied Physics*, vol. 120, no. 6, p. 064701, 2016.
- [113] T. Gilboa and A. Meller, "Optical sensing and analyte manipulation in solid-state nanopores," *Analyst*, vol. 140, no. 14, pp. 4733-4747, 2015.
- [114] A. P. Ivanov *et al.*, "DNA tunneling detector embedded in a nanopore," *Nano letters*, vol. 11, no. 1, pp. 279-285, 2010.
- [115] U. F. Keyser *et al.*, "Direct force measurements on DNA in a solid-state nanopore," *Nature Physics*, vol. 2, no. 7, p. 473, 2006.
- [116] U. Keyser, J. Van der Does, C. Dekker, and N. Dekker, "Optical tweezers for force measurements on DNA in nanopores," *Review of Scientific Instruments*, vol. 77, no. 10, p. 105105, 2006.
- [117] N. Di Fiori, A. Squires, D. Bar, T. Gilboa, T. D. Moustakas, and A. Meller, "Optoelectronic control of surface charge and translocation dynamics in solid-state nanopores," *Nature nanotechnology*, vol. 8, no. 12, p. 946, 2013.
- [118] F. Nicoli, D. Verschueren, M. Klein, C. Dekker, and M. P. Jonsson, "DNA translocations through solid-state plasmonic nanopores," *Nano letters*, vol. 14, no. 12, pp. 6917-6925, 2014.
- [119] Y. Li *et al.*, "Photoresistance switching of plasmonic nanopores," *Nano letters*, vol. 15, no. 1, pp. 776-782, 2014.
- [120] O. N. Assad, T. Gilboa, J. Spitzberg, M. Juhasz, E. Weinhold, and A. Meller, "Light-Enhancing Plasmonic-Nanopore Biosensor for Superior Single-Molecule Detection," *Advanced Materials*, vol. 29, no. 9, 2017.

- [121] M. L. Juan, R. Gordon, Y. Pang, F. Eftekhari, and R. Quidant, "Self-induced back-action optical trapping of dielectric nanoparticles," *Nature Physics*, vol. 5, no. 12, p. 915, 2009.
- [122] A. A. Al Balushi, A. Kotnala, S. Wheaton, R. M. Gelfand, Y. Rajashekara, and R. Gordon, "Label-free free-solution nanoaperture optical tweezers for single molecule protein studies," *Analyst*, vol. 140, no. 14, pp. 4760-4778, 2015.
- [123] L. K. S. Kumar and R. Gordon, "Overlapping double-hole nanostructure in a metal film for localized field enhancement," *IEEE Journal of selected topics in quantum electronics*, vol. 12, no. 6, pp. 1228-1232, 2006.
- [124] L. Kumar, A. Lesuffleur, M. Hughes, and R. Gordon, "Double nanohole apex-enhanced transmission in metal films," *Applied Physics B*, vol. 84, no. 1-2, p. 25, 2006.
- [125] M. Ghorbanzadeh, S. Jones, M. K. Moravvej-Farshi, and R. Gordon, "Improvement of Sensing and Trapping Efficiency of Double Nanohole Apertures via Enhancing the Wedge Plasmon Polariton Modes with Tapered Cusps," *ACS Photonics*, vol. 4, no. 5, pp. 1108-1113, 2017.
- [126] P. Mestres, J. Berthelot, S. S. Aćimović, and R. Quidant, "Unraveling the optomechanical nature of plasmonic trapping," *Light: Science & Applications*, vol. 5, no. 7, p. e16092, 2016.
- [127] Y. Pang and R. Gordon, "Optical trapping of 12 nm dielectric spheres using double-nanoholes in a gold film," *Nano letters*, vol. 11, no. 9, pp. 3763-3767, 2011.
- [128] A. Kotnala, D. DePaoli, and R. Gordon, "Sensing nanoparticles using a double nanohole optical trap," *Lab on a Chip*, vol. 13, no. 20, pp. 4142-4146, 2013.
- [129] A. Kotnala and R. Gordon, "Quantification of high-efficiency trapping of nanoparticles in a double nanohole optical tweezer," *Nano letters*, vol. 14, no. 2, pp. 853-856, 2014.
- [130] Y. Pang and R. Gordon, "Optical trapping of a single protein," *Nano letters*, vol. 12, no. 1, pp. 402-406, 2011.
- [131] A. A. Al Balushi, A. Zehtabi-Oskuie, and R. Gordon, "Observing single protein binding by optical transmission through a double nanohole aperture in a metal film," *Biomedical optics express*, vol. 4, no. 9, pp. 1504-1511, 2013.
- [132] A. A. Al Balushi and R. Gordon, "Label-free free-solution single-molecule protein–small molecule interaction observed by double-nanohole plasmonic trapping," *ACS Photonics*, vol. 1, no. 5, pp. 389-393, 2014.
- [133] A. A. Al Balushi and R. Gordon, "A label-free untethered approach to single-molecule protein binding kinetics," *Nano letters*, vol. 14, no. 10, pp. 5787-5791, 2014.
- [134] S. Wheaton and R. Gordon, "Molecular weight characterization of single globular proteins using optical nanotweezers," *Analyst*, vol. 140, no. 14, pp. 4799-4803, 2015.
- [135] W.-J. Lan, D. A. Holden, B. Zhang, and H. S. White, "Nanoparticle transport in conical-shaped nanopores," *Analytical chemistry*, vol. 83, no. 10, pp. 3840-3847, 2011.
- [136] W. Guan, S. X. Li, and M. A. Reed, "Voltage gated ion and molecule transport in engineered nanochannels: theory, fabrication and applications," *Nanotechnology*, vol. 25, no. 12, p. 122001, 2014.

- [137] N. Arjmandi, W. Van Roy, L. Lagae, and G. Borghs, "Measuring the electric charge and zeta potential of nanometer-sized objects using pyramidal-shaped nanopores," *Analytical chemistry*, vol. 84, no. 20, pp. 8490-8496, 2012.
- [138] K.-M. Kim *et al.*, "Surface treatment of silica nanoparticles for stable and charge-controlled colloidal silica," *International journal of nanomedicine*, vol. 9, no. Suppl 2, p. 29, 2014.
- [139] S. Bhattacharjee, "DLS and zeta potential—What they are and what they are not?," *Journal of Controlled Release*, vol. 235, pp. 337-351, 2016.

2. DIFFERENTIATION OF SPECIFIC CANCER BIOMARKERS WITH SOLID STATE NANOPORES

Reprinted (adapted) with permission from (Waqas Ali, Muhammad Raza, Mohammed Mahmood, Peter Allen, Adam Hall, Yuan Wan, and Samir Iqbal. Specific Differentiation of Cancer Biomarkers with Solid-state Nanopores. *Functional Nanostructures*. 1, no. 1 (2016): 26-34.

Copyright 2016 © One Central Press

DIFFERENTIATION OF SPECIFIC CANCER BIOMARKERS WITH SOLID-STATE NANOPORES

Waqas Ali^{1,2,3,a}, Mohammed Arif I. Mahmood^{1,2,3,b}, Peter B. Allen^{4,c}, Adam R. Hall^{5,d}, Yuan
Wan^{6,7,e}, Muhammad Usman Raza^{1,2,3,f} and Samir M. Iqbal^{1,2,3,8,9,g*}

¹Nano-Bio Lab, ²Department of Electrical Engineering, ³Nanotechnology Research Center, University of Texas at Arlington, Arlington, TX 76019, USA; ⁴Department of Chemistry, University of Idaho, Moscow, ID 83844, USA; ⁵Virginia Tech-Wake Forest School of Biomedical Engineering and Sciences, Wake Forest University School of Medicine, Winston Salem, NC 27101, USA; ⁶Ian Wark Research Institute, University of South Australia, Adelaide, South Australia 5095, Australia; ⁷PMR Institute, Shanghai, China 201203; ⁸Department of Bioengineering, University of Texas at Arlington, Arlington, TX 76019, USA; ⁹Department of Urology, University of Texas Southwestern Medical Center at Dallas, TX 75390, USA.

^awaqas.ali@mavs.uta.edu, ^barif.iftakher@gmail.com, ^cpballen@gmail.com,
^darhall@wakehealth.edu, ^emastermg@163.com, ^fraza.muhammadusman@mavs.uta.edu,
^gsmiqbal@uta.edu

Keywords: Nanopore, Biosensor, Single Molecule Detection, EGFR, Point-of-care, Cancer Diagnosis, Early Detection.

Abstract

Epidermal growth factor receptor (EGFR) is well known as an early biomarker for many cancer types. The current methods for EGFR detection lack the sensitivity and selectivity required to efficiently detect and differentiate EGFR from other proteins. We demonstrate a nanopore-based resistive pulse-sensing technique to selectively detect small amounts of EGFR from a mixture. An anti-EGFR aptamer is used to impart selectivity in the sample solution. The shift in translocation dwell time of samples both with and without a bound anti-EGFR aptamer is used to detect EGFR. EGFR with the bound aptamer results in a translocation dwell time that is about 23% shorter than that of EGFR alone, indicating a greater net charge for the complex. Thrombin is used as a control to demonstrate that the high specificity of the aptamer for EGFR enables differentiation of similar-sized proteins. The use of anti-EGFR aptamer as a targeting agent makes the label free detection of EGFR possible without nanopore surface modification or functionalization.

Introduction

EGFR detection and enumeration promises early cancer detection [1, 2] and the ability to monitor therapy and prognosis [3-5]. Elevated levels of EGFR expression in patients' serum is a strong prognostic indicator for many tumor types [6-8]. For example, Quaranta *et al.* reported the mean EGFR level in brain cancer patients' sera to be nearly twice than that of healthy subjects [9]. The total concentration of EGFR in patient serum is very small (ng/ml) and can be easily obscured by the biological noise. These facts highlight two major challenges in detection of EGFR expression levels in patients' serum: first, a useful biosensor should have molecular level sensitivity and second, it should have very high specificity. In last couple of decades, a variety of detection assays for proteins have been developed using fluorescence, electrochemical, colorimetric, chemiluminescence and surface plasmon resonance means [3, 10]. These assays lack the sensitivity and specificity required for the efficient detection of physiologically relevant EGFR levels.

Development of new approaches for point-of-care (POC) detection of protein biomarkers is a pressing need in early cancer diagnosis. Devices for POC must be ultrasensitive, fast, accurate, low priced and should be easy to use [11]. One candidate technology that has recently emerged as a potent single molecule detector is the solid- state nanopore [12-17] based on the resistive-pulse enumeration. When a molecule hinders the ionic flow through the nanopore, it registers a unique electrical pulse in the baseline ionic current trace. Analysis of these electrical pulses can be used to determine size and charge of molecules [12], length of nucleic acids [14, 18], protein size [19, 20], folding state [20, 21] and molecular agglomeration [22]. They can also be chemically modified [15, 23] for detection of specific biomarkers [17, 24] and toxic agents [25, 26].

Biological nanopores are unstable and their measurement setup is tedious due to their small fixed diameter (1.5 – 3.6 nm); only polypeptides or denatured proteins are able to translocate there [27, 28]. Moreover, preparation of large-scale protein nanopore arrays faces technical challenges [12]. On the contrary, solid-state nanopores are compatible with proteins of any conformation and size due to the tunable dimensions. These have been successfully used to detect proteins of various sizes and stochastic

sensing of proteins [14]. The current approaches have some disadvantages. First, single-ligands functionalized nanopore can only detect one type of target protein; proteins not recognized by ligands are not detected at all. If several proteins need to be simultaneously identified, different kinds of ligands should be respectively immobilized on separate nanopores [29, 30]. This means multiple copies of samples and multiple sets of nanopore frameworks need to be prepared for signal collection, analysis and calibration. Although technically feasible, such strategies for multiplexed protein detection require tremendous workload and would be unreliable from the noise and system artifacts. In addition, due to different sizes of proteins, the nanopore diameter would need to be precisely tuned in order to accommodate each analyte. If the proteins of interest have broad ranges of size that would be another challenge to decide on nanopores with suitable diameters. Another challenge is the immobilization of the specific ligands onto the inner edge of the nanopore. Surface functionalization at such small size scales is not trivial and is expected to result in insufficient immobilization sites and heterogeneous grafting especially when irregular surfaces result into various charge distribution and variations in the nanopore stoichiometry [12, 29, 30]. An ideal solid-state nanopore system should be able to simultaneously and quickly identify target proteins in a multiplexed fashion from a single miniscule sample. Such detection should be performed, from initial system setup to final data report, on one framework.

This letter reports solid-state nanopores as single-molecule sensors [31-33] for detection and enumeration of EGFR in POC setting. To keep the process simple, instead of using a functionalized nanopore [34], a bare nanopore was used and in- solution binding of EGFR with anti-EGFR aptamer was used to impart selectivity [35]. Anti-EGFR aptamer has very high affinity for EGFR and it is very selective as well [36]. Aptamer binding to the protein altered the overall charge and mass of the complex as compared to the unbound EGFR [37]. Since the speed of the translocating species strongly depended upon its charge [38-40], attachment with aptamer tweaked the translocation time for EGFR only. This change was readily identified from the analysis of registered pulses. As a negative control, the experiments were done with human α - thrombin protein. With thrombin, no change was observed in the translocation time after incubating the protein with the aptamer.

Results and Discussion

Current-voltage (I-V) characteristics of the nanopore in 20 mM Tris-acetate pH 8.2 + 5 mM Mg-acetate + 1 mM K-acetate are shown in Figure 1(b). Conductance of the nanopore was calculated to be 2.5 nS by a linear fit to the data. For the voltage range of -100 mV to 100 mV, linear I-V characteristics were observed [41, 42]. Open pore current for the nanopore at 50 mV applied bias is shown in Figure 2(a).

EGFR was introduced into the *cis* (negative) side of the nanopore that resulted in significant current blockage events. A snapshot of the nanopore current trace at 50 mV is shown in Figure 2(c). These pulses are for EGFR translocation measured in 10sec. Very uniform current pulses were observed in terms of translocation time and peak amplitude. EGFR translocation through the nanopore registered characteristic current pulses with average peak amplitude of 0.9 ± 0.21 nA and average translocation time of 80 ± 4.06 μ s (Table 1). Only one population of events was observed for the peak amplitude *versus* the translocation time for EGFR translocation through nanopore at 50 mV as shown in Figure 2(d).

TABLE 1. Pulse Statistics for Unbound EGFR & EGFR-aptamer Complex

Translocating Species	Translocation Time [μ s]	Peak Amplitude [nA]
EGFR (Unbound)	80 ± 4.06	$0. \pm 0.21$
EGFR-aptamer Complex	62 ± 5.24	1.1 ± 0.18

In the next set of experiments, again EGFR was introduced into the *cis* side of the nanopore for translocation but this time sample was incubated with anti-EGFR aptamer for a certain period under conditions mentioned in the experimental section. This time again significant current blockage events were observed. But, in contrast to the previous observations, there were two distinct types of pulses (Figure 3(a)). The two types of pulses were not very different in terms of their peak amplitudes but they were remarkably different in terms of their translocation times. The two types were different from each other by 22.5% with respect to their average translocation times and 18.2% in terms of their average

peak amplitudes.

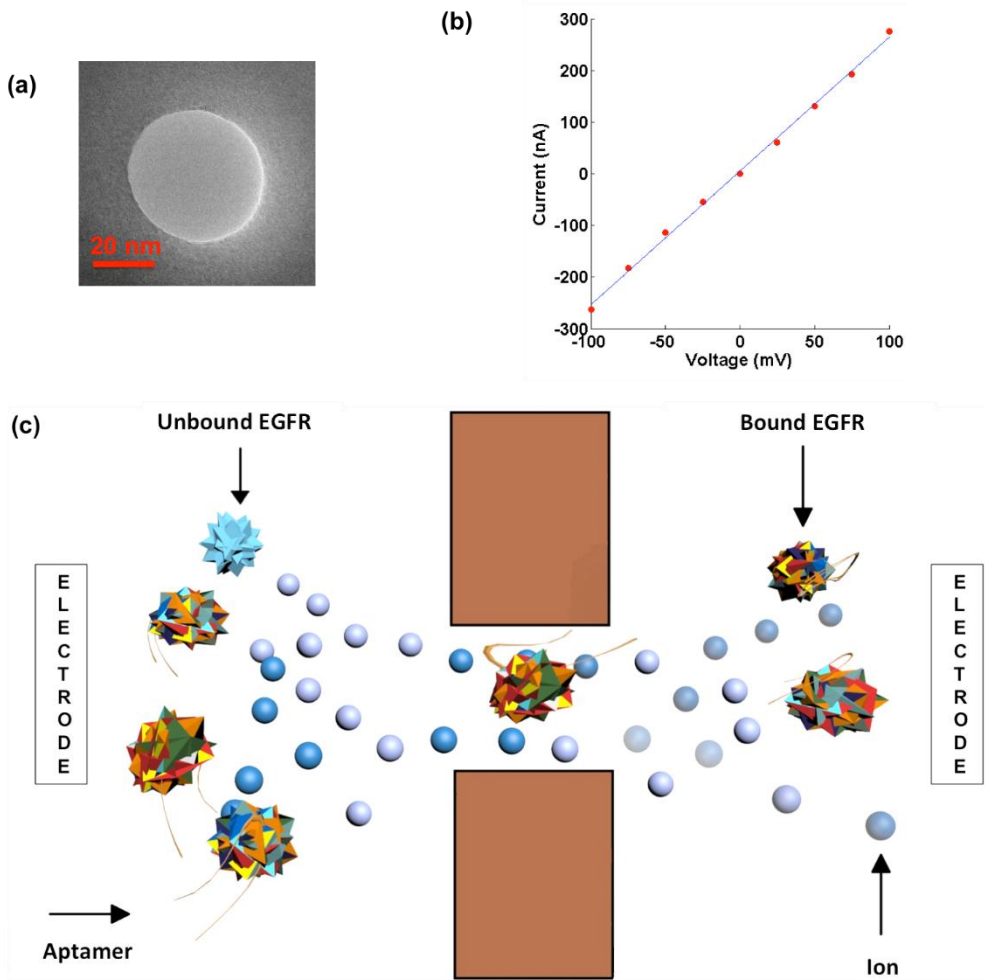


Figure 1. Nanopore for EGFR translocation experiments. (a) TEM image of a 40 nm diameter solid-state nanopore fabricated in 40 nm thick freestanding SiN membrane drilled with focused electron beam from TEM. (b) Linear I-V characteristics for the nanopore show 2.5 μ S conductivity. (c) Incubating EGFR with aptamer allows them to bind with EGFR molecules and form the complex. Complex due to their higher charge and slightly larger excluded volume than unbound EGFR cause electrical pulses that are wider and deeper as compared to those registered by unbound EGFR.

One of the two types of pulses were exactly similar (i.e. same translocation time and peak amplitude) to those that were observed for EGFR translocation without incubation with the aptamer. The second type of pulses had shorter widths i.e. higher translocation speed, and larger peak amplitudes i.e. more pore blockage, when compared to those for pulses associated with EGFR translocation without incubation with the aptamer. The second type of pulses, characterized by faster translocation speed and more pore blockage, stemmed from the translocation of the complex.

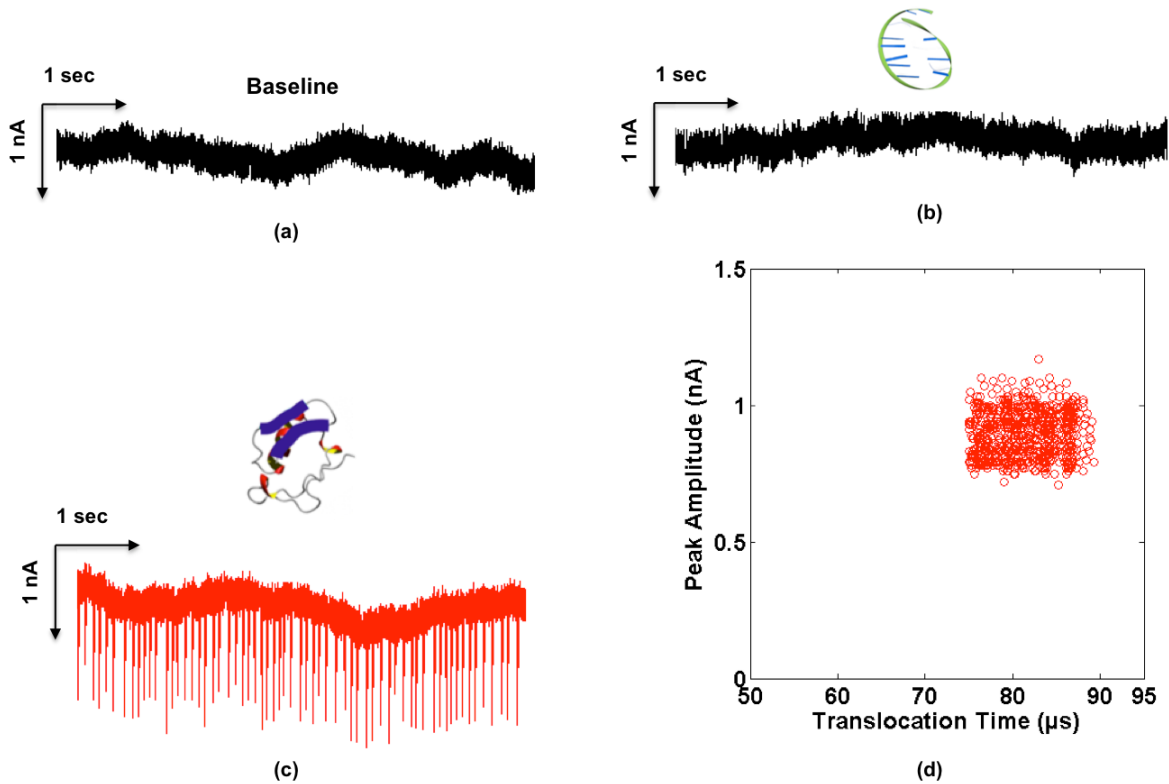
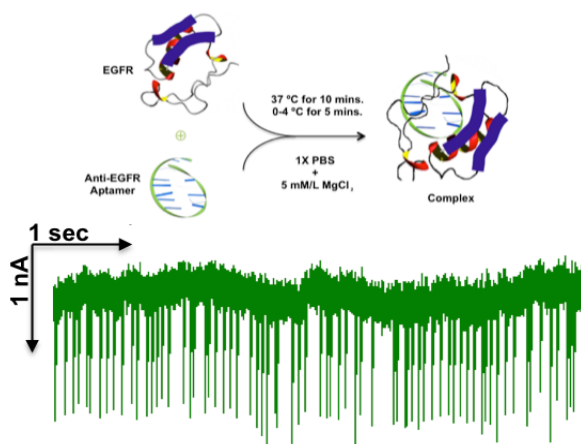


Figure 2. Snapshots of the nanopore current for 10 seconds duration for (a) Baseline, translocation of (b) Anti-EGFR aptamer (unbound only) (c) EGFR (unbound only) and (d) Scatter plot of the translocation time versus peak amplitude of the registered pulses for EGFR translocation through 40 nm nanopore at 50 mV. The registered pulses for EGFR translocation are consistent and form only one cluster of event population on the plot.

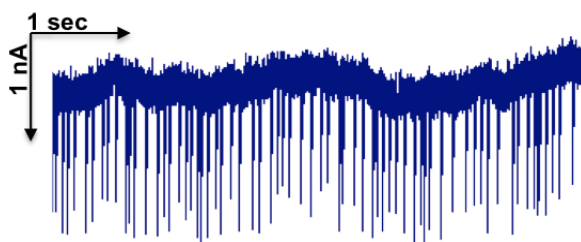
The complex translocation through a 40 nm wide and 40 nm thick solid-state nanopore under an applied voltage of 50 mV registered pulses with average peak amplitude of 1.1 ± 0.18 nA and

average translocation time of $62 \pm 5.24 \mu\text{s}$. The presence of two distinct types of populations can be clearly seen in Figure 3(d). Another important point to notice from this scatter plot is that the events frequency is not the same for the two types of pulses. There are much more events of EGFR translocation as compared to that of complex translocation. One plausible reason for that could be the abundance of unbound EGFR as compared to the EGFR-aptamer complex. To systematically prove this hypothesis, a titration series was conducted in which the molar concentration of EGFR was kept constant and the molar concentration of anti-EGFR aptamer was gradually increased. Figures 3(b) and 3(c) show the 10 sec current traces when EGFR was incubated with $4 \mu\text{M}$ and $10 \mu\text{M}$ anti-EGFR aptamer, respectively. For each case, blockage events are plotted on a scatter plot of translocation time *versus* peak amplitude (Figure 3(e) and 3(f)). A gradual increase in the event frequency for complex translocation was observed as the molar concentration of aptamer increased. The effect was opposite on the event frequency of EGFR translocation. It kept on decreasing. This shifting signal from event population of EGFR to that of complex, with the increase in aptamer concentration, indicates that more EGFR molecules were binding to aptamer as the aptamer concentration increased. So, for the first experiment with the complex translocation, there were plenty of unbound EGFR molecules present in the sample (Figure 3(d)) that reduced as the aptamer concentration increased and ultimately very few unbound EGFR molecules were left (Figure 3(f)). This is when most of the EGFR molecules were bound to the aptamer forming the complex. One might think that the second type of events can be associated with the translocation of free floating anti-EGFR aptamer in the solution. To rule this out, another experiment was carried out to record pulses for the translocation of anti-EGFR aptamer alone through the same nanopore. For this purpose, anti-EGFR aptamer was introduced into the *cis* side of the nanopore and this time no current blockage events were observed. There can be multiple reasons for that but one of the strongest reasons is that a 40 nm nanopore is probably too large to detect the translocation of aptamer (few nanometers in size [43, 44]) because for nanopore based detection scheme, nanopore size should be close to the size of the target [12, 13, 15]. In that case, even if aptamer would be indeed translocating through the nanopore but due to their much smaller size than the pore they are unlikely to block current and hence not registering any pulse, as was observed in these experiments. Another possibility can be that the charge on the aptamer is much smaller than the overall



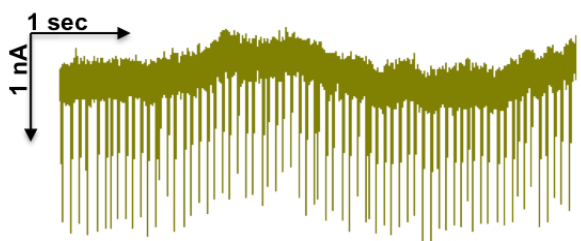
EGFR & Aptamer (3 pM : 0.5 μ M)

(a)



EGFR & Aptamer (3 pM : 4 μ M)

(b)



EGFR & Aptamer (3 pM : 10 μ M)

(c)

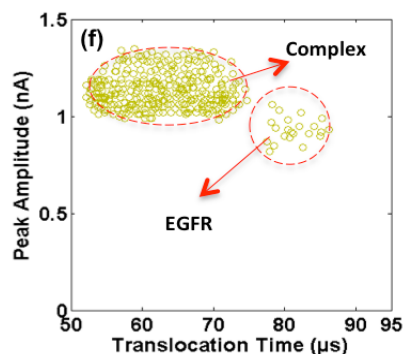
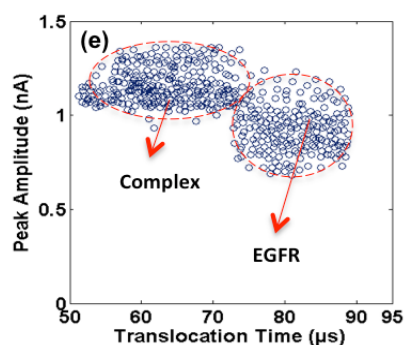
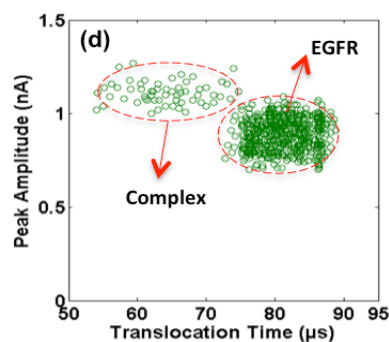


Figure 3: Snapshots of the ionic current trace for 10 seconds of the EGFR (3 pM) translocation when incubated with aptamer at (a) 0.5 μ M (b) 4 μ M and (c) 10 μ M. The scatter plots show the translocation behavior of EGFR (3 pM) when incubated with aptamer at (d) 0.5 μ M (e) 4 μ M and (f) 10 μ M. Two populations are visible: One with higher dwell time corresponds to the translocation of unbound EGFR, and second with shorter dwell time corresponds to complex's translocation.

charge of the protein. So even if 50 mV is enough to exert sufficient electrophoretic force on the protein

to translocate through the nanopore, it might not be sufficient to push aptamer alone through it due to their small charge. In that case, aptamer will not even be going through the nanopore at all and hence there will be no pulse. Though this is a less likely case but can't be ruled out completely. In any case, the point here is that, out of the two types of events that were observed for the translocation of EGFR after incubating it with aptamer, one was due to the translocation of EGFR alone and the other was due to the translocation of complex and not the free-floating aptamer.

Finally, to check the specificity of this assay, experiment was repeated with human α - thrombin protein instead of EGFR. First, thrombin was translocated through a 40 nm wide and 40 nm thick nanopore at 50 mV. Figure 4(a) shows the current trace for thrombin translocation for 10s duration. The average translocation time and average peak amplitude of the registered pulses from thrombin translocation were determined to be $68 \pm 3.17 \mu\text{s}$ and $0.5 \pm 0.15 \text{ nA}$, respectively. Thrombin ($8 \mu\text{l}$, $50 \text{ ng}/\mu\text{l}$) was then incubated with anti-EGFR aptamer ($10 \mu\text{M}$) and sample was run through the same nanopore at 50 mV. This time again, only one type of pulse was observed that was exact replica of those observed for thrombin without incubation with aptamer. The nanopore current trace for thrombin translocation after incubation with aptamer is shown in Figure 4(b). Figures 4(c) and 4(d) show the population regions of the events recorded by the translocation of unbound thrombin and thrombin-aptamer complex (i.e. after incubation with aptamer), respectively, on translocation time *versus* peak amplitude plot.

The two populations are exactly same indicating that thrombin translocation profile remained same before and after incubation with aptamer. This is because no aptamer attached to thrombin and the assay was highly selective for EGFR protein. Incubating thrombin with aptamer did not affect their translocation profile since aptamer did not attach to thrombin and no thrombin-aptamer complexes were formed.

The dynamics of protein translocation, in general, through bare as well as chemically-modified solid-state nanopores and the forces involved in this process have already been explored through simulations and experiments [14, 21, 34, 37, 45-48]. EGFR translocation through the nanopore is not different from other proteins. At a pH of 8.2, carboxylic groups in EGFR molecule have negative charge whereas amines

are protonated i.e. they attain positive charge. The isoelectric point (pI) for EGFR is 6.7 and at our buffer solution's pH the net charge on EGFR molecule is negative [49]. Due to this charge, after applying biasing voltage, electrophoretic force (EP) pushes the EGFR molecules towards the positive electrode in the *trans* compartment [50]. The velocity of this moving molecule can be calculated using Smoluchowski's equation [51, 52]: $v_{EP} = (\epsilon/\eta)\zeta_{pro}\cdot E$ where ' v_{EP} ' is the electrophoretic velocity of EGFR molecule, ' ϵ ' is the dielectric constant, ' η ' is the solution viscosity, ' ζ_{pro} ' is the zeta potential for protein molecule and ' E ' is the electric field. Electroosmotic flow (EO) in the electrolyte also affects the dynamics of the

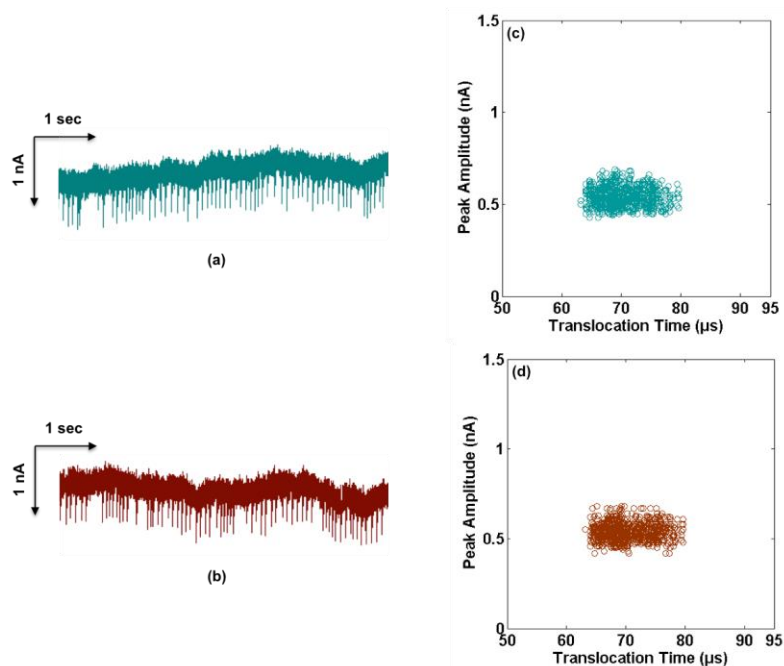


Figure 4. Snapshots of the nanopore ionic current traces for 10 seconds for the translocation of (a) Thrombin (b) Thrombin (11 pM) incubated with 10 pM of aptamer. Scatter plots of the registered pulses for the translocation of (c) Thrombin (d) Thrombin incubated with 10 pM aptamer.

EGFR movement in nanopores. In some cases EO can also cause a reverse flow of the proteins [47] i.e. negatively charged protein molecules will start moving towards the *cis* side, opposite to the EP. Reverse flow of the EGFR molecule was not observed in the experiments that meant that EO was either in the direction of EP or even if it was opposite to EP, it was not sufficient to counteract the EP and EP solely was the dominant factor in governing EGFR direction of flow.

The overall translocation process can be split into two stages; (1) Capture step, and (2) Actual translocation through the nanopore. For a 40 nm pore, the capture of EGFR molecule will be diffusion controlled as opposed to the barrier-limited case. The dynamics of this diffusion controlled capture step can be calculated with the Smoluchowski's diffusion equation [40, 51-53]: $J = 2\pi cDr_p$, where ' J ' is the rate at which the EGFR arrives at the nanopore entrance, ' c ' is the bulk analyte concentration, ' D ' is the diffusion constant and ' r_p ' is the nanopore radius. Once EGFR has entered the nanopore, the translocation depends upon the zeta potential of the EGFR molecule and of the nanopore [50]. Cressiot *et al.* simulated the interaction of proteins with nanopore walls formed by FIB as well as TEM. They found that due to the absence of dangling atoms [54] and rearrangement of silica in nanopores formed by TEM, the interaction between proteins and nanopore walls is very weak [48]. Blockage time, $t_b = L/v_{EP}$ (' L ' is nanopore channel length) is a function of the applied voltage [48] as well as the charge of the translocating species [19, 47]. Increasing either of these would increase the EP on the EGFR molecules and hence will decrease the blockage time and vice versa. At fixed applied bias of 50 mV, the pulses were pretty consistent in their width i.e. translocation time or blockage time for EGFR translocation. Coagulation of molecules, if happened, would have either blocked the pore completely or much longer translocation times would have been present [45]. However, none of such events were observed so it can be concluded that no EGFR coagulation occurred under these experimental conditions. Concurrent translocations of multiple EGFR molecules were observed though, but these events were very few and were discarded from the analysis. From single EGFR translocation events, very consistent pulse depths were observed, that was a clear indication of the uniform excluded volume of the EGFR molecules.

The specificity of anti-EGFR aptamer for EGFR and their attachment chemistry is quite well established [35, 36, 55]. When EGFR is incubated with the aptamer, they form a complex with 1:1 stoichiometry. It is just like aptamer, which has its own charge and mass, riding on the EGFR molecule. Since the estimated pI for aptamer is 5.5, at pH 8.2 it has almost the same charge as the EGFR. The attachment of EGFR with aptamer enhances the overall charge of the complex as well as the complex has more mass now than EGFR alone. These changes influence the overall dynamics of the complex translocation through the nanopore and make the translocation profile of complex different from that of

EGFR. The additional charge of the complex very well explains the faster translocation of the complex through the nanopore. One might argue here that due to the additional mass it might be possible that the complex actually moved slower than the EGFR. However, this is not the dominant factor in determining the translocation profile of the complex [37], since due to the binding of aptamer with EGFR, the overall change in charge is much more than the overall change in mass. That's why much more shift in the translocation time was observed rather than the peak amplitudes between the pulses associated with complex and EGFR translocation.

The shifting of the EGFR translocation behavior, as the molar concentration of aptamer increased, can be explained with Smoluchowski's diffusion equation. According to this equation, the capture rate ' J ' increases by increasing the analyte concentration ' c ' in the solution. In Figure 3(d), the event rate is low for complex and higher for EGFR but as we increased the aptamer molar concentration, many more complexes were formed causing the event rate for them to shoot up (Figure 3(e) & 3(f)). With thrombin, since aptamer didn't bind to it, no complexes were formed, and the translocation profile remained the same as before when no aptamer was involved.

The nanopores depicted a very selective and sensitive framework for label-free detection of EGFR from a sample. The use of bare nanopore made the process very simple and provided much more flexibility in the choice of nanopore size, unlike functionalized nanopore in which the ligand would be tethered inside the nanopore walls and the target must interact with the nanopore walls [37]. A functionalized nanopore is usable for one type of target and functionalization itself is a time consuming and labor extensive process. The use of bare nanopore with ligands to bind specific targets in solution increase the usability of the device since the same device can be used for multiple targets. There are no stringent limitations on the size of the nanopore as well.

Materials and Methods

Materials: Recombinant Human EGFR/ErbB1 Fc Chimera, CF (EGFR ~134 KDa) was purchased from R&D Systems and human α -thrombin (Thrombin ~37 KDa) was purchased from Abcam, plc. Anti-EGFR

aptamer (~10 KDa) had the sequence GGGCGCUCCGACCUUAGUCUCUGUGCCGCUAUAU
GCACGGAUUUAAUCGCCGUAGAAAAGCAUGUCAAAAGCCGGAACCGUGUAGCACAGCAGAGAAUJAAU
GCCCCGCAUGACCAG [36, 56]. All other chemicals were obtained from Sigma-Aldrich unless specified
otherwise.

Nanopore Fabrication and Electrical Measurements: A solid-state nanopore of 40 nm diameter and 40 nm length (Figure 1(a)) was used for all the translocation experiments. The nanopore was drilled in a thin suspended silicon nitride membrane by focusing an electron beam of a transmission electron microscope (TEM). Nanopore diameter was controlled by the exposure time [57]. The detailed fabrication process for membranes is reported elsewhere [58]. The nanopore chip was sandwiched between two PDMS gaskets that were further sandwiched between two Teflon blocks that contained the electrophoresis buffer solution (20 mM Tris-acetate pH 8.2 + 5 mM Mg- acetate + 1 mM K-acetate). Protein unfolding has strong dependence on the applied voltage [21, 48]. To keep proteins in their native states and to avoid any unfolding all the translocation experiments were done at a very low voltage i.e. 50 mV. For current measurement and to apply the voltage, Ag/AgCl electrodes were immersed in the buffer solution and were connected to Axopatch 200B through the headstage. Figure 1(c) shows the schematic of nanopore measurement system. Current recording was done at a bandwidth of 250 kHz whereas filtering was done at 100 kHz with a lowpass Bessel filter. A custom-made MATLAB routine [59] was used for analysis of the data. The *t*-test was done for statistical analysis.

In-solution Binding of Protein and Aptamer: For in-solution binding, EGFR protein and anti-EGFR aptamer were mixed in the binding buffer (Figure 2c). The binding buffer constituted of 1X PBS and 5 mM/L MgCl₂. Three separate mixtures were prepared by mixing EGFR and anti-EGFR aptamer in different concentrations. In mixture 1, 8 μl of 50 ng/μl (3 pM) EGFR was mixed with 0.5 μM aptamer. In mixture 2 and 3, EGFR concentration was kept same as mixture 1 but aptamer concentration was 4 μM and 10 μM, respectively. The mixtures were incubated at 37 °C for 10 minutes and then were placed in freezer (0-4 °C) for 5 minutes. The details on binding dynamics have been explained before [36]. For control experiments, 8 μl of human α-thrombin protein at 50 ng/μl (11 pM) concentration was also

mixed with anti-EGFR aptamer (10 μ M) and was incubated first at 37 °C for 10 minutes and then at 0-4 °C for 5 minutes.

Conclusions

In summary, the use of nanopore based resistive-pulse sensors for rapid and reliable detection of EGFR has been presented. Due to high single molecule sensitivity of nanopore sensors, very small amount of EGFR has been detected. EGFR overexpression, though an early biomarker for different types of cancers, have not yet been utilized properly for early cancer detection because available methods are not sensitive enough to detect very small changes in the quantities of EGFR. Besides high sensitivity and rapid detection, the scheme of nanopore with complex detection does not require pre-processing of the samples. The simplicity of this label-free detection method can enable the use of the nanopore device in a POC setting for early cancer diagnosis. The methodology can be further expanded for the detection of other biomarkers as well if there are matching ligands available. Additionally, this technique can be used to determine the affinity of the aptamer-protein complex as well.

Acknowledgement

We thank Raja Raheel Khanzada for his help with the graphics of this paper. We would also like to thank Dr. Andrew Ellington from the University of Texas at Austin for providing us the aptamer molecules. This work was supported by grant ECCS-12000 from National Science Foundation, USA.

References

1. Pepe MS, Etzioni R, Feng Z, Potter JD, Thompson ML, Thornquist M, Winget M, Yasui Y. Phases of biomarker development for early detection of cancer, Journal of the National Cancer Institute. 93 (2001) 1054-61.
2. Wulfkuhle JD, Liotta LA, Petricoin EF. Proteomic applications for the early detection of cancer, Nature Reviews Cancer. 3 (2003) 267-75.

3. Rusling JF. Multiplexed electrochemical protein detection and translation to personalized cancer diagnostics, *Analytical Chemistry*. 85 (2013) 5304-10.
4. Gabos Z, Sinha R, Hanson J, Chauhan N, Hugh J, Mackey JR, Abdulkarim B. Prognostic significance of human epidermal growth factor receptor positivity for the development of brain metastasis after newly diagnosed breast cancer, *Journal of Clinical Oncology : Official Journal of the American Society of Clinical Oncology*. 24 (2006) 5658-63.
5. Mak MP, William WN, Jr. Targeting the epidermal growth factor receptor for head and neck cancer chemoprevention, *Oral oncology*. 50 (2014) 918-23.
6. Maheswaran S, Sequist LV, Nagrath S, Ulkus L, Brannigan B, Collura CV, Inserra E, Diederichs S, Iafrate AJ, Bell DW, et al. Detection of mutations in EGFR in circulating lung-cancer cells, *The New England Journal of Medicine*. 359 (2008) 366-77.
7. Voldborg BR, Damstrup L, Spang-Thomsen M, Poulsen HS. Epidermal growth factor receptor (EGFR) and EGFR mutations, function and possible role in clinical trials, *Annals of Oncology : Official Journal of the European Society for Medical Oncology / ESMO*. 8 (1997) 1197-206.
8. Mendelsohn J, Baselga J. Epidermal growth factor receptor targeting in cancer, *Seminars in Oncology*. 33 (2006) 369-85.
9. Quaranta M, Divella R, Daniele A, Di Tardo S, Venneri MT, Lolli I, Troccoli G. Epidermal growth factor receptor serum levels and prognostic value in malignant gliomas, *Tumori*. 93 (2007) 275-80.
10. Nam JM, Thaxton CS, Mirkin CA. Nanoparticle-based bio-bar codes for the ultrasensitive detection of proteins, *Science*. 301 (2003) 1884-6.
11. Gubala V, Harris LF, Ricco AJ, Tan MX, Williams DE. Point of care diagnostics: status and future, *Analytical Chemistry*. 84 (2012) 487-515.

12. Venkatesan BM, Bashir R. Nanopore sensors for nucleic acid analysis. *Nature Nanotechnology*. 6 (2011) 615-24.
13. Bell NA, Engst CR, Ablay M, Divitini G, Ducati C, Liedl T, Keyser UF. DNA origami nanopores, *Nano Letters*. 12 (2012) 512-7.
14. Wei R, Gatterdam V, Wieneke R, Tampe R, Rant U. Stochastic sensing of proteins with receptor-modified solid-state nanopores, *Nature Nanotechnology* 7 (2012) 257-63.
15. Iqbal SM, Akin D, Bashir R. Solid-state nanopore channels with DNA selectivity, *Nature Nanotechnology*. 2 (2007) 243-8.
16. Soni GV, Dekker C. Detection of nucleosomal substructures using solid-state nanopores, *Nano Letters*. 12 (2012) 3180-6.
17. Niedzwiecki DJ, Iyer R, Borer PN, Movileanu L. Sampling a biomarker of the human immunodeficiency virus across a synthetic nanopore, *ACS Nano*. 7 (2013) 3341-50.
18. Chen P, Mitsui T, Farmer DB, Golovchenko J, Gordon RG, Branton D. Atomic Layer Deposition to Fine-Tune the Surface Properties and Diameters of Fabricated Nanopores, *Nano Letters* 4 (2004) 1333-7.
19. Fologea D, Ledden B, McNabb DS, Li J. Electrical characterization of protein molecules by a solid-state nanopore, *Applied Physics Letters*. 91 (2007) 539011- 3.
20. Talaga DS, Li J. Single-molecule protein unfolding in solid state nanopores, *Journal of the American Chemical Society*.131 (2009) 9287-97.
21. Rodriguez-Larrea D, Bayley H. Multistep protein unfolding during nanopore translocation, *Nature Nanotechnology*. 8 (2013) 288-95.

22. Uram JD, Ke K, Hunt AJ, Mayer M. Submicrometer pore-based characterization and quantification of antibody-virus interactions, *Small*. 2 (2006) 967-72.
23. Ali M, Bayer V, Schiedt B, Neumann R, Ensinger W. Fabrication and functionalization of single asymmetric nanochannels for electrostatic/hydrophobic association of protein molecules, *Nanotechnology*. 19 (2008) 485711.
24. Majd S, Yusko EC, Billeh YN, Macrae MX, Yang J, Mayer M. Applications of biological pores in nanomedicine, sensing, and nanoelectronics, *Current Opinion in Biotechnology*. 21 (2010) 439-76.
25. Bayley H, Cremer PS. Stochastic sensors inspired by biology, *Nature*. 413 (2001) 226-30.
26. Liu A, Zhao Q, Guan X. Stochastic nanopore sensors for the detection of terrorist agents: current status and challenges, *Analytica Chimica Acta*. 675 (2010) 106- 15.
27. Maglia G, Heron AJ, Stoddart D, Japrun D, Bayley H. Analysis of single nucleic acid molecules with protein nanopores, *Methods in Enzymology*. 475 (2010) 591- 623.
28. Nivala J, Marks DB, Akeson M. Unfoldase-mediated protein translocation through an alpha-hemolysin nanopore, *Nature Biotechnology*. 31 (2010) 247-50.
29. Movileanu L. Interrogating single proteins through nanopores: challenges and opportunities, *Trends in Biotechnology*. 27 (2009) 333-41.
30. Hernandez-Ainsa S, Keyser UF. DNA origami nanopores: developments, challenges and perspectives, *Nanoscale*. 6 (2014) 14121-32.
31. Payet L, Martinho M, Pastoriza-Gallego M, Betton JM, Auvray L, Pelta J, Mathe J. Thermal unfolding of proteins probed at the single molecule level using nanopores, *Analytical Chemistry*. 84 (2012) 4071-6.

32. Han A, Creus M, Schurmann G, Linder V, Ward TR, de Rooij NF, Stauffer U. Label-free detection of single protein molecules and protein-protein interactions using synthetic nanopores, *Analytical Chemistry*. 80 (2008) 4651-8.
33. Howorka S, Siwy Z. Nanopore analytics: sensing of single molecules, *Chemical Society Reviews*. 38 (2009) 2360-84.
34. Rotem D, Jayasinghe L, Salichou M, Bayley H. Protein detection by nanopores equipped with aptamers, *Journal of the American Chemical Society*. 134 (2012) 2781-7.
35. Bunka DH, Stockley PG. Aptamers come of age - at last, *Nature Reviews Microbiology*. 4 (2006) 588-96.
36. Wan Y, Mahmood MA, Li N, Allen PB, Kim YT, Bachoo R, Ellington AD, Iqbal SM. Nanotextured substrates with immobilized aptamers for cancer cell isolation and cytology, *Cancer*. 118 (2012) 1145-54.
37. Mahmood MA, Ali W, Adnan A, Iqbal SM. 3D structural integrity and interactions of single-stranded protein-binding DNA in a functionalized nanopore, *The Journal of Physical Chemistry B*. 118 (2014) 5799-806.
38. He Y, Tsutsui M, Scheicher RH, Fan C, Taniguchi M, Kawai T. Mechanism of how salt-gradient-induced charges affect the translocation of DNA molecules through a nanopore, *Biophysical Journal*. 105 (2013) 776-82.
39. Kowalczyk SW, Dekker C. Measurement of the docking time of a DNA molecule onto a solid-state nanopore, *Nano Letters*. 12 (2012) 4159-63.
40. Plesa C, Kowalczyk SW, Zinsmeister R, Grosberg AY, Rabin Y, Dekker C. Fast translocation of proteins through solid state nanopores, *Nano Letters*. 13 (2013) 658-63.

41. Ho C, Qiao R, Heng JB, Chatterjee A, Timp RJ, Aluru NR, Timp G. Electrolytic transport through a synthetic nanometer-diameter pore, *Proceedings of the National Academy of Sciences of the United States of America*. 102 (2005) 10445-50.
42. Kowalczyk SW, Kapinos L, Blosser TR, Magalhaes T, van Nies P, Lim RY, Dekker C. Single-molecule transport across an individual biomimetic nuclear pore complex, *Nature Nanotechnology*. 6 (2011) 433-8.
43. Zhang H, Li XF, Le XC. Tunable aptamer capillary electrophoresis and its application to protein analysis, *Journal of the American Chemical Society*. 130 (2008) 34-5.
44. van den Hout M, Skinner GM, Klijnhout S, Krudde V, Dekker NH. The passage of homopolymeric RNA through small solid-state nanopores, *Small*. 7 (2011) 2217- 24.
45. Yusko EC, Johnson JM, Majd S, Prangko P, Rollings RC, Li J, Yang J, Mayer M. Controlling protein translocation through nanopores with bio-inspired fluid walls, *Nature Nanotechnology*. 6 (2011) 253-60.
46. Kowalczyk SW, Hall AR, Dekker C. Detection of local protein structures along DNA using solid-state nanopores, *Nano Letters*. 10 (2010) 324-8.
47. Firnkes M, Pedone D, Knezevic J, Doblinger M, Rant U. Electrically facilitated translocations of proteins through silicon nitride nanopores: conjoint and competitive action of diffusion, electrophoresis, and electroosmosis, *Nano Letters*. 10 (2010) 2162-7.
48. Cressiot B, Oukhaled A, Patriarche G, Pastoriza-Gallego M, Betton JM, Auvray L, Muthukumar M, Bacri L, Pelta J. Protein transport through a narrow solid-state nanopore at high voltage: experiments and theory, *ACS Nano*. 6 (2012) 6236-43.
49. Ceresa BP, Peterson JL. Cell and molecular biology of epidermal growth factor receptor, *International Review of Cell and Molecular Biology*. 313 (2014) 145-78.

50. Lu B, Hoogerheide DP, Zhao Q, Yu D. Effective driving force applied on DNA inside a solid-state nanopore, *Physical Review E, Statistical, Nonlinear, and Soft Matter Physics*. 86 (2012) 011921.
51. Peters B, Bolhuis PG, Mullen RG, Shea JE. Reaction coordinates, one- dimensional Smoluchowski equations, and a test for dynamical self-consistency, *The Journal of Chemical Physics*. 138 (2013) 054106.
52. Egorova EM. The validity of the Smoluchowski equation in electrophoretic studies of lipid membranes, *Electrophoresis*. 15 (1994) 1125-31.
53. Family F, Meakin P, Deutch JM. Kinetics of coagulation with fragmentation: Scaling behavior and fluctuations, *Physical Review Letters*. 57 (1986) 727-30.
54. Cruz-Chu ER, Aksimentiev A, Schulten K. Ionic Current Rectification Through Silica Nanopores, *The Journal of Physical Chemistry C, Nanomaterials and Interfaces*. 113 (2009) 1850.
55. Wan Y, Tan J, Asghar W, Kim YT, Liu Y, Iqbal SM. Velocity effect on aptamer- based circulating tumor cell isolation in microfluidic devices, *The Journal of Physical Chemistry B*. 115 (2011) 13891-6.
56. Wan Y, Liu Y, Allen PB, Asghar W, Mahmood MA, Tan J, Duhon H, Kim YT, Ellington AD, Iqbal SM. Capture, isolation and release of cancer cells with aptamer-functionalized glass bead array, *Lab On a Chip*. 12 (2012) 4693-701.
57. Fischbein MD, Drndic M. Sub-10 nm device fabrication in a transmission electron microscope, *Nano Letters*. 7 (2007) 1329-37.
58. Asghar W, Ilyas A, Deshmukh RR, Sumitsawan S, Timmons RB, Iqbal SM. Pulsed plasma polymerization for controlling shrinkage and surface composition of nanopores, *Nanotechnology*. 22 (2011) 285304.
59. Billo JA, Asghar W, Iqbal SM. An Implementation for the Detection and Analysis of Negative Peaks

in an Applied Current Signal across a Silicon Nanopore, Micro- and Nanotechnology Sensors, Systems, and Applications III. 8031 (2011) 80312T.

3. CROSSTALK BETWEEN ADJACENT NANOPORES IN A SOLID- STATE MEMBRANE ARRAY FOR MULTI-ANALYTE HIGH- THROUGHPUT BIOMOLECULE DETECTION

Reprinted (adapted) With permission from (M.U. Raza, S. Saleem, W. Ali, and S. M. Iqbal, Crosstalk between adjacent nanopores in a solid-state membrane array for multi-analyte high-throughput biomolecule detection, Journal of Applied Physics, 120, no. 6 (2016): 064701), with the permission of AIP Publishing.

Copyrights 2016 © AIP Publishing

Crosstalk between Adjacent Nanopores in a Solid-state Membrane Array for Multi-analyte High-throughput Biomolecule Detection

Muhammad Usman Raza^{1,2,3}, Sajid Saleem⁴, Waqas Ali^{1,2,3}

and Samir M. Iqbal^{1,2,3,5,6,a)}

¹Nano-Bio Lab, University of Texas at Arlington, Arlington, Texas 76019, USA

²Department of Electrical Engineering, University of Texas at Arlington, Arlington, TX 76011, USA

³Nanotechnology Research Center, University of Texas at Arlington, Arlington, Texas 76019, USA

⁴Department of Electrical and Power Engineering, National University of Sciences and Technology, Karachi, Pakistan

⁵Department of Bioengineering, University of Texas at Arlington, Arlington, TX 76010, USA

⁶Department of Urology, University of Texas Southwestern Medical Center at Dallas, Dallas, TX 75390, USA

Abstract

Single nanopores are used to detect a variety of biological molecules. The modulations in ionic current under applied bias across the nanopore contain important information about translocating species, thus providing single analyte detection. These systems are, however, challenged in practical situations where multiple analytes have to be detected at high-throughput. This paper presents analysis of a multi-nanopore system that can be used for the detection of analytes with high throughput. As a scalable model, two nanopores were simulated in a single solid-state membrane. The interactions of the electric fields at the mouths of the individual nanopores were analyzed. The data elucidated the electrostatic properties of the nanopores from a single membrane and provided a framework to calculate the -3 dB distance, akin to the debye length, from one nanopore to the other. This distance was the minimum distance between the adjacent nanopores such that their individual electric fields did not significantly interact with one another. The results can help in the optimal experimental design conditions to construct solid-state nanopore arrays, for any given nanopore size and applied bias.

Introduction

Certain diseases such as cancer can lead to severe complications and drastically reduced survival rates if not detected early. Early detection is the key in fight against cancer which killed about 574,743 people in the US in 2010 (or 186 deaths per 100,000 population) as shown by the data from Center for Disease Control (CDC).[68] These trends have not improved for many years. Survival rate of patients affected with cancer improve dramatically when diagnosis is made early in the disease lifecycle.

The clinical symptoms of cancer do not show up until it has reached an advanced stage. Little can be done to contain or eliminate it then. The usual diagnostic tests leave much to be desired towards early and effective cancer detection. The need is for cheap, readily available and specific cancer diagnostic tools and methods.

In this paper, the problems associated with solid-state nanopore based detection of biomolecules are analyzed. A framework of nanopore arrays can sense multiple cancer biomarkers. The simulations lay foundations for rational design of electrically isolated nanopore arrays. The distance between adjacent nanopores, applied bias and nanopore sizes define some basic design principles. In the end, the flow of an elliptical molecule is presented through a nanopore at two different adjacent nanopore distances. This demonstrates the utility of the solid-state nanopores in an array format for real-time sensing of protein molecules.

A. Solid-state Nanopores.

The nanopore biosensors are increasingly used for rapid and cost-effective detection of various biological analytes. The main reason for their emergence is the specific, label free and robust single molecule analysis capability. These can be used with varying functionalization for detection of multiple analytes.[69][70] There are two different kinds of nanopores. First are the biologically occurring α -hemolysin nanopores which are suspended in lipid bilayers made from *Staphylococcus aureus* which contains homoheptameric subunits leading to transmembrane channels of about 1.5 nm in diameter.[71][72][73] Second, the solid-state nanopores are made using silicon fabrication processes. Solid-state nanopores are relatively more robust and practical than the biological nanopores. Nanopores

have been used to detect proteins, DNA and RNA complexes which may be linked to the detection of cancer.

Solid-state nanopores are fabricated by drilling holes in silicon nitride or silicon oxide membranes. Silicon nitride is generally preferred over silicon dioxide because it has low stress and remains intact even when its thickness is reduced to less than 10 nm.[74][45][43] However, the thickness of the membranes can further be reduced to a mere nanometer by using graphene.[75][76][48]

In the experiments, each nanopore chip is sandwiched between two containers filled with ionic solution. The *cis-trans* containers are separated by the nanopore in the membrane. The analyte to be detected is introduced in the appropriate side. Ag/AgCl electrodes are immersed in each container of ionic solution and a voltage is applied across the nanopore. The analyte travels under the effect of bias through the solid-state nanopore. The ionic current through the nanopore gets disrupted when analytes pass through.[77] A large variety of biological molecules like DNA, RNA, disease biomarkers, and viruses have been detected with nanopores.[78][79][80] The side to which the analytes are introduced depends on the isoelectric point of the analyte,[81][82] the pH of the solution and the polarity of the electrodes. The drop in the ionic current when the analyte passes through the nanopore results into the detection of the particular analyte.[83] This detection has been made specific by attaching ligands on the nanopore walls for a specific analyte under consideration.[84] The interaction of translocating species with nanopore surface grafted species results into characteristic negative peaks in the ionic current which makes detection of the specific analytes possible.[85] Single nanopore biosensors have many issues related to their practical implementations like baseline shifting, low throughput, and challenges in reproducible measurements.[86] On the measurements of nanopores, first, there is no self-referencing capability for the baseline current at any time when the analyte is passing through. Second, it cannot detect multiple analytes because the nanopore functionalization makes it specific to only one analyte. Third, the single nanopore sensor does not have the ability for differential operation that can be used to reduce noise for enhanced detection.[87] Fourth, if the single nanopore is blocked by a large molecule somehow,[88] it requires replacement of the nanopore, which means it lacks robustness. Last, and most importantly, the single nanopore biosensor has severely low throughput. This means that it takes a lot of time to process the millions of molecules in a sample

looking for a few hundred copies of target biomolecule such as a cancer biomarker, especially at the early stages of the disease.

In order to circumvent problems associated with single nanopore technology, a framework of multiple nanopores made in the same membrane is presented here. Fig 1 shows a model two-nanopore array.

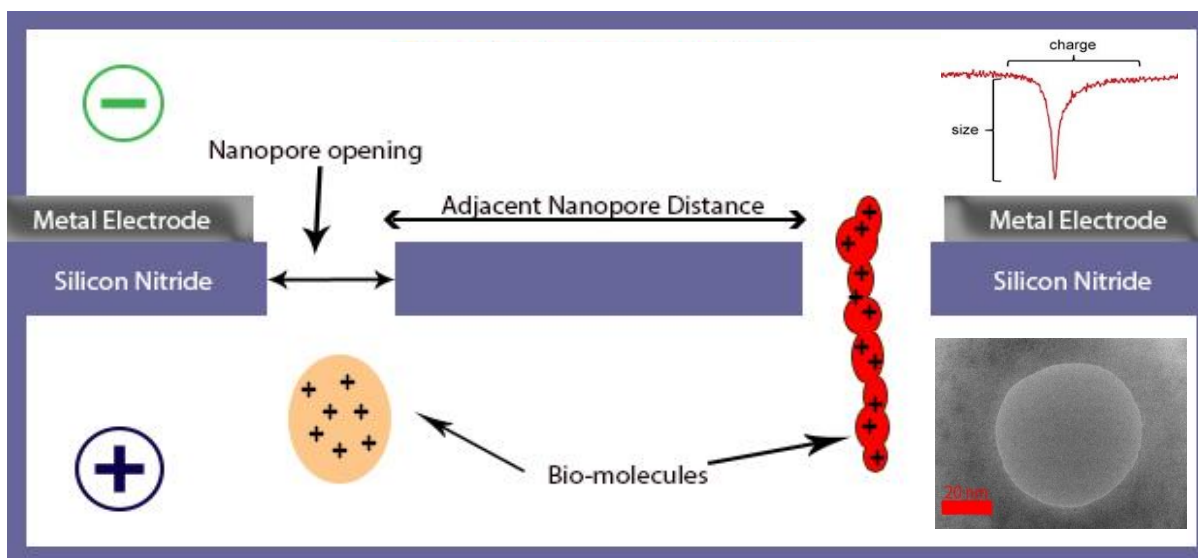


FIG.1. Two nanopore array. The biasing electrodes are shown in circle. These are immersed in the electrolyte solution. In the inset above, the translocation time of the molecule is plotted against the translocation current through the nanopore. This shows that as the molecule passes through the nanopore, it results in a downward pulse in the current. The lower-right inset shows an actual 60 nm nanopore drilled in a silicon nitride membrane using transmission electron microscope.

B. Nanopore Arrays

In a nanopore array, each nanopore has to be addressed with its own sensing electrodes, made on the membrane right close by. In line with this concept, the simulations consisted of two nanopores made in one membrane. When voltage bias was applied across the nanopores, a field was generated across the nanopores. This field resulted in the ionic current across the nanopores, moving the molecules through and ultimately causing pulses in the ionic current. The electrodes right next to the respective nanopores would detect the individual pulses in respective ionic currents. The measurements from each nanopore would thus provide quantitative pulse statistics related to the specific biomolecules. The system can detect multiple biomolecules at the same time and with throughput double than that through a two-nanopore array.

The problem of paramount importance in the nanopore array is that the adjacent nanopores have to be at a specific distance away from each other. If the distance is less, the electric fields from adjacent nanopores intersect with each other. This results in the ionic current drop at the metal electrodes to be affected by the adjacent nanopore current leading to false results. Also, the distance between the nanopore mouth and the metal electrode has to be optimized so that maximum detection is possible through the electrodes.

I. Nanopore Model

A two-dimensional model was constructed to simulate the effects of adjacent nanopore electric

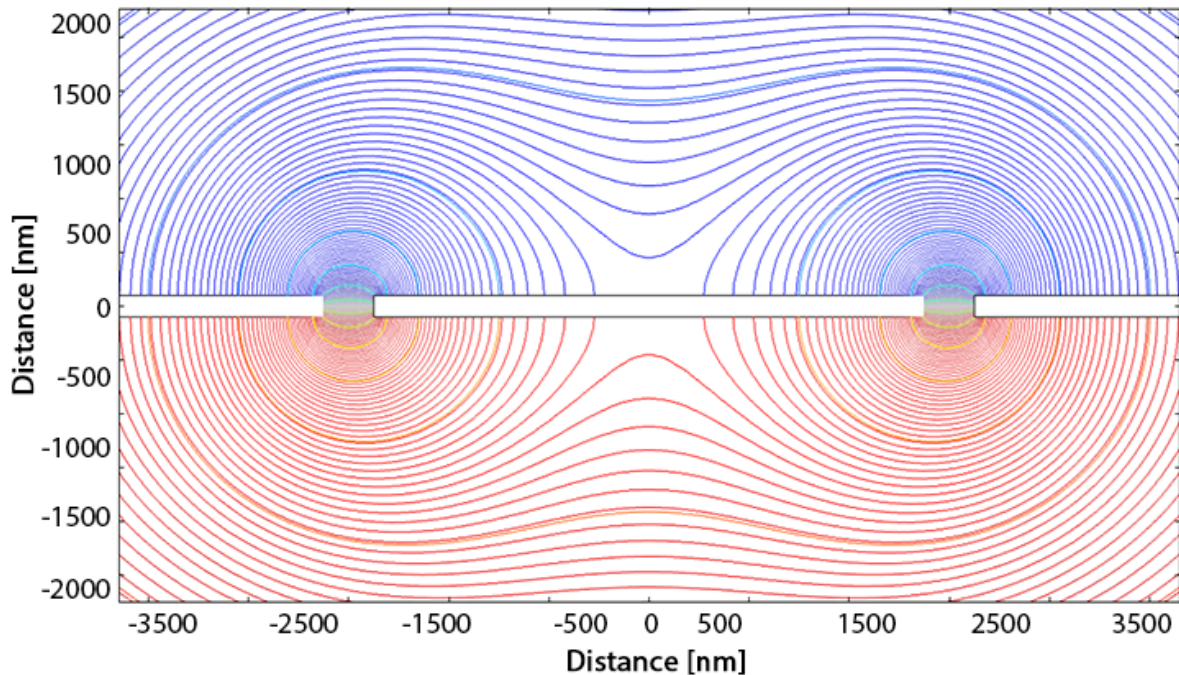


FIG. 2. The two-nanopore array model. The contour lines depict the electric field

fields on the translocation profile. The nanopores were made in a silicon nitride membrane of 20 nm thickness. A 1 M KCl ionic solution was used in the model. It was contained in two containers of silicon nitride insulator separated in the middle by the silicon nitride membrane. The only path between the two containers for the ionic current to flow was through the two nanopores. The depth of the 2D model was set

at 5 nm. Electric potential was applied as a line source at the top and bottom extremes of the 2D model (Fig. 2).

The materials used in the model consisted of silicon nitride with an electrical conductivity of 0 S/m, relative permittivity of 9.7 and density of 3100 kg/m³. For 1 M KCl, the electrical conductivity was taken as 11 S/m and a relative permittivity of 60 [89]. The material KCl was assigned to be the ionic solution that was contained by the silicon nitride boundaries.

The COMSOL simulations used time-invariant electric currents physics model. The top and bottom plate was assigned as high potential and ground in this model, respectively. This resulted in the change in electric potential across the nanopore through the ionic solution (Fig. 3).

II. Experimental Setup

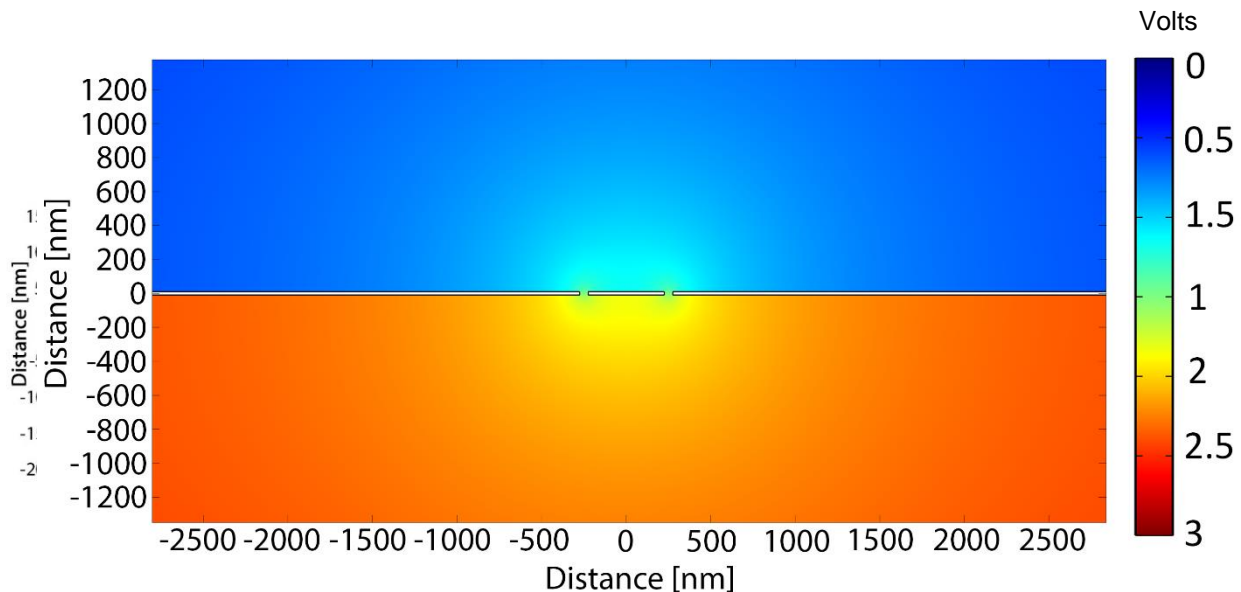


FIG. 3. A two nanopore array at 500 nm distance showing the interaction of the electric fields

In order to simulate the properties of a two nanopore array using the electric currents model, the DC bias was applied across a silicon nitride membrane. The ionic current flow was through the two adjacent nanopores. The simulations provided electric potential at the mouth of the nanopores to measure the best distance feasible between the two adjacent nanopores. It is important to note that the potential was the largest at the mouth of the nanopore where the molecules would exit the nanopore. There were three

variables in the nanopore array setup. These were the adjacent nanopore distance, the applied voltage bias and the size of the nanopore. The three specific scenarios were simulated to measure their effects on electric potential through the two nanopores while keeping the other two factors constant. First, the distance between the adjacent nanopores was varied to find the optimum distance between two nanopores of certain size at fixed DC bias. Second, the effect of varying the DC bias applied across the nanopores was measured on the electric potential of adjacent nanopores. Third, the effect of varying the size of the nanopores was found as it changed with the electric potential through two adjacent nanopores at fixed distance and fixed DC bias. These three parameters translated into the properties of measurement system that can be tailored to design for optimum results.

III. Results

The results of the simulations were plotted to get the best possible distance between the nanopores. At the end of each simulation and once equilibrium was achieved, the system snapshot was taken (Fig. 4). The field values clearly showed the drop across a region much wider than the unperturbed area.

A. Variation in Nanopore Distance

Figure 4, shows two cases, out of many (Fig. 5), with inter-nanopore distances of 1000 nm and 4000 nm. As can be seen in Fig. 4(a), the electric fields of two nanopores intercept each other in the ionic solution, while the ionic solution is passing through the nanopore. The direction of flow of anions and cations in the 1 M KCl solution is opposite to one another as these pass through the nanopore. This is due to the net charge on the individual K^+ and Cl^- ions in the solution and the effect of electric field on them. The net movement of charge through the nanopores created an ionic current flowing through these nanopores. The nanopores provided resistance to the flow of ionic current due to the small size of the opening. This resulted in the maximum potential drop across the nanopores, hence leading to the maximum magnitude of electric field at the nanopore mouth.

Fig. 5 shows the effects of the variation in adjacent nanopore distance on the electric potential at the DC bias of 3 V and at the nanopore size of 50 nm. As the adjacent nanopore distance increased, the electric potential between the nanopores decreased significantly. The peak electric potential was thus at the mouth of the nanopore and it degraded significantly as the distance from the mouth of the nanopore increased. For two adjacent nanopores to be independent of the electric fields of each other, the amplitude of electric potential should drop by at least -3 dB at the adjacent nanopore midpoint. So, if the peak amplitude is V_0 , then the -3 dB amplitude of the electric potential should be less than $0.709V_0$. The simulations showed that at an adjacent nanopore distance of 2 microns or higher, the value of the electric potential at the adjacent nanopore midpoint was less than -3 dB value of peak electric potential at the mouth

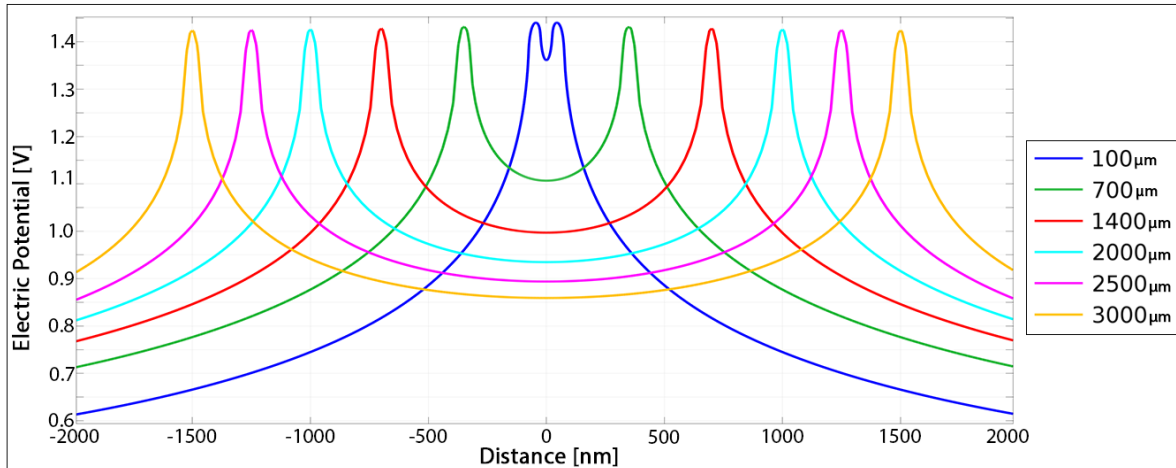


FIG. 5. The electric potential at the adjacent nanopores separated by increasing distance show that as the adjacent nanopore distance increases the electric potential at the middle of the two nanopores also decreases.

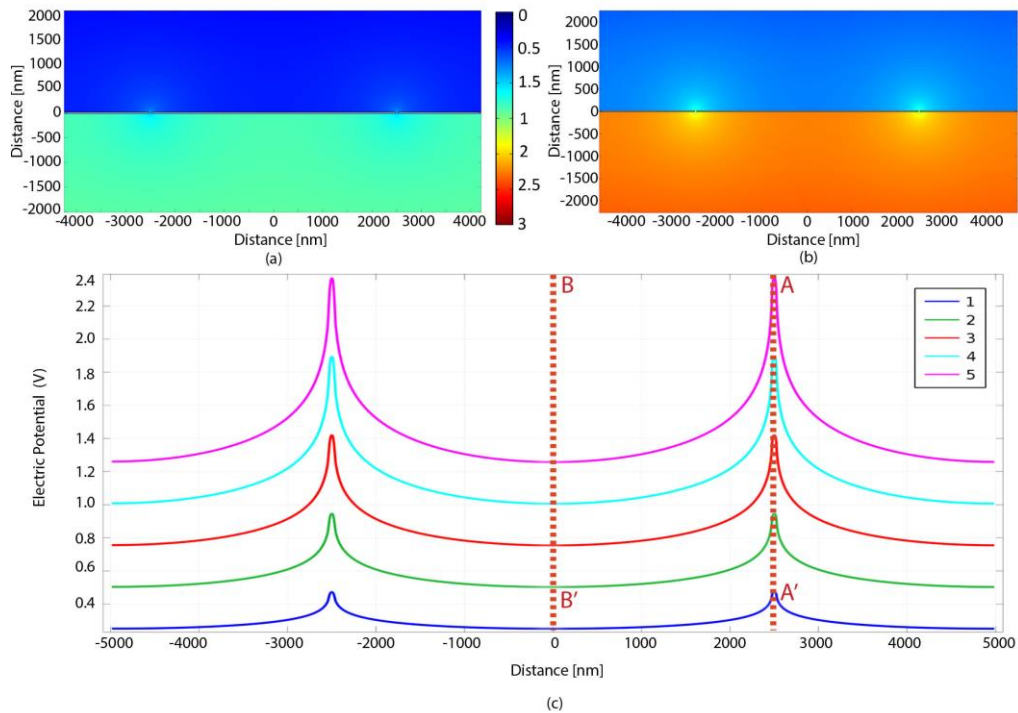


FIG. 6. The field at DC bias of (a) 2 V and (b) 3 V. (c) The change in electric potential as the DC Bias is varied. This shows that as the DC bias is reduced, the adjacent nanopore distance required to minimize crosstalk also lessens. AA' and BB' slices are explored further to analyze change in the electric potential with respect to the applied bias in later text.

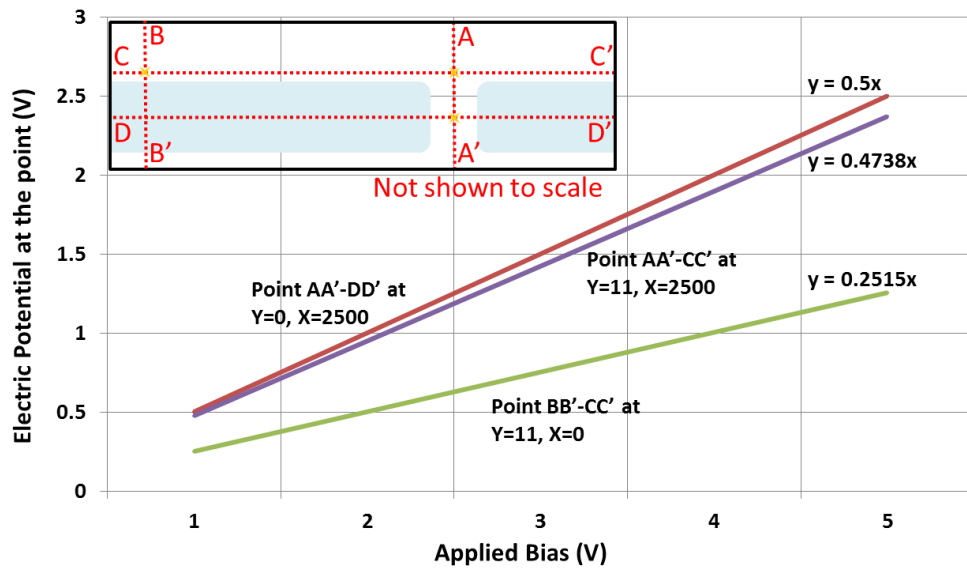


FIG. 7. The plot shows the linear behavior of electric potential at various points in the ionic solution. The rate of change of applied bias is largest at the center of the nanopore and reduces at points away from the center of the nanopore

of the nanopore which is also the debye length. This distance was enough for the adjacent nanopore electric fields to not interfere with each other.

B. Variation in DC Bias

The electric potential interference change was linear at all points of interest when the distance between 50 nm nanopores was kept at 5000 nm and the DC bias across the nanopore was reduced from 5 V to 1 V (Figs. 6 and 7). From the data, it can be seen that the required adjacent nanopore distance is less for systems with lower applied bias, and the rate of change of applied bias at the center of the nanopore is the highest (Fig. 8(a)). This shows that for optimum detection of the translocating biomolecule through the nanopore, electrodes should be placed at the center of the nanopore sandwiched inside the nanopore membrane. Sensitivity of the electrodes will be thus maximum if placed in the middle of the nanopore which is experimentally challenging.

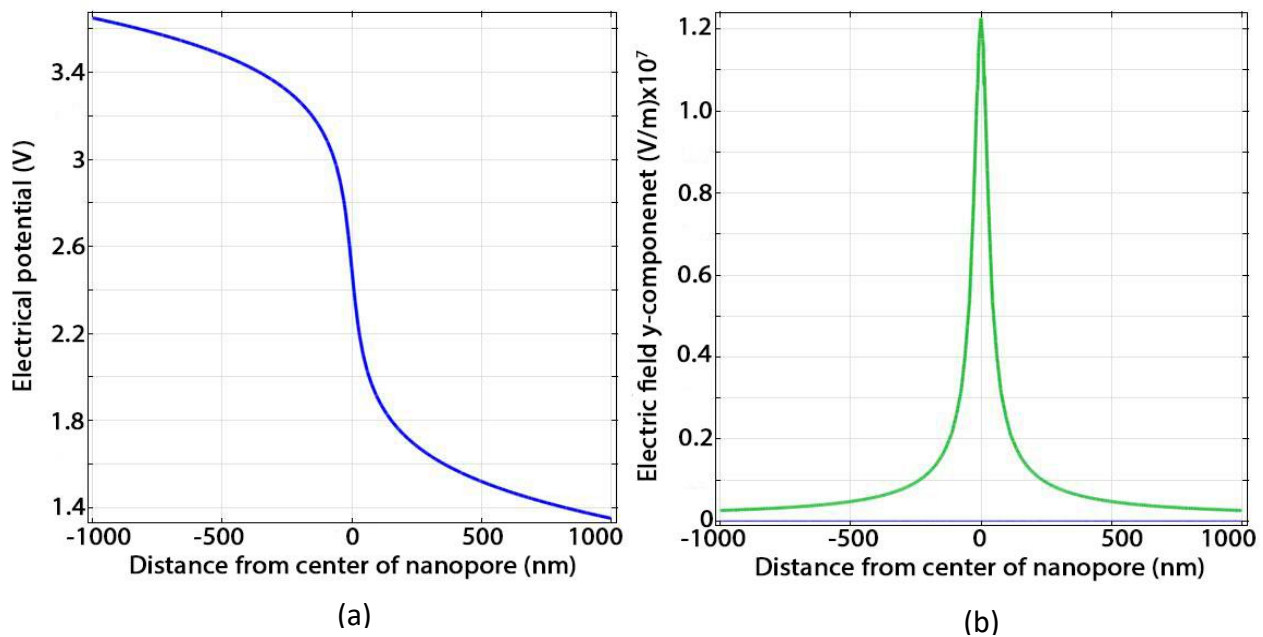


FIG. 8. Plot shows the relationship of electric potential and the y-component of the electric field along the line AA' (line AA' is shown in inset of Fig. 7).

In line with the limitations of actual fabrication, the electrodes were placed at the mouth of the nanopore where the rate of change was relatively lower. The y-component of electric field was also the highest at the center of the nanopore (Fig. 8(b)). This shows that the pull on the biomolecule will be the highest at the center and would decrease as it moves outwards towards the mouth of the nanopore. As a

consequence, the translocation acceleration of the biomolecule will be the highest at the center of the nanopore. This shows that even a distance of less than the required 3 microns would be enough between adjacent nanopores at a bias of 1 V, which is in the range of voltages employed in the nanopore

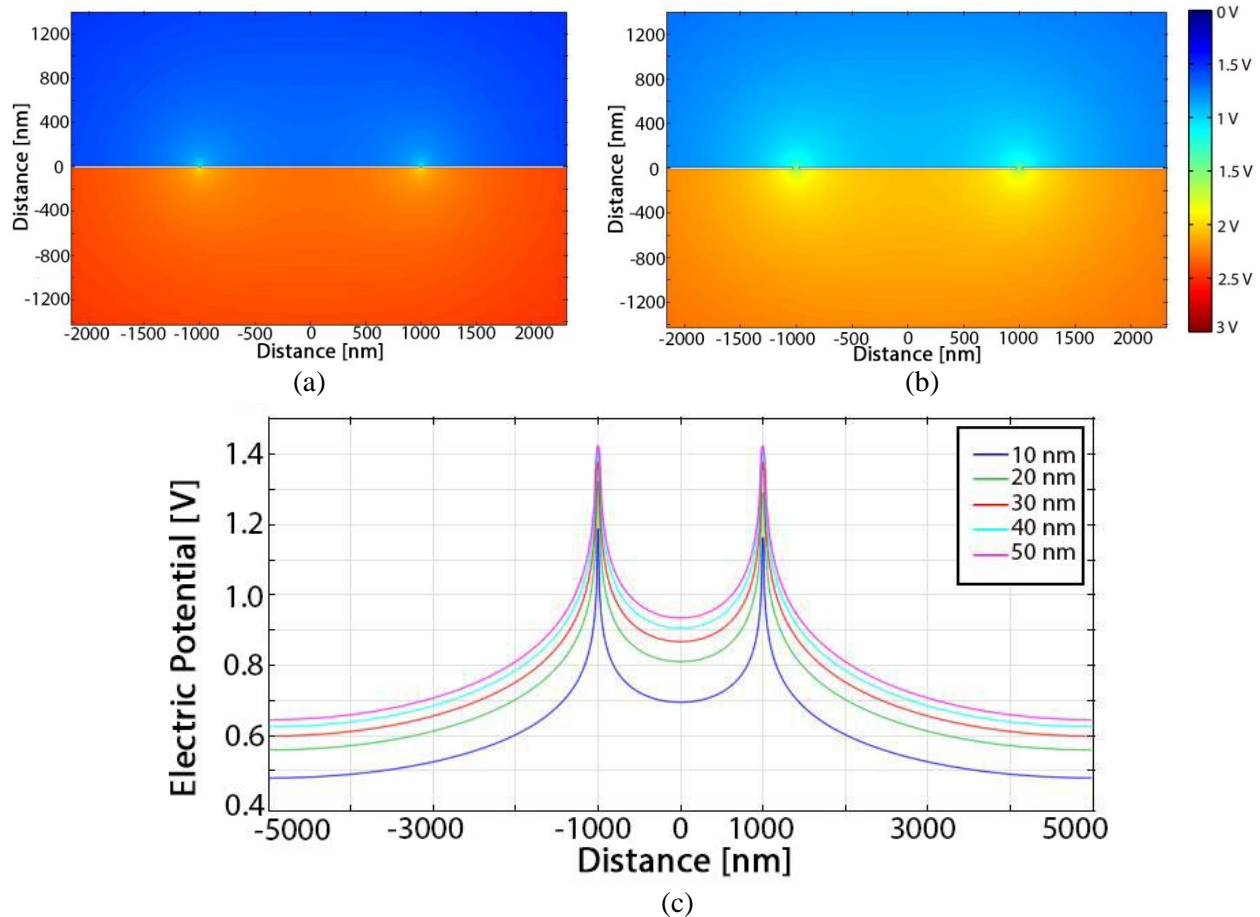


FIG. 9. The field with nanopore diameter of (a) 10 nm and (b) 50 nm (c) The variations in electric potential as the nanopore diameters are changed show that the larger diameter nanopores require more adjacent nanopore separation.

experiments.^[90]

As shown in Fig 1, the nanopore sensors are used to selectively detect biomolecules passing through the nanopore. These biomolecules can behave as anions or cations when suspended in solutions of different pH according to their isoelectric points. The net charge on the individual molecules determines whether the target biomolecule will be suspended in the *cis* or *trans* side of the nanopore. As the biomolecules have complex structures, if the electric fields at the mouth of the nanopore are high, the

molecules start to lose their shape and characteristics [85]. This can result in flawed experimental results. The higher the DC bias, more field is felt by the biomolecule to translocate through the nanopore. This behaves as an accelerating force on the biomolecule and leads it to pass through the nanopore in less time leading to less interaction of the biomolecule with the nanopore or the nanopore grafted ligands. This high acceleration is thus undesirable in nanopore experiments as it may result in the loss of selective biomolecule detection.

The DC bias across the nanopore membranes thus has to adjust to values that lead to translocation of these biomolecules across the nanopore without disrupting their molecular structure and without interfering with sub-molecular forces. That is one of the reasons of using very low bias values in actual nanopore experiments; down to about 100 mV in some experiments.

C. Variation in Nanopore Size

The third variable was the nanopore size, varied while keeping the adjacent nanopore distance and the applied DC bias constant. The need for change in nanopore size is dictated by the fact that the biomolecules used in the experiments (as shown in Fig 1) are of varying shapes and sizes. If the biomolecule size is much smaller than the size of the nanopore, the biomolecule may not significantly block the flow of ionic current through the nanopore. This would result in nonspecific and insignificant drops in ionic current during translocation. On the other hand, if the size of the biomolecules is larger than that of the nanopore, it would cause permanent blockage or may result in molecule deformation and loss of their shape, structure and functionality.

The detection of specific biomolecules requires that the nanopore walls are functionalized with specific ligands that attach selectively with the translocating biomolecules of interest. Larger nanopore may result in lack of significant interactions between the translocating biomolecules and the ligands functionalized on the walls of the nanopore. Therefore, the size of the nanopore has to be designed based on the size of the translocating species and the layer thickness of ligands.

Fig 9 shows the electric potential between adjacent nanopores as the nanopore size was varied but the adjacent nanopore distance was kept constant at 2000 nm and DC bias was set at 3 V. This data further elucidates that a nanopore size of 50 nm is good enough when the next nanopore is just 2 micron away. The 2 micron inter-nanopore distance at 3 V bias provides smooth operation of the nanopore array biosensor without adjacent nanopore crosstalk. It is thus easy to decide the configurations for a multi-nanopore multi-analyte detection scheme.

IV. Biomolecule translocation through the nanopore

To further validate the preceding results with a biomolecule, simulation were also done with an elliptically shaped protein. EGFR is a cell surface receptor that is overexpressed in many cancers. The radius of EGFR is about 20 nm and it is 40 nm long. The molecule is negatively charged at neutral pH, so a charge number of -1 was used to simulate the negatively charged molecule. The applied bias was 3 V and the nanopore diameter was 50 nm. For this simulation, two distances (between adjacent nanopores) were used. First adjacent nanopore distance was 100 nm which was less than the debye length. The second adjacent nanopore distance used was 3000 nm which was more than the minimum distance for these conditions.

Fig. 10(a) shows the electric potential contours at 100 nm while the molecule is passing through the nanopore on the left. It can be seen that the nanopore on the right is so close that it is significantly affected by the electrical interference from the changes in electric field from the adjacent nanopore. This shows that at a distance less than debye length; 100 nm distance in this instance; the results may be false and nonspecific. The adjacent nanopore distance of 3000 nm, which is much more than the debye length of 2000 nm, shows no electric potential distortion when the molecule passed through the left nanopore (Fig 10(b)).

Fig 10(c) shows that at an adjacent nanopore distance of 100 nm, when the molecule passes through the left nanopore there is significant change in electric potential at the mouth of the nanopore as well. However, there is absolutely no change in electric potential at the right nanopore when it is 3000 nm

apart. So in this case there will be no false results in the experiments when electrodes are placed at the mouth of the nanopore.

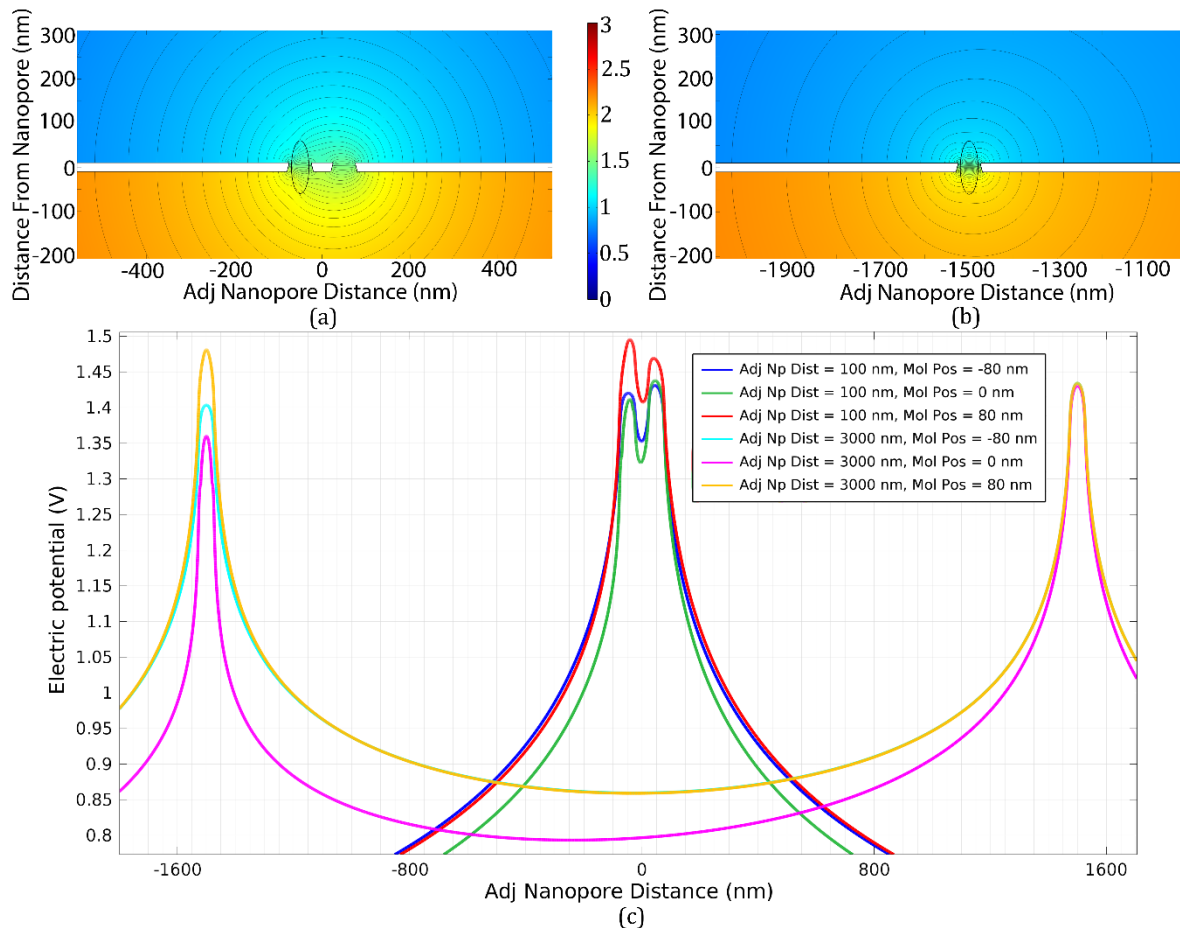


FIG. 10 (a) & (b). shows an elliptical molecule translocating through the nanopores. The adjacent nanopore distance in (a) is 100 nm and in (b) is 3000 nm. The molecule is right at the nanopore center in both (a) and (b). The contour lines represent the electric potential. (c) Shows the electric potential at the mouth of the nanopore.

The data shows that a protein would be difficult to detect and give nonspecific results if the design constraints are not met. Hence, a nanopore with an adjacent nanopore more than Debye length away would result in negligible crosstalk and true molecule detection. Calculating the Debye length i.e. is the -3 dB drop

in voltage from the peak to the midpoint is done in Fig. 11. It shows clearly the case of a translocating molecule at 80 nm from the nanopore. The debye length has been calculated by calculating the length at which the midpoint voltage is – 3 dB the peak voltage. It is clearly shown for a case when the nanopore diameter is 50 nm and applied voltage is 3 V the Debye length is 2000 nm between the adjacent nanopores. At 2000 nm adjacent nanopore distance V_o is 1.37 V at the mouth the nanopore with the translocating molecule. At midpoint of the two nanopores the voltage is 0.97 V. This turns out to be 0.709 V_o which is what we require. So, we conclude that the debye length in this case is 2000 nm adjacent nanopore distance. Finally, for construction of the nanopore array system, for 3 V applied voltage, our adjacent nanopore distance should be more than 2000 nm apart.

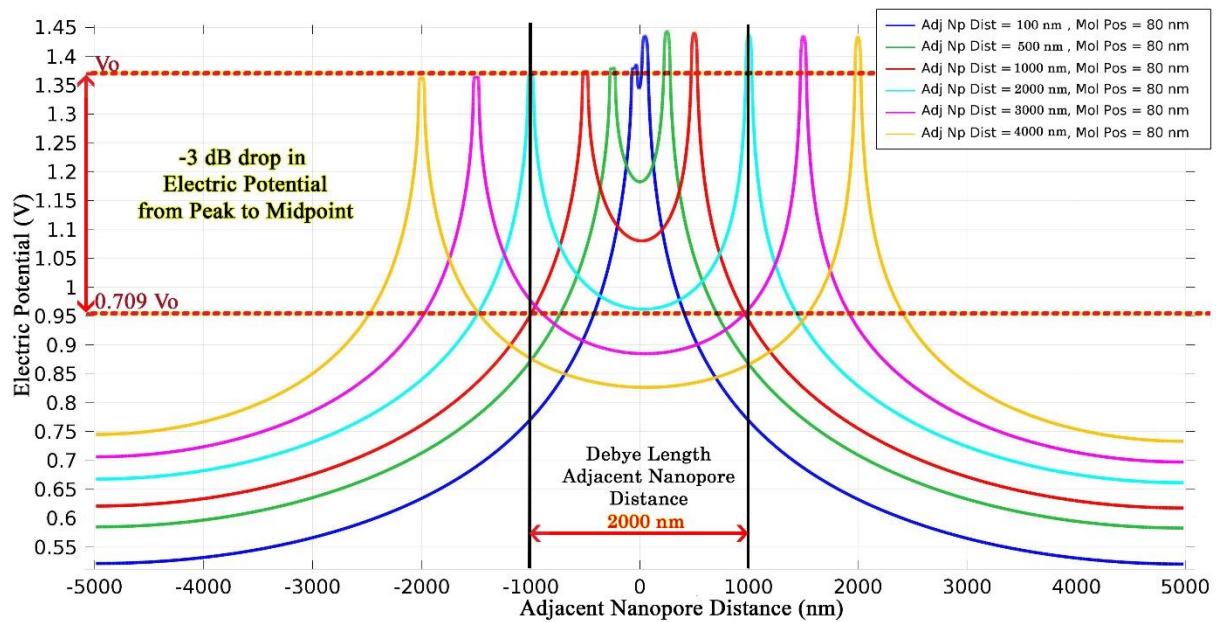
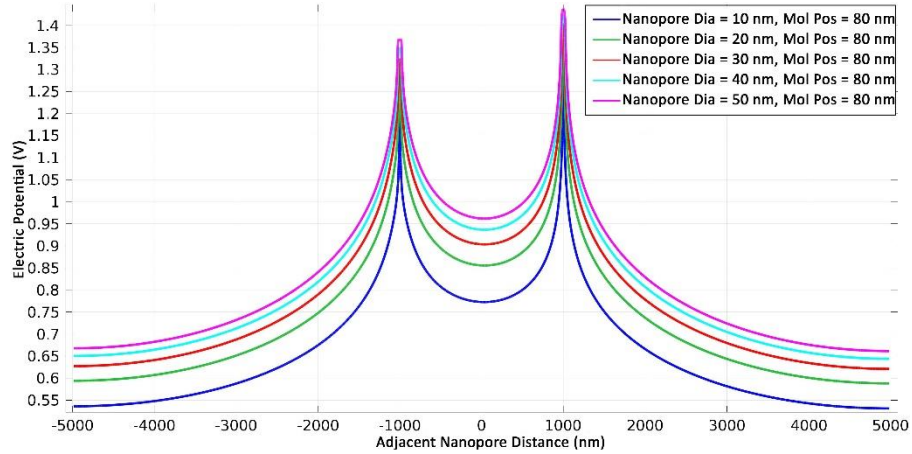
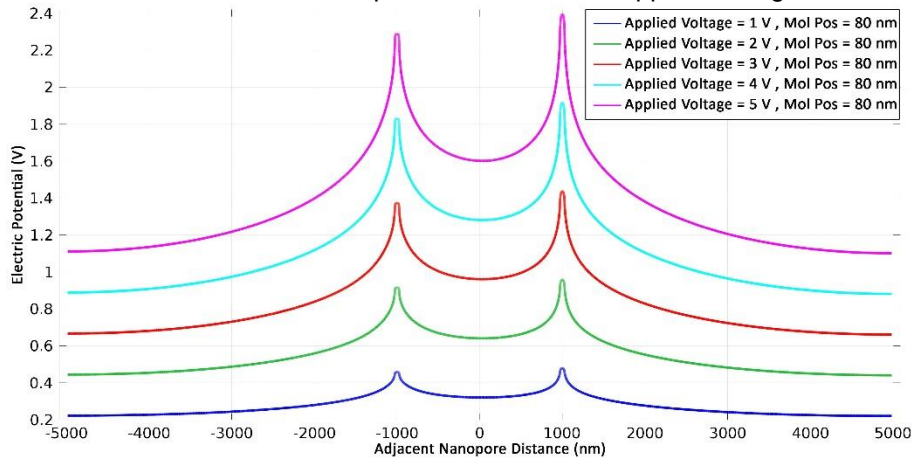


Fig.11: Shows the case of voltage at the mouth of the nanopore as the elliptical molecule passes through the nanopore. We clearly see that the debye length is 2000 nm as the -3 dB drop in electric potential between the peak and midpoint is 0.709 V_o .

Another important aspect of a multiple nanopore array is to see how the voltage drop from the molecule translocation change at variable voltages and for variable nanopore sizes. The relationship of molecular translocation to nanopore diameter and applied voltage is depicted in Fig. 12, where the adjacent



nanopore distance has been kept at 2000 nm. It is clear that the distance between adjacent nanopore has to be increased if we increase either the nanopore diameter or the applied voltage across the nanopore.



(a)

(b)

Fig.12. (a) Change in nanopore diameter when the applied voltage is constant at 3 V and the adjacent nanopore distance is 2000 nm. The voltage drop is for the mouth of the nanopore as the elliptical molecule passes through the nanopore. (b) The case of change in applied voltage as the nanopore diameter is kept at 50 nm and the adjacent nanopore distance is kept at 2000 nm.

V. Conclusions

Nanopore arrays have the potential to build more robust, faster and highly selective molecular sensors. The throughput of the currently used single nanopore devices can be increased manifold if these were employed in array formats. With differential operation, noises can be subtracted from the experimental results leading to more sensitive detection of biomolecules. However, nanopore arrays bring forward a new set of design challenges. The simulations presented can guide fabrication towards optimum distance between two adjacent nanopores for them to function relatively independent of each other. It is also established that the nanopore array devices need electrodes at the mouth of the nanopores for differential measurements unlike conventional nanopores. The simulations show that the adjacent nanopore fabrication must be done keeping in view the size and electrical characteristics of the biomolecule being investigated. The size of the nanopore and the applied bias has to be varied depending on the biomolecule. In short, all parameters have to be evaluated before fabrication of the nanopore array device as increase in applied bias or in nanopore size require increase in the adjacent nanopore distance. The reduction in adjacent nanopore interference can open roadmap for multi-nanopore self-referencing systems that can go beyond current single nanopore frameworks.

VI. References:

- ¹ Sherry L Murphy, JQ Xu, and Kenneth D Kochanek, *National Vital Statistics Reports* **61** (4), 1 (2013).
- ² Samir M Iqbal, Demir Akin, and Rashid Bashir, *Nature Nanotechnology* **2** (4), 243 (2007).
- ³ Haiying He, Ralph H Scheicher, Ravindra Pandey, Alexandre Reily Rocha, Stefano Sanvito, Anton Grigoriev, Rajeev Ahuja, and Shashi P Karna, *The Journal of Physical Chemistry (C)* **112** (10), 3456 (2008).
- ⁴ Toshihisa Osaki, Hiroaki Suzuki, Bruno Le Pioufle, and Shoji Takeuchi, *Analytical Chemistry* **81** (24), 9866 (2009).
- ⁵ L. Song, M. R. Hobaugh, C. Shustak, S. Cheley, H. Bayley, and J. E. Gouaux, *Science (New York, N.Y.)* **274** (5294), 1859 (1996).
- ⁶ Giovanni Maglia, Marcela Rincon Restrepo, Ellina Mikhailova, and Hagan Bayley, *Proceedings of the National Academy of Sciences* **105** (50), 19720 (2008).
- ⁷ Jiali Li, Derek Stein, Ciaran McMullan, Daniel Branton, Michael J Aziz, and Jene A Golovchenko, *Nature* **412** (6843), 166 (2001).
- ⁸ AJ Storm, JH Chen, XS Ling, HW Zandbergen, and C Dekker, *Nature Materials* **2** (8), 537 (2003).
- ⁹ Cees Dekker, *Nature Nanotechnology* **2** (4), 209 (2007).
- ¹⁰ Slaven Garaj, W Hubbard, A Reina, J Kong, D Branton, and JA Golovchenko, *Nature* **467** (7312), 190 (2010).
- ¹¹ Zuzanna S Siwy and Matthew Davenport, *Nature Nanotechnology* **5** (10), 697 (2010).

- ¹² Grégory F Schneider, Stefan W Kowalczyk, Victor E Calado, Grégory Pandraud, Henny W Zandbergen, Lieven MK Vandersypen, and Cees Dekker, *Nano Letters* **10** (8), 3163 (2010).
- ¹³ Farzin Haque, Jinghong Li, Hai-Chen Wu, Xing-Jie Liang, and Peixuan Guo, *Nano Today* **8** (1), 56 (2013).
- ¹⁴ Giovanni Maglia, Andrew J Heron, David Stoddart, Deanpen Japrun, and Hagan Bayley, *Methods in Enzymology* **475**, 591 (2010).
- ¹⁵ Stefan Howorka and Zuzanna Siwy, *Chemical Society Reviews* **38** (8), 2360 (2009).
- ¹⁶ Ruoshan Wei, Thomas G Martin, Ulrich Rant, and Hendrik Dietz, *Angewandte Chemie* **124** (20), 4948 (2012).
- ¹⁷ Yong Li, Huang-Hao Yang, Qi-Hua You, Zhi-Xia Zhuang, and Xiao-Ru Wang, *Analytical Chemistry* **78** (1), 317 (2006).
- ¹⁸ Jie-Ren Ku and Pieter Stroeve, *Langmuir* **20** (5), 2030 (2004).
- ¹⁹ Amit Meller, Lucas Nivon, and Daniel Branton, *Physical Review Letters* **86** (15), 3435 (2001).
- ²⁰ Erik C. Yusko, Jay M. Johnson, Sheereen Majd, Panchika Prangkio, Ryan C. Rollings, Jiali Li, Jerry Yang, and Michael Mayer, *Nature Nanotechnology* **6** (4), 253 (2011).
- ²¹ Mohammed Arif I Mahmood, Waqas Ali, Ashfaq Adnan, and Samir M Iqbal, *The Journal of Physical Chemistry B* **118** (22), 5799 (2014).
- ²² Deqiang Wang, Jingwei Bai, Sung-wook Nam, Hongbo Peng, Robert Bruce, Lynn Gignac, Markus Brink, Ernst Kratschmer, Stephen Rossnagel, Philip S. Waggoner, Kathy Reuter, Chao Wang, Yann Astier, Venkat Balagurusamy, Binqun Luan, Young Kwark, Eric Joseph, Michael Guillorn, stas Polonsky, Ajay Royyuru, Satyavolu Papa Rao, and Gustavo A. Stolovitzky, *Nanoscale* (2014).

²³ Daniel Branton, David W Deamer, Andre Marziali, Hagan Bayley, Steven A Benner, Thomas Butler, Massimiliano Di Ventra, Slaven Garaj, Andrew Hibbs, and Xiaohua Huang, *Nature Biotechnology* **26** (10), 1146 (2008).

²⁴ Liviu Movileanu, *Trends in Biotechnology* **27** (6), 333 (2009).

²⁵ (PubChem Substance Database, 2015), Vol. 2015.

²⁶ Waseem Asghar, Azhar Ilyas, Rajendra R Deshmukh, Sulak Sumitsawan, Richard B Timmons, and Samir M Iqbal, *Nanotechnology* **22** (28), 285304 (2011).

4. SIBA ACTUATED NANOPORE ELECTROPHORESIS (SANE)

Reprinted with permission from (M.U. Raza, S.S.S. Peri, L-C. Ma, S. M. Iqbal and G. Alexandrakis, SIBA actuated nanopore electrophoresis (SANE), In review, 2018, IOP Nanotechnology.

SIBA ACTUATED NANOPORE ELECTROPHORESIS

(SANE)

Muhammad Usman Raza^{*1}, Sai Santosh Sasank Peri^{*1}, Liang-Chieh Ma², Samir M. Iqbal^{2,3,#}, and George Alexandrakis^{2,#}

*Equal Author

¹ Department of Electrical Engineering, University of Texas at Arlington, Arlington, TX, 76019, USA

² Department of Bioengineering, University of Texas at Arlington, Arlington, TX, 76019, USA

³ Nano-bio Lab, Department of Electrical Engineering, and School of Medicine, University of Texas Rio Grande Valley, Edinburg, TX 78539, USA

Email: SMIQBAL@ieee.org and galex@uta.edu

ABSTRACT

We present a novel method to trap nanoparticles in Double Nanohole (DNH) nanoapertures integrated on top of solid-state nanopores (ssNP). The nanoparticles were propelled by an electrophoretic force from the cis towards the trans side of the nanopore but were trapped in the process when they reached the vicinity of the DNH-ssNP interface. The Self-Induced Back Action (SIBA) plasmonic force existing between the tips of the DNH opposed the electrophoretic force and enabled simultaneous optical and electrical sensing of a single nanoparticle for seconds. The novel SIBA Actuated Nanopore Electrophoresis (SANE) sensor was fabricated using two-beam GFIS FIB. Firstly, Ne FIB milling was used to create the DNH features and was combined with end pointing to stop milling at the metal-dielectric interface. Subsequently, He FIB was used to drill a 25 nm nanopore through the center of the DNH. Proof of principle experiments to demonstrate the potential utility of the SANE sensor were performed with 20 nm silica nanoparticles. The addition of optical trapping to electrical sensing extended translocation times by four orders of magnitude. The extended electrical measurement times revealed newly observed high frequency charge transients that were attributed to bobbing of the nanoparticle driven by the competing optical and electrical forces. Frequency analysis of this bobbing behavior hinted at the possibility of distinguishing single from multi-particle trapping events. We also discuss how SANE sensor measurements could be used to estimate the total charge around a nanoparticle. The SANE sensor therefore shows promise as an enabling tool for selective detection of biomolecules and quantification of their interactions.

INTRODUCTION

Nanopore biosensors utilize resistive pulse sensing of ion currents to detect biological analytes. Translocation of the analyte through a nanometer aperture is driven by the applied bias [43, 50, 91]. This technique has been used to detect DNA [92-95], proteins [61, 96-101], miRNA [58, 63, 102, 103] and other bio-analytes [64]. It has also been proposed as an affordable DNA sequencing tool [104, 105]. Although nanopores have been made from biological membranes [106, 107], solid state nanopores (ssNPs) have been widely used as a more robust alternative [108]. SsNPs are fabricated in silicon chips with suspended dielectric membranes in which the nanopores are etched or milled [45, 109-111]. Over the past two decades, numerous enhancements in nanopore technology have been reported for biosensing, including surface attachment to nanopore walls [63, 95], nanopore arrays [112], optically enhanced nanopores [113] and embedded tunneling electrode nanopores [114]. These technologies were developed to address challenges relating to low throughput, high sensor noise, lack of self-referencing, and high pore translocation speeds [46, 91].

To enhance nanopore sensing further, attempts have been made to combine it with optical sensing. Optical enhancement of nanopore sensing has garnered much interest since Keyser et al [115, 116] used a tightly focused laser on a DNA-tethered micrometer bead translocating through an ssNP. Optical forces acted as a tweezer for controlling bead translocation thus enabling study of biomolecular interactions inside the nanopore by force spectroscopy. However, tweezing cannot be extended to sub-diffraction limit nanoparticles directly due to the exponential reduction in optical trapping force with size. Surface charge control by optical excitation has also been used as an alternative approach employing electroosmotic flow to slow down the translocation of analytes through the nanopores [117]. Nevertheless, this technique only works in small nanopores due to Debye length restriction and requires fluorescent labeling for optical detection. Jonsson et al. [118] used gold bowtie plasmonic nanoantennas to create optical field enhancement in the nanogap over the mouth of a TEM-milled silicon nitride nanopore. The plasmonic focusing led to increased ionic conductance due to localized heating but did not slow down translocation through the nanopore. They also reported photoresistive switching in plasmonic nanopores [119], which

was attributed to plasmon-induced gaseous air bubble formation at the nanopore mouth. Recently, Meller et al. [120] reported a plasmonic nanopore with a circular gold nanowell on the trans side of the nanopore. This resulted in dual-mode detection of nanopore current and plasmonically excited fluorescence from the labelled DNA, without any control on nanopore translocation speed.

Nanoaperture-focused plasmons in metallic films are a potentially enabling technology for controlling analyte translocation through a nanopore, but this has been explored very little to date. Optical trapping at low laser powers can be attained in the immediate vicinity of metallic nanoapertures through a self-induced back action (SIBA) mechanism [121]. In SIBA, when a dielectric nanoparticle has a slightly higher refractive index than its surrounding medium a photon-mediated feedback force is actuated due to conservation of momentum against diffusion forces near the nanoaperture. The resulting coupling of light to the far field via the dielectric nanoparticle results in increased light transmission through the plasmonic nanoaperture and therefore enables label-free detection [122]. Double nanohole (DNH) nanoapertures have been reported as SIBA-mediated optical traps by Gordon et al. for high local field enhancement at the intersection of the nanoholes [123]. The Gordon group has reported a series of studies on the design characteristics of the DNH structure [124-126] and their use in many applications, including the trapping of nanoparticles [127-129] and single protein molecules [130-133].

Here we report nanofabrication and proof of principle studies for a DNH-ssNP sensor enabling simultaneous SIBA-mediated optical trapping by the DNH and electrophoresis through the ssNP. We name this a SIBA Actuated Nanopore Electrophoresis (SANE) sensor. The nanopore is milled between the tips of the DNH where the highest plasmonic energy is focused, resulting in trapping of the nanoparticle due to dielectric loading at the mouth of the nanopore. The nanoparticle translocates through the nanopore after it escapes trapping and yields the characteristic drop in ionic current due to pore blockage. Two types of focused ion beam (FIB) milling enabled nanofabrication of the DNH structure in an Au layer deposited on top of a thin silicon nitride layer without damaging it. Furthermore, the DNH structure is known to dissipate heat very effectively with minimal temperature increases at optical trapping powers [134]. In proof of principle experiments, we show that the DNH-nanopore structure trapped 20 nm dielectric nanoparticles for several

seconds, while enabling their concurrent electrical sensing during the same time interval. The SANE sensor controlled the nanoparticle translocation through the nanopore, which extended the duration of electrical sensing by up to four orders of magnitude compared to nanopore sensing alone. The extended electrical measurement times revealed a newly observed high frequency charge transient phenomenon related to occupancy of the optical trap by one or more nanoparticles. Finally, we discuss how upon sensor calibration, these bimodal measurements could be used to estimate the total charge around a nanoparticle.

MATERIALS AND METHODS

DUAL NANO HOLE – NANO PORE CHIP FABRICATION

The fabrication was done on double side polished, (100) orientation 4-inch silicon. Wet oxidation was done to grow 500 nm SiO_2 followed by a 60 nm LPCVD non-stoichiometric low stress silicon nitride (Si_xN_y). For each wafer, individual 15 mm x 15 mm square chips were created with one side patterned using S1813 photoresist with a darkfield backside mask. The first mask contained square windows of 786 μm size in the center. The 786 μm square etch windows were opened in Si_xN_y using DRIE to etch through its entire 60 nm layer thickness and then a 6:1 Buffered Hydrofluoric acid (BHF) solution was used to etch the SiO_2 to reveal the bare silicon (Fig. 1). The wafers were placed in 22 % tetramethylammonium hydroxide (TMAH) solution at 90 °C to anisotropically etch the wafer all the way to the front side revealing the 100 μm square $\text{SiO}_2/\text{Si}_x\text{N}_y$ membranes at the other side, henceforth called the front side. The SiO_2 was a sacrificial layer to protect the membrane during further processing and was etched away at the last step of the chip fabrication. The wafers were cleaned in Piranha solution and inspected under an optical microscope to confirm the design parameters of the anisotropic etch. E-beam evaporation was used to deposit 5 nm of Cr as the adhesion layer on which 100 nm of Au was subsequently deposited on the front side of the wafer on top of the suspended Si_xN_y membranes. The S1813 positive resist was used to coat the front side of the wafer to pattern four diagonal FIB alignment markers in Au. A backside aligner (EVG 620) was used to align the dark field second mask and to expose the front side while aligned to the backside patterns. Au and Cr were wet etched using commercially available wet etchants (Sigma Aldrich). The etched and cleaned wafers were inspected under an optical microscope for proper placement of FIB alignment markers on the

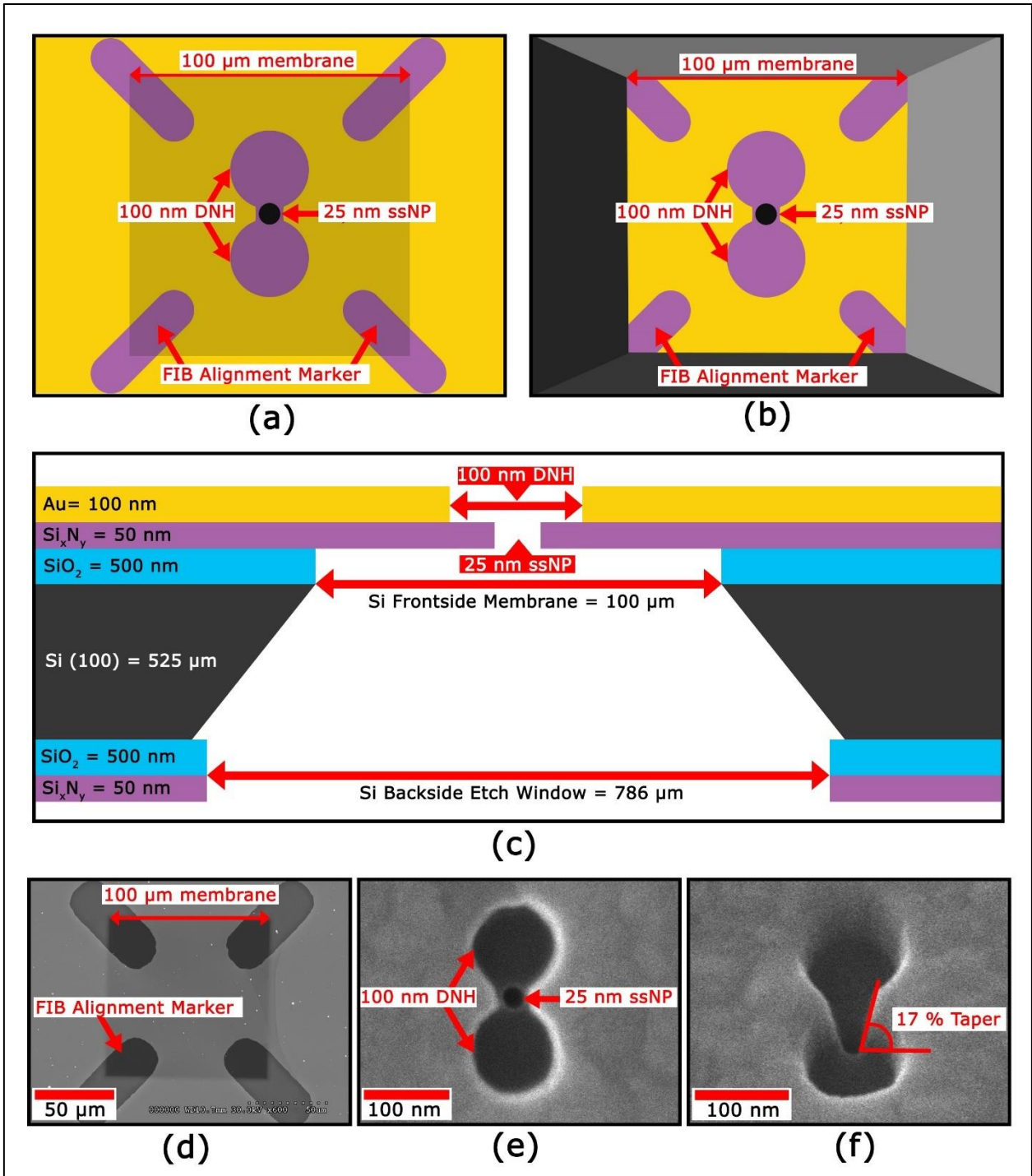


Fig. 1: (a) (b) (c) Not to scale. (a) Front side view of SANE chip. (b) Back side view of SANE chip. (c) Cross-section of the SANE sensor chip. (d) SEM micrograph of front side of the SANE chip before FIB drilling. He ion microscope image of top view (e) and tilted view (f) of milled DNH with 17% sidewall taper and a 25 nm ssNP drilled at its center.

suspended Si_xN_y membrane from the front side and the back side [Fig. 1(d)]. The front side of the wafers

was coated in thick S1813 photoresist and hard baked. The individual chips were diced and separated from each other. The sacrificial SiO₂ layer beneath the Si_xN_y was then wet etched from the back side using 6:1 BHF for 8 min and the photoresist layer on the front side was removed in acetone. The individual chips were dried and inspected under an optical microscope to confirm the integrity of the membrane and of the alignment markers on it. The membrane area now consisted of a 50 nm thick Si_xN_y layer with a 5 nm Cr / 100 nm Au metal stack [Fig. 1(c)]. These 15 mm x 15 mm individual chips were now ready for FIB milling [Fig. 1(d)].

The FIB milling on these individual chips was done using a mix of Ne and He GFIS focused ion beams (Carl Zeiss, ORION NanoFab, Peabody, MA). The Ga FIB or TEM beam could not be used due to the complex requirements of the dual layer design [Fig. 1(c)]. The dumbbell shape of the DNH was milled into the Au film (Critical Dimension = 25 nm) and the milling had to be stopped at the metal/dielectric interface. The DNH shape was designed to have 15-20 % tapered edges [Fig. 1(f)], in line with a prior feature optimization study [125], converging towards the metal/dielectric interface. A Ne ion beam was used to mill the DNH shape in the Au/Cr metal stack (500 fA beam current, 25 kV acceleration voltage, 10 μm aperture and 8.5 mm working distance). A beam dose of 0.2 – 0.225 nC/μm² was determined to be optimum to reach the Au/Cr – Si_xN_y interface. The secondary electron current was used in the nanopatterning visualization engine to determine when the dielectric interface was reached to terminate the Ne FIB milling. At that point, the beam was switched to He ions and a 25 nm circle was drilled through the suspended Si_xN_y membrane in the middle of the DNH shape (2 pA beam current, 30 kV acceleration voltage with 150 nC/μm² dose, 10 μm aperture and 8.5 mm working distance). He FIB nanopore drilling through the Si_xN_y film was stopped when the secondary electron current suddenly decreased to almost zero [Fig. 1(e)].

EXPERIMENTAL SETUP

The beam from an 820 nm laser diode (L820P200, Thorlabs) was collimated to a 2 mm diameter and circularly polarized through a QWP (WPQ05M, Thorlab), followed by a Glan-Thompson linear polarizer (GTH10M, Thorlabs) for controlling the polarization of light incident on the chip. The light then passed

through a tunable HWP (WPH05M, Thorlabs) to make the direction of polarization perpendicular to the DNH's long axis to excite maximally wedge plasmons for trapping [46]. A downstream 4x beam expander (Newport) was used in combination with an 8 mm circular aperture (ID.1.0, Newport) to make the intensity profile of the cylindrical beam flatter. The beam then went through a periscope and into the back aperture

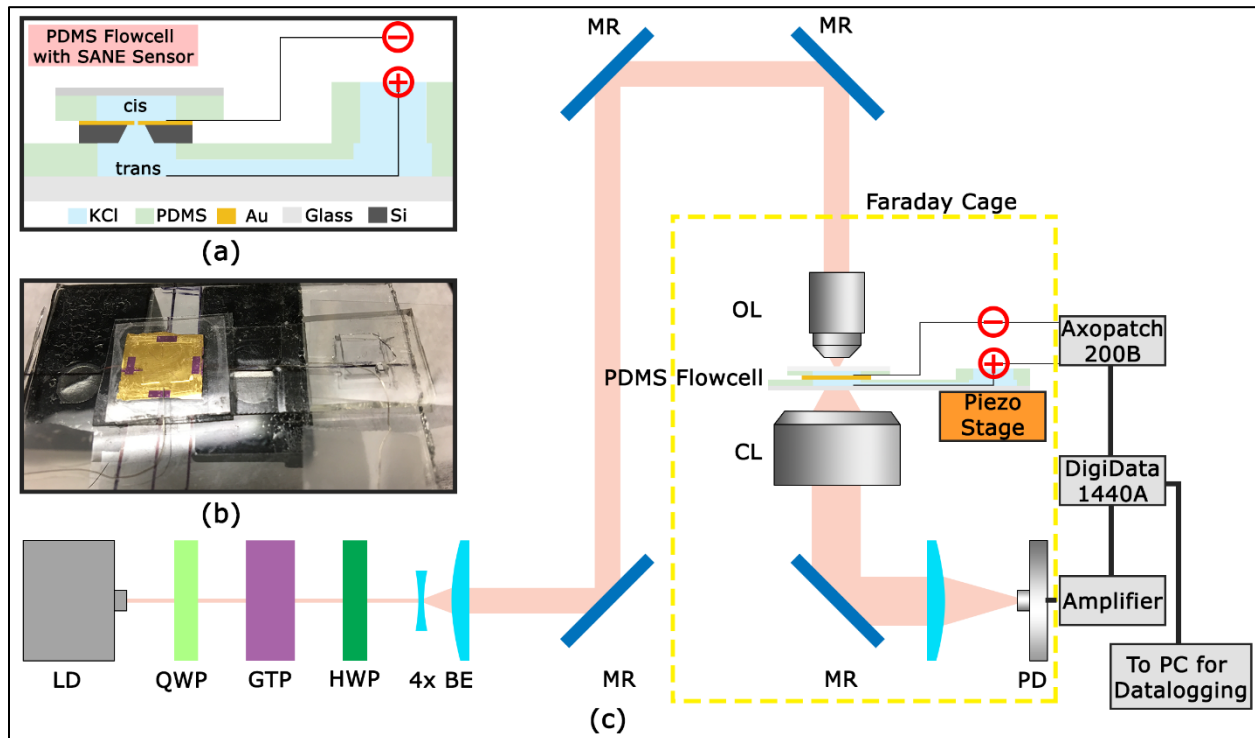


Fig. 2: (a) PDMS flow cell cross-sectional view with SANE sensor. (b) Image of prepared PDMS flow cell with SANE chip ready for placement on piezo-controlled stage. (c) Complete optical setup with PDMS flow cell placement and measurement instruments. LD: Laser Diode, QWP: Quarter Wave Plate, GTP: Glan-Thompson Polarizer, HWP: Half Wave Plate, 4x BE: 4x Beam Expander, MR: Mirror, OL: Carl-Zeiss 1.3 N.A. 63x Objective Lens, CL: Condenser Lens, PD: Photodiode.

of a 63x oil immersion objective lens and focused onto the front Au side of the SANE chip. The objective's focal spot was aligned with the DNH center by adjusting the piezoelectric stage controls until polarized light transmission was maximized. Light transmission through the FIB alignment markers was used as a first coarse step to find the DNH on the chip. The light transmitted through the chip's center and any leakage

light scattering through alignment markers was collected by a condenser lens and focused onto a photodiode (PDA36A, Thorlabs).

The standard soft lithography techniques were used for fabrication of a flow cell that could house the SANE sensor chip with a cis and a trans chamber for the nanopore and to provide optical access to the DNH. The flow cell was made from polydimethylsiloxane (PDMS) mixed in a 10:1 ratio of polymer to initiator as prescribed by the manufacturer (Dow Corning). This mixture was degassed to remove air bubbles and subsequent fabrication was performed in three steps. In the first step, a flat PDMS slab of 2 mm thickness was created by adding the bubble-free mixture to a cavity created on a polished side of a silicon wafer and curing it on a hotplate at 100°C for 10 min. After peeling this PDMS slab, a pattern was cut into it consisting of a 10 mm square opening at the center and a 2 mm wide rectangular channel connecting it to another 10 mm square opening towards the end of the slab [Fig. 2(a)]. The PDMS slab was bonded onto a 3 in x 2 in glass slide using oxygen plasma (Electro-Technic). In the second step, the SANE sensor was placed over the central square opening using a double-sided tape (3M) sealing the square opening underneath and creating the trans chamber of the nanopore. Another flat PDMS slab of 3 mm thickness was created using the same procedure and a hollow rectangle was cut and placed over the square opening at the end of the slab using double-sided tape [Fig. 2(b)]. This secondary chamber acted as a reservoir holding enough ionic solution to keep the bottom of the nanopore always wet. The rectangular channel connecting these openings was also covered with the same double-sided tape to completely seal the flow path. In the third step, a 1-inch coverslip of 170 μm thickness (VWR) was plasma-bonded onto a very thin PDMS layer of 200 μm thickness, with a square opening of 10 mm cut through the center of this layer to form a cis chamber over the SANE sensor. An additional 1 mm wide gap was cut at the edge of this PDMS layer to allow introduction of analyte into the cis chamber along with the cis chamber electrode. Subsequently, the trans side was gently filled with ionic solution using Teflon tubing connected to a syringe up to the brim of the 3 mm PDMS reservoir wall. To complete the electrical path, the trans side electrode was introduced through the reservoir wall and pushed along the rectangular channel until its tip was located right below the sensor. Finally, the secondary reservoir was topped with a coverslip to confine the ionic solution within the flow cell. This flow cell was attached to a holder and the assembly was screwed onto a piezo-controlled translation

stage (MDT6938, Thorlabs) immediately below the objective lens. The prepared PDMS flow cell with the SANE chip is shown in Fig. 2(b).

To implement electrical sensing the cis and trans chamber Ag/AgCl electrodes were attached to the Axon Headstage (CV 203BU) of the Axon Axopatch 200B patch clamp in voltage clamp mode. A custom-made Faraday cage using copper wire mesh (PSY405, Thorlabs) was installed to cover the entire optical assembly and shield the PDMS flow cell from low-frequency electromagnetic noise during highly sensitive patch clamp ionic current recordings. Subsequently, the nanopore was first tested for wetting. If the nanopore was blocked, an alternating ± 5 volts square wave was applied to the two electrodes for 60 sec to unblock the nanopore through electrophoretic pressure. After wetting, the trans side reservoir of the PDMS flow cell was filled with 7.4 pH 1M KCl solution and the cis reservoir was filled with 1 % solution of 20 ± 4 nm silica nanoparticles (MEL0010, NanoComposix) suspended in the same solution. The PDMS flow cell was attached to the piezo-controlled stage using screws and the laser beam was aligned to the DNH center as described above. A 250 mV bias was applied through the patch clamp in voltage clamp mode. The photodiode and Axopatch 200B signals were both sent through an Axon Digidata 1440 ADC to a PC for recording and data analysis in Axon Clampfit 10.6 software. The complete experimental setup schematic is shown in Fig. 2(c).

RESULTS

Fig. 3 shows the first proof of principle measurements with the SANE sensor that demonstrate multi-second trapping of a single 20 nm silica nanoparticle with concurrent electrophoretic measurements through the nanopore at the center of the DNH. When the 20 nm nanoparticle was trapped by the DNH, a step increase of 11 % in optical transmission was seen due to dielectric loading of the trap [Fig. 3(a)]. Concurrently, high frequency transients were seen in the raw ionic current [Fig. 3(b)], registering a positive charge peak of ~ 38 nA which was 19 times more than the baseline nanopore current. These ionic current oscillations were likely caused by axial nanoparticle oscillations, which we will henceforth refer to as ‘bobbing’, in the nanopore vicinity due to opposing optical and electrical forces. It is noteworthy that optical trapping enabled

ionic current sensing of the nanoparticle for a few seconds, which is about four orders of magnitude longer than the typical current sensing times for nanoparticle translocation events through a nanopore alone.

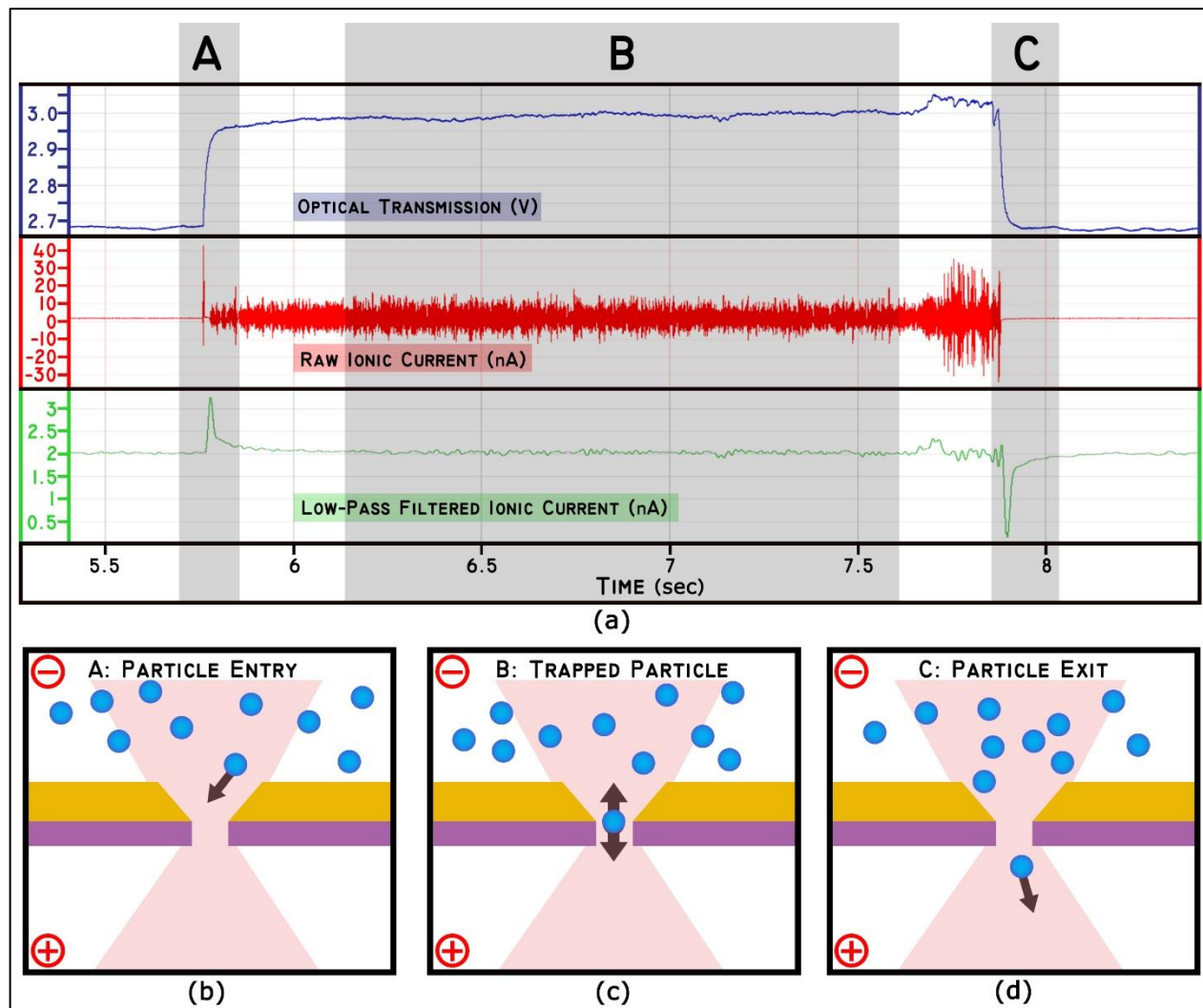


Fig. 3: (a) Plots of simultaneously recorded optical transmission (top, blue; V), raw ionic current (middle, red; nA) and 20 Hz low-pass filtered ionic current [bottom, green; nA) versus time (sec) for the single 20 nm silica nanoparticle trapped in the SANE sensor. Physical interpretation schematics for the signals recorded within gray-shaded regions A, B and C are shown in panels (b), (c) and (d), respectively. (b) Region A: Negatively charged nanoparticle entering the DNH-ssNP under applied bias. (c) Region B: Nanoparticle trapped and bobbing inside the DNH near the ssNP mouth. (d) Region C: Nanoparticle exiting the optical trap after the electrophoretic force dominates translocation.

The recorded raw ionic current was also filtered with a 20 Hz, low pass 8-pole Bessel filter in Axon Clampfit 10.6 to enable visualization of the nanoparticle movement effects on low frequency ionic current. A distinct

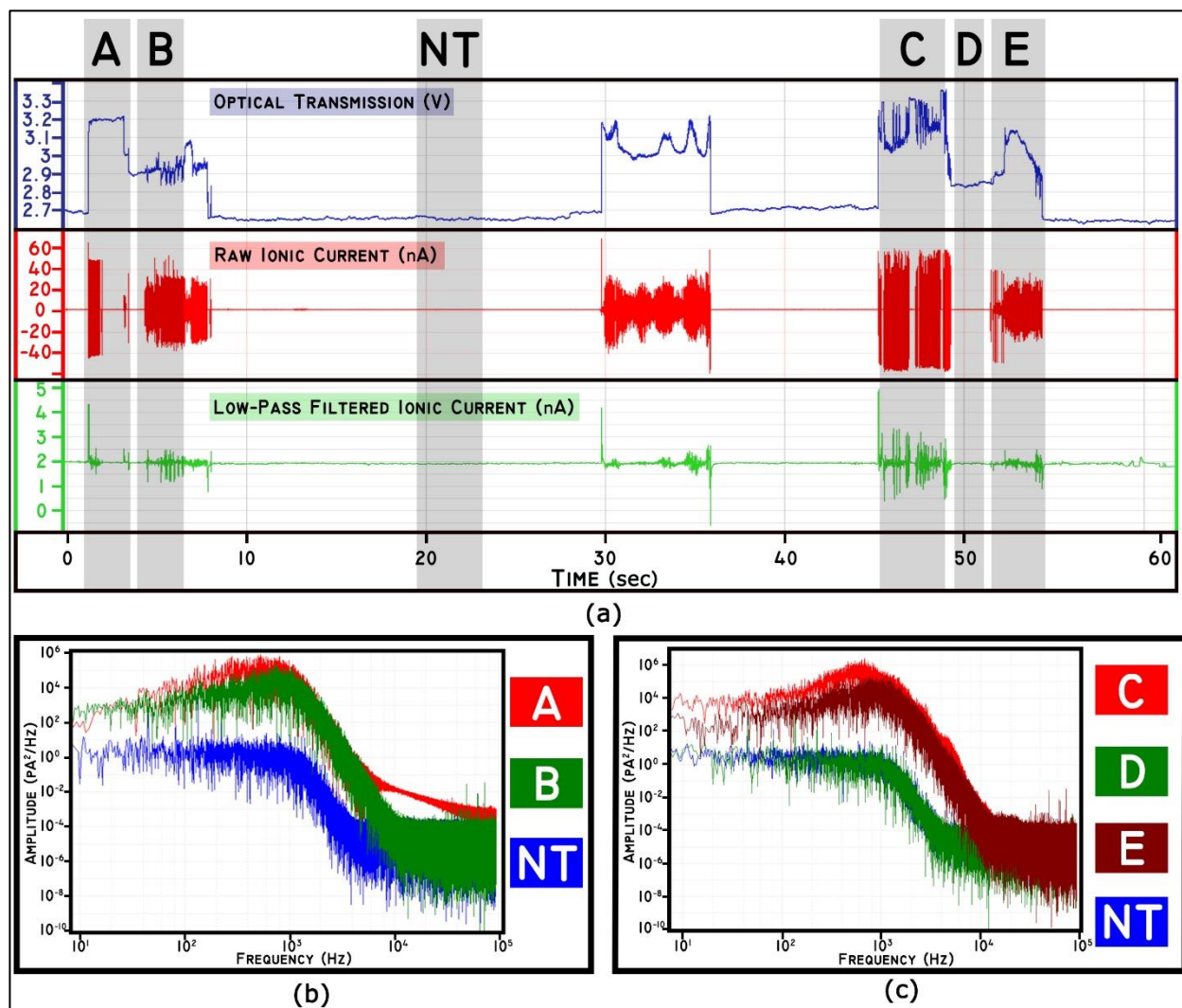


Fig 4: (a) Plots of simultaneously recorded optical transmission (top, blue; V), raw ionic current (middle, red; nA) and 20 Hz low-pass filtered ionic current (bottom, green; nA) versus time (sec) for a 1 min trace with three complex multi-particle trapping events. (b) Power spectrum analysis of the raw ionic current signal for Regions A, B and a No-Trapping (NT) region. (c) Power spectrum analysis of raw ionic current signal for Regions C, D, and E including NT for reference.

positive peak of 26.2 ms was registered during charged nanoparticle entry in the DNH, when the trapping started [Fig. 3(a), Region A, green curve in third row]. The nanoparticle was bobbing inside the DNH trap for about 2.15 sec [Fig. 3(a), Region B] and the low-pass filtered ionic signal did not show any appreciable

changes during that time. Towards the end of the trapping period, the amplitude of high frequency transients increased concurrently with a slight increase in optical transmission before the nanoparticle escaped and translocated through the nanopore [Fig. 3(a), Region C]. When the nanoparticle translocated across the ssNP from the cis to the trans region, a characteristic negative ionic current pulse was seen (third row, green) due to nanopore blockage during translocation (1.84 nA, translocation time 58.6 ms) taking place concurrently with a drop in optical transmission decrease back to the baseline (first row, blue).

In addition to single trapping events, more complex multiple nanoparticle trapping events were recorded and analyzed as well. Fig. 4(a) provides a 1 min trace showing three such trapping events. The gray-shaded Region A in that figure highlights a two-nanoparticle trapping event, as deduced from the nearly doubled optical transmission amplitude compared to the trapping event in Region B ($10 \pm 2\%$ versus $18.5 \pm 1\%$). Frequency spectrum analysis of raw ionic current signals for Regions A and B is shown in Fig. 4(b). Interestingly, the peak of the frequency spectrum for Region A was found in the 850 Hz range whereas it was in the 1kHz range for Region B. The latter had a remarkably similar power spectrum for the single nanoparticle trapping event described in Fig. 3 (frequency spectrum not shown for brevity). Furthermore, the frequency spectrum from a No-Trapping (NT) period is included for comparison in Fig. 4(b), demonstrating a plateau rather than a peak frequency and spectral amplitudes that were up to four orders of magnitude lower than those for trapping events. These spectral differences suggest the possibility of differentiating single versus double nanoparticle trapping events over background signals with the SANE sensor. A representative sequence of multiple nanoparticle trapping events is highlighted in Regions C and D of Fig. 4(a). Fig. 4(c) shows the power spectra of these Regions and compares them to the NT condition. The power spectrum of Region C with an amplitude peak at 850 Hz and a $19.5 \pm 1\%$ increase in optical transmission shows a two-nanoparticle trapping event. Optical transmission in region D was $8.7 \pm 1\%$ over baseline, indicating single nanoparticle trapping. However, the raw ionic current showed no high frequency transients in Region D, making its frequency spectrum indistinguishable from the NT condition, even though optical transmission indicated single nanoparticle trapping. We hypothesize, that during this period the nanoparticle attained transient equilibrium in the DNH-ssNP trap and was not bobbing significantly. In Region E, another nanoparticle entered the trapping site, indicated by an increase in optical transmission

to 15 ± 1 % and shifted the ionic current fluctuation spectral peak from ~ 1 kHz to ~ 900 Hz. These observations are interpreted as the entry of an additional nanoparticle instigating bobbing for both nanoparticles inside the trap before these translocated through the nanopore.

DISCUSSION

The dynamics of a nanoparticle in electrophoretic flow through a ssNP have been studied in detail [43]. In our study, the nanoparticle translocation dynamics changed drastically due to the SIBA-actuated trapping of the nanoparticle in the DNH nanocavity. The trapping force acting on the nanoparticle remained balanced for several seconds, e.g. 2.15 sec for the particle shown in Fig. 3(a). Furthermore, the characteristic negative peak due to ionic current blockage lasted 58.76 ms for the single 20 nm nanoparticle translocation event shown in Fig. 3(d), which is much longer than the 200 ± 30 μ s translocation times of similar nanoparticles [135]. Therefore, optical trapping enabled ionic current recordings of the nanoparticle in the vicinity of the nanopore that were about four orders of magnitude longer than typical translocation times for similar nanoparticles and also slowed down their translocation through the nanopore.

The greatly extended ionic current recording times also revealed a newly observed high frequency charge transient phenomenon. We hypothesize that this originates from bobbing of the nanoparticle through the mouth of the nanopore due to the competing electrophoretic and SIBA forces. These high frequency transients were seen both for single nanoparticle [Fig. 3(a)] and multiple nanoparticle [Fig. 4(a)] trapping. At the end of the single trapping event seen in Fig. 3(a) (Region D), the nanoparticle started bobbing, which resulted in larger amplitudes for both ionic current and optical transmission. These observations suggest that the electrophoretic force led the nanoparticle to translocate through the ssNP.

It was observed that the peak amplitude of high frequency transients for raw ionic current decreased as dielectric loading in the trap increased from a single nanoparticle (~ 1 kHz) to two nanoparticles (~ 850 Hz). Therefore, frequency spectrum analysis of the SANE sensor's raw ionic current shows promise for distinguishing single nanoparticles from more complex trapping events. In addition to periods of high

frequency ionic current transients, instances of trapping with relatively quiet ionic current signals were also observed. For example, the single nanoparticle trapping in Fig. 4(a) (Region D), with similar optical transmission amplitude as Region B did not show any high frequency transients. We hypothesize that this behavior was a result of transient equilibrium achieved by the single nanoparticle in the trap as it temporarily stopped bobbing. However, when another nanoparticle entered the DNH trap this equilibrium was disturbed and the high frequency charge transients returned with a peak frequency of ~900 Hz (Region E) in the raw ionic current trace [Fig. 4(c)]. The latter behavior was consistent with two-nanoparticle trapping. The subsequent gradual decrease in optical transmission and low-amplitude spikes in the low-passed ionic current in Region E suggest that the two nanoparticles translocated through the nanopore sequentially and not as a single unit. These findings indicate that the SANE sensor can provide information on the dynamics of single and two-nanoparticle dynamics inside the optical trap.

Finally, it is worth pointing out the possibility of using calibrated SANE sensor measurements in future work to estimate the number of total surface charges around unknown analytes. The Grahame equation [136] can be used to calculate total surface charge using the experimentally determined zeta potential of the analytes by the SANE sensor. The zeta potential can be deduced from the electrophoretic mobility of the analytes, which entails measurement of their translocation time and knowledge of the applied bias and nanopore size [137]. Concurrent optical measurements of analyte radius can be used to determine which approximation of Smoluchowski's theory is appropriate for deducing the zeta potential [138]. For experimental parameters relevant to this work the appropriate approximation is the Hückel equation, which would yield the zeta potential estimate for the analytes [139]. These considerations indicate the possibility of calibrating the SANE sensor's optical and ionic current signals in future work to estimate the charge around unknown analytes by direct measurement of their radius and electrophoretic mobility.

CONCLUSIONS

We have demonstrated multi-second optical trapping of electrophoretically translocating nanoparticles through a ssNP. The competing electrophoretic and SIBA forces induced bobbing inside the optical trap

that led to high frequency ionic current oscillations sensed through the nanopore. Frequency analysis of these oscillations demonstrated the possibility of distinguishing between single nanoparticles versus two nanoparticles inside the trap. Furthermore, the SANE chip's bimodal sensing ability showcased the possibility of using it as a tool to estimate the charge around a nanoparticle. This framework demonstrated the significant potential of the SANE sensor as an enabler for analyzing the charge and selective interactions between biological molecules.

ACKNOWLEDGEMENTS

We are grateful to Mr. Soeren Eyhusen and Mr. Chuong Huynh for allowing access and providing technical guidance on focused ion beam milling at the Zeiss ORION NanoFab facility in Peabody, MA. We are also grateful to Mr. Huan (Mick) Nguyen, Mr. Dennis Bueno and Mr. Richard K. Chambers for their invaluable technical guidance on fabrication at the Shimadzu Institute Nanotechnology Research Center, University of Texas at Arlington. Support for this work was provided through a Pilot Research Program for Interdisciplinary Collaboration funded by the Vice-President of Research Office of the University of Texas at Arlington.

REFERENCES:

- [1] Dekker C 2007 Solid-state nanopores *Nature nanotechnology* **2** 209
- [2] Yuan Z, Wang C, Yi X, Ni Z, Chen Y and Li T 2018 Solid-State Nanopore *Nanoscale research letters* **13** 56
- [3] Shi W, Friedman A K and Baker L A 2016 Nanopore sensing *Analytical chemistry* **89** 157-88
- [4] Butler T Z, Pavlenok M, Derrington I M, Niederweis M and Gundlach J H 2008 Single-molecule DNA detection with an engineered MspA protein nanopore *Proceedings of the National Academy of Sciences* **105** 20647-52
- [5] Harrell C C, Choi Y, Horne L P, Baker L A, Siwy Z S and Martin C R 2006 Resistive-pulse DNA detection with a conical nanopore sensor *Langmuir* **22** 10837-43
- [6] Fologea D, Gershow M, Ledden B, McNabb D S, Golovchenko J A and Li J 2005 Detecting single stranded DNA with a solid state nanopore *Nano letters* **5** 1905-9
- [7] Iqbal S M, Akin D and Bashir R 2007 Solid-state nanopore channels with DNA selectivity *Nature nanotechnology* **2** 243
- [8] Hasan M R, Mahmood M A I, Khanzada R R, Mansur N, Adnan A and Iqbale S M Molecular Dynamics Study of Protein Deformation through Solid-State Nanopore
- [9] Khan M S, Dosoky N S, Mustafa G, Patel D, Berdiev B and Williams J D 2017 Electrophysiology of Epithelial Sodium Channel (ENaC) Embedded in Supported Lipid Bilayer Using a Single Nanopore Chip *Langmuir* **33** 13680-8
- [10] Talaga D S and Li J 2009 Single-molecule protein unfolding in solid state nanopores *Journal of the American Chemical Society* **131** 9287-97

- [11] Nir I, Huttner D and Meller A 2015 Direct sensing and discrimination among Ubiquitin and Ubiquitin chains using solid-state nanopores *Biophysical journal* **108** 2340-9
- [12] Varongchayakul N, Huttner D, Grinstaff M W and Meller A 2018 Sensing Native Protein Solution Structures Using a Solid-state Nanopore: Unraveling the States of VEGF *Scientific reports* **8** 1017
- [13] Freedman K J, Haq S R, Edel J B, Jemth P and Kim M J 2013 Single molecule unfolding and stretching of protein domains inside a solid-state nanopore by electric field *Scientific reports* **3** 1638
- [14] Japruno D, Dogan J, Freedman K J, Nadzeyka A, Bauerdick S, Albrecht T, Kim M J, Jemth P and Edel J B 2013 Single-molecule studies of intrinsically disordered proteins using solid-state nanopores *Analytical chemistry* **85** 2449-56
- [15] Wanunu M, Dadosh T, Ray V, Jin J, McReynolds L and Drndić M 2010 Rapid electronic detection of probe-specific microRNAs using thin nanopore sensors *Nature nanotechnology* **5** 807
- [16] Venkatesan B M and Bashir R 2011 Nanopore sensors for nucleic acid analysis *Nature nanotechnology* **6** 615
- [17] Gu L-Q, Wanunu M, Wang M X, McReynolds L and Wang Y 2012 Detection of miRNAs with a nanopore single-molecule counter *Expert review of molecular diagnostics* **12** 573-84
- [18] Zahid O K, Wang F, Ruzicka J A, Taylor E W and Hall A R 2016 Sequence-specific recognition of microRNAs and other short nucleic acids with solid-state nanopores *Nano letters* **16** 2033-9
- [19] Ali W, Raza M U, Mahmood M A I, Allen P B, Hall A R, Wan Y and Iqbal S M Differentiation of Specific Cancer Biomarkers with Solid-state Nanopores
- [20] Deamer D, Akeson M and Branton D 2016 Three decades of nanopore sequencing *Nature biotechnology* **34** 518

- [21] Steinbock L and Radenovic A 2015 The emergence of nanopores in next-generation sequencing *Nanotechnology* **26** 074003
- [22] Khan M S, Dosoky N S, Berdiev B K and Williams J D 2016 Electrochemical impedance spectroscopy for black lipid membranes fused with channel protein supported on solid-state nanopore *European Biophysics Journal* **45** 843-52
- [23] Manrao E A, Derrington I M, Laszlo A H, Langford K W, Hopper M K, Gillgren N, Pavlenok M, Niederweis M and Gundlach J H 2012 Reading DNA at single-nucleotide resolution with a mutant MspA nanopore and phi29 DNA polymerase *Nature biotechnology* **30** 349
- [24] Li J, Stein D, McMullan C, Branton D, Aziz M J and Golovchenko J A 2001 Ion-beam sculpting at nanometre length scales *Nature* **412** 166
- [25] Storm A, Chen J, Ling X, Zandbergen H and Dekker C 2003 Fabrication of solid-state nanopores with single-nanometre precision *Nature materials* **2** 537
- [26] Lo C J, Aref T and Bezryadin A 2006 Fabrication of symmetric sub-5 nm nanopores using focused ion and electron beams *Nanotechnology* **17** 3264
- [27] Gierak J, Mailly D, Hawkes P, Jede R, Bruchhaus L, Bardotti L, Prevel B, Mélinon P, Perez A and Hyndman R 2005 Exploration of the ultimate patterning potential achievable with high resolution focused ion beams *Applied Physics A* **80** 187-94
- [28] Emmrich D, Beyer A, Nadzeyka A, Bauerdick S, Meyer J, Kotakoski J and Götzhäuser A 2016 Nanopore fabrication and characterization by helium ion microscopy *Applied Physics Letters* **108** 163103
- [29] Raza M U, Saleem S, Ali W and Iqbal S M 2016 Crosstalk between adjacent nanopores in a solid-state membrane array for multi-analyte high-throughput biomolecule detection *Journal of Applied Physics* **120** 064701

- [30] Gilboa T and Meller A 2015 Optical sensing and analyte manipulation in solid-state nanopores *Analyst* **140** 4733-47
- [31] Ivanov A P, Instuli E, McGilvery C M, Baldwin G, McComb D W, Albrecht T and Edel J B 2010 DNA tunneling detector embedded in a nanopore *Nano letters* **11** 279-85
- [32] Miles B N, Ivanov A P, Wilson K A, Doğan F, Japrun D and Edel J B 2013 Single molecule sensing with solid-state nanopores: novel materials, methods, and applications *Chemical Society Reviews* **42** 15-28
- [33] Keyser U F, Koeleman B N, Van Dorp S, Krapf D, Smeets R M, Lemay S G, Dekker N H and Dekker C 2006 Direct force measurements on DNA in a solid-state nanopore *Nature Physics* **2** 473
- [34] Keyser U, Van der Does J, Dekker C and Dekker N 2006 Optical tweezers for force measurements on DNA in nanopores *Review of Scientific Instruments* **77** 105105
- [35] Di Fiori N, Squires A, Bar D, Gilboa T, Moustakas T D and Meller A 2013 Optoelectronic control of surface charge and translocation dynamics in solid-state nanopores *Nature nanotechnology* **8** 946
- [36] Nicoli F, Verschueren D, Klein M, Dekker C and Jonsson M P 2014 DNA translocations through solid-state plasmonic nanopores *Nano letters* **14** 6917-25
- [37] Li Y, Nicoli F, Chen C, Lagae L, Groeseneken G, Stakenborg T, Zandbergen H W, Dekker C, Van Dorpe P and Jonsson M P 2014 Photoresistance switching of plasmonic nanopores *Nano letters* **15** 776-82
- [38] Assad O N, Gilboa T, Spitzberg J, Juhasz M, Weinhold E and Meller A 2017 Light-Enhancing Plasmonic-Nanopore Biosensor for Superior Single-Molecule Detection *Advanced Materials* **29**
- [39] Juan M L, Gordon R, Pang Y, Eftekhari F and Quidant R 2009 Self-induced back-action optical trapping of dielectric nanoparticles *Nature Physics* **5** 915

- [40] Al Balushi A A, Kotnala A, Wheaton S, Gelfand R M, Rajashekara Y and Gordon R 2015 Label-free free-solution nanoaperture optical tweezers for single molecule protein studies *Analyst* **140** 4760-78
- [41] Kumar L K S and Gordon R 2006 Overlapping double-hole nanostructure in a metal film for localized field enhancement *IEEE Journal of selected topics in quantum electronics* **12** 1228-32
- [42] Kumar L, Lesuffleur A, Hughes M and Gordon R 2006 Double nanohole apex-enhanced transmission in metal films *Applied Physics B* **84** 25
- [43] Ghorbanzadeh M, Jones S, Moravvej-Farshi M K and Gordon R 2017 Improvement of Sensing and Trapping Efficiency of Double Nanohole Apertures via Enhancing the Wedge Plasmon Polariton Modes with Tapered Cusps *ACS Photonics* **4** 1108-13
- [44] Mestres P, Berthelot J, Acimović S S and Quidant R 2016 Unraveling the optomechanical nature of plasmonic trapping *Light: Science & Applications* **5** e16092
- [45] Pang Y and Gordon R 2011 Optical trapping of 12 nm dielectric spheres using double-nanoholes in a gold film *Nano letters* **11** 3763-7
- [46] Kotnala A, DePaoli D and Gordon R 2013 Sensing nanoparticles using a double nanohole optical trap *Lab on a Chip* **13** 4142-6
- [47] Kotnala A and Gordon R 2014 Quantification of high-efficiency trapping of nanoparticles in a double nanohole optical tweezer *Nano letters* **14** 853-6
- [48] Pang Y and Gordon R 2011 Optical trapping of a single protein *Nano letters* **12** 402-6
- [49] Al Balushi A A, Zehtabi-Oskuie A and Gordon R 2013 Observing single protein binding by optical transmission through a double nanohole aperture in a metal film *Biomedical optics express* **4** 1504-11

- [50] Al Balushi A A and Gordon R 2014 Label-free free-solution single-molecule protein–small molecule interaction observed by double-nanohole plasmonic trapping *ACS Photonics* **1** 389-93
- [51] Al Balushi A A and Gordon R 2014 A label-free untethered approach to single-molecule protein binding kinetics *Nano letters* **14** 5787-91
- [52] Wheaton S and Gordon R 2015 Molecular weight characterization of single globular proteins using optical nanotweezers *Analyst* **140** 4799-803
- [53] Lan W-J, Holden D A, Zhang B and White H S 2011 Nanoparticle transport in conical-shaped nanopores *Analytical chemistry* **83** 3840-7
- [54] Guan W, Li S X and Reed M A 2014 Voltage gated ion and molecule transport in engineered nanochannels: theory, fabrication and applications *Nanotechnology* **25** 122001
- [55] Arjmandi N, Van Roy W, Lagae L and Borghs G 2012 Measuring the electric charge and zeta potential of nanometer-sized objects using pyramidal-shaped nanopores *Analytical chemistry* **84** 8490-6
- [56] Kim K-M, Kim H M, Lee W-J, Lee C-W, Kim T-i, Lee J-K, Jeong J, Paek S-M and Oh J-M 2014 Surface treatment of silica nanoparticles for stable and charge-controlled colloidal silica *International journal of nanomedicine* **9** 29
- [57] Bhattacharjee S 2016 DLS and zeta potential—What they are and what they are not? *Journal of Controlled Release* **235** 337-51

5. CONCLUSION

In this dissertation, we investigated solid state nanopore technologies for the sensitive detection of nanoparticles and protein biomarkers of cancer. Firstly, a study was performed by use of solid state nanopores to determine the binding of EGFR, a biomarker overexpressed in multiple cancers, to its RNA aptamer. This study demonstrated the promise of nanopore sensing technology for protein biomarker detection and led to our next goal, which was to explore the feasibility of detecting multiple biomarkers simultaneously to improve the specificity of disease diagnosis. As a first step towards that goal, in the second part of this dissertation we investigated the feasibility of resolving the throughput and multiplexing problems with single ion channel solid state nanopores by fabricating multiple nanopores on a single chip for simultaneous detection of biomarkers and self-referencing capability. Simulations were done to investigate the adjacent distance required so that electronic crosstalk between nearest-neighbor nanopores could be minimized for fabrication of nanopore arrays. In the last part of this dissertation, we have tried to resolve another long-time problem associated with current nanopore technology, namely the limited translocation time and lack of selectivity through solid state nanopores which impedes their use in real world situations where millions of biomolecules must be parsed to find the biomarker for a certain disease. A significant first step towards resolving this challenge was attained by fabricating a novel dual modality optical and electrical DNH-nanopore biosensor. A DNH aperture was milled at the mouth of a solid state nanopore and an NIR laser was focused onto the nanopore leading to trapping of the translocating nanoparticles at the mouth of the nanopore. The nanopore particle oscillated at the trapping site and translocated after some time when the electrophoretic force was able to overcome the plasmonic trapping force. Proof of principle experiments on this novel plasmonic solid state nanopore biosensor were accomplished by demonstrating optical trapping induced control of translocation of 20 nm silica nanoparticles through the nanopore. The extraordinary four orders of magnitude increase in electrical signal sensing time for any single particle trapped near the mouth of the nanopore opens up many future possibilities for use of the DNH-nanopore sensor as a fingerprinting tool for biomolecular applications. Much future work remains to be done to enable practical use of this sensor's ground-breaking properties in diverse

possible applications such as early cancer detection, DNA sequencing, Dual modality Mass Spectrometry, and active virus identification and analysis.

6. APPENDICES

PERMISSION FROM AUTHORS AND PUBLISHERS

CHAPTER 3- PERMISSION FROM AUTHORS AND PUBLISHERS

4/26/2018

One Central Press » Copyright Policy

- [Home](#)
- [Subjects](#)
- [Proceedings](#)
- [Journals](#)
- [Books](#)
- [Open Access](#)
- [About Us](#)
- [News](#)
- [Contact](#)
-

Copyright Policy

1. OCP acknowledges and agrees that the Author(s) retain(s) the copyright to their work submitted for publication.

2. The author assigns to OCP all rights:

– to publish the Work, in whole or in part, by various means such as hard copy or electronic copy formats, and in any and all forms of media, now or hereafter known; and

– to republish, distribute, promote, publicly perform, and publicly display the Work at any time and in all One Central Press projects.

3. The author(s) must comply to the following:

– only submit original work that has neither appeared elsewhere for publication, nor is under review for another refereed publication

– should determine whether disclosure of their material, content and photographs requires the prior consent of other parties and, if so, should obtain it; and

– research carried out in collaboration with other scholars necessitates that all authors approve of submitting the published work.

Statements and opinions expressed in the published work are those of the Author(s) and not those of the editors or One Central Press. No responsibility is accepted for the accuracy of information contained in the published work. OCP assumes no responsibility or liability for any damage or injury to persons or property arising out of the use of any materials, instructions, methods or ideas contained inside the published work.

4. By accepting the Copyright Agreement the corresponding Author:

– warrants that he/she is the Author and has the power and authority to make and execute this assignment

– affirms that, for jointly authored Chapters, he/she is empowered to accept this form on behalf of all authors

– warrants that the Chapter is original, has not previously been published and is not currently under consideration for publication by any other entity

– affirms that permission will be obtained for all previously published and/or copyrighted material contained in this manuscript (to the extent that the chapter incorporates text, passages, figures, data or other material from the work of others), it is the authors collective responsibility to obtain all copyright permissions – they can be obtained during the publishing process and need to be collected before publication; and

<http://www.onecentralpress.com/copyright-policy/>

1/3

– agrees to indemnify One Central Press against all losses, costs and expenses (including legal costs and expenses) arising from claims made by other parties due to the exceptional circumstance that the author has breached any terms, conditions and/or warranties concerning the authorship of the chapter (the whole or parts of it), the rights to publish the chapter or the infringement of any third party's rights.

If the Author has prepared the work as part of that his/her official duties as an employee or officer of a Government agency, public institution or company and has copyrights that belong to the Government agency, public institution, or company, One Central Press agrees to accept their terms and conditions if they are not in conflict with OCP's Copyright Policy.

CALL FOR CHAPTERS

Submit Chapters to our Books... [Read More](#)

[PUBLISH WITH ONE CENTRAL PRESS](#)



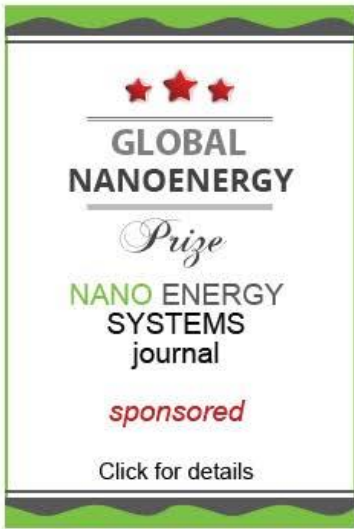
Waivers and Discounts on Article Publication Charges



One Central Press Blog

Latest News

[READ MORE](#)



NANO WORLD CURRENT/PAST ISSUES



CONTACT DETAILS

- One Central Press
Atlantic Business Centre
Atlantic Street
Altrincham
Cheshire
WA14 5NQ
United Kingdom
- @ admin@onecentralpress.com

[Home](#) | [Subjects](#) | [Books](#) | [Open Access](#) | [About Us](#) | [Blog](#) | [Contact](#) | [Publish](#) | [Frequently Asked Questions](#) | [Copyright Policy](#) | [Privacy Policy](#)



Email: _____


To whom it may concern

Subject: Permission to reuse/reprint an in-preparation/in-press/published manuscript in PhD dissertation.

I am a co-author on the paper titled "Differentiation of Specific Cancer Biomarkers with Solid-state Nanopores" that is published in OCP Functional Nanostructures.

I grant permission to Mr. Muhammad Usman Raza to reuse/reprint this manuscript in his PhD dissertation.

Name: Waqas Ali

Signature: 

Email: waqas.ali@mavs.uta.edu

Date: 04/26/2018

To whom it may concern

Subject: Permission to reuse/reprint an in-preparation/in-press/published manuscript in PhD dissertation.

I am a co-author on the paper titled "Differentiation of Specific Cancer Biomarkers with Solid-state Nanopores" that is published in OCP Functional Nanostructures.

I grant permission to Mr. Muhammad Usman Raza to reuse/reprint this manuscript in his PhD dissertation.

Name: Mohammed Arif Iftaker Mahmood

Signature: 

Email: arif_iftaker@rumy.io

Date: 27th April 2018

To whom it may concern

Subject: Permission to reuse/reprint an in-preparation/in-press/published manuscript in PhD dissertation.

I am a co-author on the paper titled "Differentiation of Specific Cancer Biomarkers with Solid-state Nanopores" that is published in OCP Functional Nanostructures.

I grant permission to Mr. Muhammad Usman Raza to reuse/reprint this manuscript in his PhD dissertation.

Name: Peter Allen

Signature: 

Email: pballen@uidaho.edu

Date: 4/27/18

To whom it may concern

Subject: Permission to reuse/reprint an in-preparation/in-press/published manuscript in PhD dissertation.

I am a co-author on the paper titled "Differentiation of Specific Cancer Biomarkers with Solid-state Nanopores" that is published in OCP Functional Nanostructures.

I grant permission to Mr. Muhammad Usman Raza to reuse/reprint this manuscript in his PhD dissertation.

Name: _____ Adam R. Hall _____

Signature: _____  _____

Email: _____ arhall@wakehealth.edu _____

Date: _____ 04/31/18 _____


To whom it may concern

Subject: Permission to reuse/reprint an in-preparation/in-press/published manuscript in PhD dissertation.

I am a co-author on the paper titled "Differentiation of Specific Cancer Biomarkers with Solid-state Nanopores" that is published in OCP Functional Nanostructures.

I grant permission to Mr. Muhammad Usman Raza to reuse/reprint this manuscript in his PhD dissertation.

Name: _____Yuan Wan_____

Signature:  _____

Email: _____mangendoc@gmail.com_____

Date: _____04/27/2018_____


To whom it may concern

Subject: Permission to reuse/reprint an in-preparation/in-press/published manuscript in PhD dissertation.

I am a co-author on the paper titled "Differentiation of Specific Cancer Biomarkers with Solid-state Nanopores" that is published in OCP Functional Nanostructures.

I grant permission to Mr. Muhammad Usman Raza to reuse/reprint this manuscript in his PhD dissertation.

Name: DR. SAMIR IQBAL

Signature: 

Email: SMIQBAL@IEEE.ORG

Date: 04/28/2018

RE: Form submission from: Thesis & Dissertation Questions

Turner, Diane L

Mon 4/23/2018 11:17 AM

To: Raza, Muhammad Usman <raza.muhammadusman@mavs.uta.edu>;

1. Since you are equal authors, you can use this article.
2. The Office of Graduate Studies has a template on their website for article-based theses.
https://www.uta.edu/gradstudies/_documents/General%20Information/Article%20based%20thesis%20dissertation%20final%202.26.16.pdf

Diane Turner

From: raza.muhammadusman@mavs.uta.edu [mailto:raza.muhammadusman@mavs.uta.edu]

Sent: Monday, April 16, 2018 12:05 PM

To: Turner, Diane L

Subject: Form submission from: Thesis & Dissertation Questions

Submitted on Monday, April 16, 2018 - 12:04pm

Submitted by anonymous user: 76.185.89.111

Submitted values are:

Contact Information

Name Muhammad Usman Raza

Student ID Number 1000878773

Email Address raza.muhammadusman@mavs.uta.edu

Phone Number 2142089774

Preferred contact method Phone

Graduation Information

Graduation Semester Spring

Graduation Year 2018

Thesis or Dissertation? Dissertation

Question

Hi,

I have the following questions.

1- I am equal author in a publication with my lab mate. He used that publication in his dissertation. Can I also use that publication in my dissertation as I was equal author? Will it be an issue as he has attached that publication in his dissertation?

2- Can I attached the published papers as is in the dissertation or do i need to format them in single coloumn style ususally used in dissertation?

Kindly reply to these queries ass soon as possible.

5/1/2018

Mail - raza.muhammadusman@mavs.uta.edu

Thanks

Usman
Question

The results of this submission may be viewed at:

<https://library.uta.edu/node/1519/submission/119836>

CHAPTER 3- PERMISSION FROM AUTHORS AND PUBLISHERS

4/30/2018

Mail - raza.muhammadusman@mavs.uta.edu

RE: URGENT: Permission to reprint my JAP published manuscript in PhD Dissertation

AIPRights Permissions <Rights@aip.org>

Mon 4/30/2018 10:08 AM

To: Raza, Muhammad Usman <raza.muhammadusman@mavs.uta.edu>;

Dear Dr. Raza:

You are permitted to include your published article in your thesis, provided you also include a credit line referencing the original publication.

Our preferred format is (please fill in the citation information):

“Reproduced from [FULL CITATION], with the permission of AIP Publishing.”

Please let us know if you have any questions.

Sincerely,

Susann Brailey

Manager, Rights & Permissions

AIP Publishing

1305 Walt Whitman Road | Suite 300 | Melville NY 11747-4300 | USA

t +1.516.576.2268

rights@aip.org | publishing.aip.org

Follow us: [Facebook](#) | [Twitter](#) | [LinkedIn](#)

From: Raza, Muhammad Usman [mailto:raza.muhammadusman@mavs.uta.edu]

Sent: Monday, April 30, 2018 11:01 AM

To: AIPRights Permissions <Rights@aip.org>

Subject: Re: URGENT: Permission to reprint my JAP published manuscript in PhD Dissertation

Hi,

I require permission to reprint my JAP published manuscript in my PhD dissertation. The manuscript's citation is provided below:

Raza, Muhammad Usman, et al. "Crosstalk between adjacent nanopores in a solid-state membrane array for multi-analyte high-throughput biomolecule detection." *Journal of Applied Physics* 120.6 (2016): 064701.

<https://outlook.office.com/owa/?path=/mail/inbox>

1/3

4/30/2018

Mail - raza.muhammadasman@mavs.uta.edu

Please grant me this permission for my PhD dissertation. The manuscript will be published 'as is' in the dissertation document. Kindly also let me know any requirements that you may have for the reprint.

Thanks

Muhammad Usman Raza

GTA, Electrical Engineering

Doctoral Student, Nano Bio Lab

University of Texas at Arlington

Mob: +1 214 208 9774

From: Raza, Muhammad Usman

Sent: Thursday, April 26, 2018 11:05 AM

To: rights@aip.org

Subject: URGENT: Permission to reprint my JAP published manuscript in PhD Dissertation

Hi,

I require permission to reprint my JAP published manuscript in my PhD dissertation. The manuscript's citation is provided below:

Raza, Muhammad Usman, et al. "Crosstalk between adjacent nanopores in a solid-state membrane array for multi-analyte high-throughput biomolecule detection." *Journal of Applied Physics* 120.6 (2016): 064701.

Please grant me this permission for my PhD dissertation. The manuscript will be published 'as is' in the dissertation document. Kindly also let me know any requirements that you may have for the reprint.

Thanks

Muhammad Usman Raza

<https://outlook.office.com/owa/?path=/mail/inbox>

2/3

4/30/2018

Mail - raza.muhammadusman@mavs.uta.edu

GTA, Electrical Engineering

Doctoral Student, Nano Bio Lab

University of Texas at Arlington

Mob: +1 214 208 9774


To whom it may concern

Subject: Permission to reuse/reprint an in-preparation/in-press/published manuscript in PhD dissertation.

I am a co-author on the paper titled "Crosstalk between adjacent nanopores in a solid-state membrane array for multi-analyte high-throughput biomolecule detection" that is published in Journal of Applied Physics.

I grant permission to Mr. Muhammad Usman Raza to reuse/reprint this manuscript in his PhD dissertation.

Name: DR. SAMIR IQBAL

Signature: 

Email: SMIQBAL@IEEE.ORG

Date: 04/28/2018

To whom it may concern

Subject: Permission to reuse/reprint an in-preparation/in-press/published manuscript in PhD dissertation.

I am a co-author on the paper titled "Crosstalk between adjacent nanopores in a solid-state membrane array for multi-analyte high-throughput biomolecule detection" that is published in Journal of Applied Physics.

I grant permission to Mr. Muhammad Usman Raza to reuse/reprint this manuscript in his PhD dissertation.

Name:

Sajid Saleem

Signature:

Sajid Saleem

Email:

ssaleem@pnee.nust.edu.pk

Date:

27 April 2018

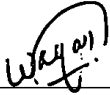
To whom it may concern

Subject: Permission to reuse/reprint an in-preparation/in-press/published manuscript in PhD dissertation.

I am a co-author on the paper titled "Crosstalk between adjacent nanopores in a solid-state membrane array for multi-analyte high-throughput biomolecule detection" that is published in Journal of Applied Physics.

I grant permission to Mr. Muhammad Usman Raza to reuse/reprint this manuscript in his PhD dissertation.

Name: Waqas Ali

Signature: 

Email: waqas.ali@mavs.uta.edu

Date: 04/26/2018

CHAPTER 4- PERMISSION FROM AUTHORS AND PUBLISHERS

To whom it may concern

Subject: Permission to reuse/reprint an in-preparation/in-press/published manuscript in PhD dissertation.

I am a co-author on the paper titled "SIBA Actuated Nanopore Electrophoresis (SANE)" that is in review in IOP Nanotechnology.

I grant permission to Mr. Muhammad Usman Raza to reuse/reprint this manuscript in his PhD dissertation.

Name: SAI SANTOSH SASANK PERI

Signature: 

Email: Saisantosh.sasan.peri@mavs.uta.edu

Date: 4/26/18

To whom it may concern

Subject: Permission to reuse/reprint an in-preparation/in-press/published manuscript in PhD dissertation.

I am a co-author on the paper titled "SIBA Actuated Nanopore Electrophoresis (SANE)" that is in review in IOP Nanotechnology.

I grant permission to Mr. Muhammad Usman Raza to reuse/reprint this manuscript in his PhD dissertation.

Name: Liang-Chieh Ma

Signature: Liang-Chieh Ma

Email: liangchieh.ma@uta.edu

Date: 04/27/18

To whom it may concern

Subject: Permission to reuse/reprint an in-preparation/in-press/published manuscript in PhD dissertation.

I am a co-author on the paper titled "SIBA Actuated Nanopore Electrophoresis (SANE)" that is in review in IOP Nanotechnology.

I grant permission to Mr. Muhammad Usman Raza to reuse/reprint this manuscript in his PhD dissertation.

Name: DR. SAMIR IQBAL

Signature: 

Email: SMIQBAL@IEEE.ORG

Date: 04/28/2018

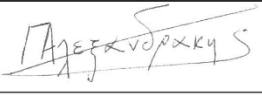
To whom it may concern

Subject: Permission to reuse/reprint an in-preparation/in-press/published manuscript in PhD dissertation.

I am a co-author on the paper titled "SIBA Actuated Nanopore Electrophoresis (SANE)" that is in review in IOP Nanotechnology.

I grant permission to Mr. Muhammad Usman Raza to reuse/reprint this manuscript in his PhD dissertation.

Name: George Alexandrakis

Signature: 

Email: galex@uta.edu

Date: 04/27/18